Title
Visualizing Synapses between Specific Neurons In vivo with Light Microscopy

Author
Chen, Yi

Publication Date
2014

Peer reviewed|Thesis/dissertation

UNIVERSITY OF CALIFORNIA

Los Angeles

Visualizing Synapses between Specific Neurons In vivo with Light Microscopy

A dissertation submitted in partial satisfaction of the

requirements for the degree of Doctor of Philosophy

in Biological Chemistry

By

Yi Chen

2014

ABSTRACT OF THE DISSERTATION

Visualizing Synapses between Specific Neurons In vivo with Light Microscopy

by

Yi Chen

Doctor of Philosophy in Biological Chemistry

University of California, Los Angeles, 2014

Professor S. Lawrence Zipursky, Chair

Specific synaptic connections underlie the ability of our nervous systems to perform the complex computations that account for our daily perception and behavior. How these connections arise during development is a central question in neuroscience. Due to the cellular complexity of the central nervous system (CNS) and the small size of synapses, it is difficult to efficiently visualize synapses of identified neurons in vivo, and this has become a major obstacle to studying mechanisms of synapse formation and synaptic specificity. Synapses are traditionally visualized with Electron Microscopy (EM), which can generate comprehensive and accurate synaptic connectivity maps. However, EM techniques are time consuming and labor intensive, making it difficult to study the dynamic process of synaptic development and identify molecular pathways involved in synapse formation using this method. Therefore, my thesis research has focused on developing techniques facilitating synapse visualization in vivo with light microscopy. I first adapted a technique originally developed in *C elegans* called GFP reconstitution across synaptic

partners (GRASP) to the nervous system of *Drosophila melanogaster*. I showed that adapted GRASP effectively detected synapses between known synaptic partner neurons within the fly visual system. It also successfully mapped neuronal connections within the neural circuit that underlies fly mating behavior. Due to some caveats in the design, in certain cell types GRASP failed to distinguish synapses from general cell-cell contacts. Inspired by GRASP and the prospect of addressing its limitations, I designed a new method called Synaptic Tagging with Recombination (STaR), which labels endogenous presynaptic and postsynaptic proteins in a cell-type-specific fashion. I modified genomic loci encoding synaptic proteins within bacterial artificial chromosomes such that these proteins, expressed at endogenous levels and with normal spatiotemporal patterns, were labeled in an inducible fashion in specific neurons through targeted expression of site-specific recombinases. Within the fly visual system, the number and distribution of synapses labeled with STaR correlate with EM studies. Using two different recombination systems, presynaptic and postsynaptic specializations of synaptic pairs can be co-labeled, and synapses between specific partners can be identified by assessing the apposition of these specializations. With STaR, I characterized synaptic development in photoreceptor neurons and uncovered a novel transformation phase of growth cones to synaptic terminals. This has led to the generation of gene expression profiles before, during and after the transformation phase and an in vivo RNAi screen to identify genes regulating photoreceptor synaptogenesis using the STaR markers. Furthermore, combining STaR with two-photon microscopy allowed visualization of synapse formation in live animals. In principle, STaR can be adapted to the mammalian nervous system. Both GRASP and STaR will facilitate our future investigation of key questions in synapse biology.

The dissertation of Yi Chen is approved.

Utpal Banerjee

Eddy De Robertis

Alvaro Sagasti

S. Lawrence Zipursky, Committee Chair

University of California, Los Angeles

2014

TABLE OF CONTENTS

LIST OF FIGURES

Chapter 1.

Chapter 2.

LIST OF TABLES

ACKNOWLEDGEMENT

This dissertation would not have been possible without the support of many people throughout the course of my graduate training.

First and foremost, I am tremendously grateful to my mentor, Larry Zipursky. I am thankful to Larry for his constant support, guidance and encouragement. I have learnt many things from Larry that will be my most valuable assets continuously throughout my scientific career. Larry has taught me how to think creatively, how to address scientific problems rigorously, and how to communicate with others efficiently. Most importantly, Larry has always encouraged me to follow my passion in science, which I will always remember in my future career.

I am also appreciative to the members of my committee, Utpal Banerjee, Eddy De Robertis and Alvaro Sagasti for their valuable guidance and support throughout my graduate training.

I am also grateful to other members of the Zipursky lab for guidance, intellectual simulation and friendship. First, I am very thankful to Jason McEwen, Orkun Akin, and Dorian Gunning for their tremendous help in my thesis project. Jason taught me many important techniques in molecular biology, which made my thesis project possible. Orkun and Dorian helped me with key experiments in my thesis project. I would also like to thank Kimberly Tsui, an excellent undergraduate student that worked with me in my thesis project. I am also grateful for Aljoscha Nern, who has provided me with intelligent discussions and useful reagents throughout my graduate training. Lastly, I would like to thank all the past and present members of the Zipursky lab for valuable comments and suggestions on my projects.

My PhD would not be possible without the support of my family. I am thankful to my husband Matthew Pecot. I am indebted to his unwavering encouragement, support and friendship throughout the years, especially at difficult times. I am eternally grateful to my parents for their unconditional love, trust and support.

My dissertation work was supported in part by the Dissertation Year Fellowship from UCLA Graduate Divisions. I wish to express my appreciation for the financial support.

Chapter 2, section 2, subsection 3 entitled, "Mapping the neural circuit underlying Drosophila mating behavior using GRASP" is a version of the manuscript from: Fan, P., Manoli, D.S., Ahmed, O.M., Chen, Y., Agarwal, N., Kwong, S., Cai, A.G., Neitz, J., Renslo, A., Baker, B.S., and Shah, N.M. (2013). Genetic and neural mechanisms that inhibit Drosophila from mating with other species. Cell 154, 89-102.

Chapter 3 is a version of: Chen, Y., Akin, O., Nern, A., Tsui, C.Y., Pecot, M.Y., and Zipursky, S.L. (2014). Cell-type-specific labeling of synapses in vivo through synaptic tagging with recombination. Neuron 81, 280-293. The authors of this manuscrip thank Dorian Gunning for help in generating the Ort antibody. We thank Martin Wallner and Richard Ohlsen for recordings in Xenopus oocytes to test different locations for tagging Ort. We thank Koen Venken and Hugo Bellen for providing reagents and advice for BAC recombineering, Tzumin Lee for providing DNA constructs containing LexA::VP16, Gerry Rubin and Barrett Pfeiffer for flies containing various cell-type-specific Gal4s and DNA con- structs, and Stephan Sigrist for providing brp mutant flies. We thank Mitya Chklovskii, Louis Scheffer, Shinya Takemura, Marta Rivera-Alba, and Ian Meinertzhagen for providing the latest results from the fly EM project at Janelia Farm Research Campus. For critical reading of the manuscript, we would also like to

thank Ian Meinertzhagen, Kelsey Martin, Eddy De Robertis, Utpal Banerjee, Alvaro Sagasti, and members of the S.L.Z. laboratory. This work was supported by a UCLA Dissertation Year Fellowship and the Howard Hughes Medical Institute. S.L.Z. is an investigator of the Howard Hughes Medical Institute.

VITA

June, 2007	B.S., Chemical Biology Tsinghua University Beijing, China
2007	Boyer Award for New Graduate Students ACCESS Graduate Program University of California, Los Angeles Los Angeles, California
2013	David Sigman Award Department of Biological Chemistry University of California, Los Angeles Los Angeles, California
2013	Dissertation Year Fellowship Graduate Divisions University of California, Los Angeles Los Angeles, California

PUBLICATIONS AND PRESENTATIONS

Pecot MY, Chen Y, Akin O, Chen Z, Tsui CY, Desplan C, & Zipursky SL (2014) Sequential axon-derived signals couple target survival and layer specificity in the Drosophila visual system. Neuron 82(2), 320-33

Chen Y, Akin O, Nern A, Tsui CY, Pecot MY, Zipursky SL (2014) Cell-type-specific labeling of Synapses in vivo through Synaptic Tagging with Recombination. Neuron 81(2), 280-93

Pecot MY, Tadros W, Nern A, Bader M, Chen Y, Zipursky SL. (2013) Multiple interactions control synaptic layer specificity in the Drosophila visual system. Neuron 77(2), 299-310

Fan P, Manoli DS, Ahmed OM, Chen Y, Agarwal N, Kwong S, Cai AG, Neitz J, Renslo A, Baker BS, Shah NM. (2013) Genetic and neural mechanisms that inhibit Drosophila from mating with other species. Cell 154 (1), 89-102

Chen Y, Nern A, Zipursky SL (2012) Cell-type-specific labeling of Synapses in vivo. Poster presented at the Cold Spring Harbor Laboratory Conference: Axon Guidance, Synapse Formation and Regeneration

Chen Y, Nern A, Zipursky SL (2012) Cell-type-specific labeling of Synapses in vivo. Poster presented at the Janelia Farm Research Conference: Wiring the Brain

Langenbacher AD, Huang J, Chen Y, Chen JN. (2012) Sodium pump activity in the yolk syncytial layer regulates zebrafish heart tube morphogenesis. Dev Biol 362 (2), 263-270

Hattori D, Chen Y, Matthews BJ, Salwinski L, Sabatti C, Greuber WB, Zipursky SL. (2009) Robust discrimination between self and non-self neurites requires thousands of Dscam1 isoforms. Nature 461 (7264), 644-648

Chapter 1 Introduction

Overview

Due to the small size of synapses and the extraordinary density of neuronal processes in the central nervous system (CNS), it has been a major challenge to examine how specific synaptic connections are established between different neuronal processes. Fortunately, the pace of discovery in this area is increasing rapidly: the cellular and molecular mechanisms of synapse formation have been extensively studied in cultured neurons. In some cases, the analysis is being extended to the nervous system *in vivo* (McAllister, 2007). Several molecular strategies have been implicated in achieving synaptic specificity (Sanes and Yamagata, 2009). New microscopic and genetic tools have been developed to facilitate visualizing synapses between specific neurons *in vivo*, which will lead to further advancement of our understanding of synapse formation and synaptic specificity.

In this introduction, I will provide a framework within which the progress on understanding synapse formation and synaptic specificity from different aspects can be considered.

Cellular mechanisms of synapse formation

A synapse is the fundamental unit underlying neural circuits where neurotransmitter release occurs in a spatially and temporally coordinated manner. It is generally composed of three structures: the presynaptic site, the synaptic cleft and the postsynaptic site. At the presynaptic site, the active zone (AZ) provides the platform for rapid fusion of neurotransmitter-filled synaptic vesicles (SVs) after calcium influx. At the postsynaptic site, neurotransmitter receptors accumulate within a compartment referred to as the postsynaptic density (PSD), which is critical

for the stability and dynamic regulation of neurotransmitter receptor populations. AZ and PSD each consists of special protein complexes that are transported to these sites and assembled during synapse formation (Margeta et al., 2008; McAllister, 2007).

For a synapse to form, contact must be made between the presynaptic axon and the postsynaptic dendrite. These contacts can be initiated by either axonal growth cones or dendritic filopodia. Some of these axo-dendritic contacts are transitory, resulting in retraction of the filopodium. However, a small subset of these filopodia become stabilized, and nascent synapses form at those sites. The signals that lead to the stabilization of filopodia contacts, thought to be cell adhesion molecules, are likely to be some of the first signals that lead to synapse formation (see next section) (Sanes and Yamagata, 2009; Yamagata et al., 2003).

Ultimately, the transport of presynaptic and postsynaptic proteins must be altered by signals at sites of axo-dendritic contact to cause their accumulation at those sites. The time course of synaptogenesis is usually measured by the time-course of stable accumulation of the presynaptic and postsynaptic proteins. In cultured neurons, three possible sequences of events were observed with time-lapse imaging (Figure 1-1) (McAllister, 2007). Friedman and colleagues showed that presynaptic differentiation occurred well before postsynaptic development in cultured rodent cortical neurons (Friedman et al., 2000). In contrast, another report showed that in cultured hippocampal neurons a significant proportion of postsynaptic protein complexes are stabilized at nascent postsynaptic sites at least 2 hours before the accumulation of presynaptic vesicles at the apposing axonal membrane (Gerrow et al., 2006). Yet a third report by Sabo and Washbourne indicated that presynaptic and postsynaptic proteins were recruited simultaneously to new axo-dendritic contacts within a few minutes (Sabo et al., 2006; Washbourne et al., 2002).

Taken together, there appear to be multiple mechanisms for the recruitment and stabilization of presynaptic and postsynaptic proteins to new sites of axo-dendritic contact in cultured neurons. Many of them remain to be tested *in vivo* in the intact nervous system.

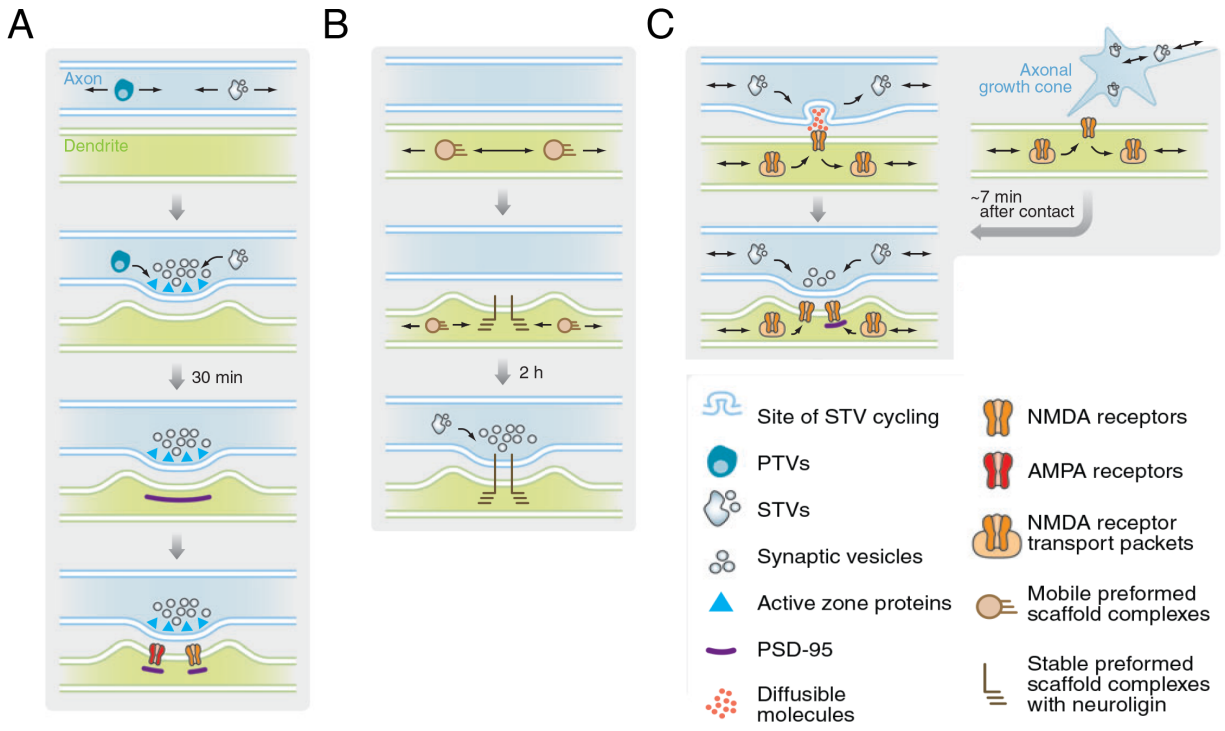

Figure 1-1 Three possible sequences of events during synaptogenesis in cultured neurons

Multiple mechanisms account for the recruitment and stabilization of presynaptic and postsynaptic proteins to new sites of axo-dendritic contact. (A) Glutamatergic synapses between axon and dendrite shafts of hippocampal neurons can form in about an hour after the initial accumulation of presynaptic vesicles. Presynaptic proteins, including synaptic vesicle precursors (STVs) and piccolo-transport vesicles (PTVs), are mobile in axons before synapses are formed. These precursors are the first proteins recruited to nascent synapses. After approximately 30 min, PSD-95 accumulates at these sites followed by glutamate receptors (Friedman et al., 2000). (B) Glutamatergic synapses can also form at pre-specified sites along dendritic shafts of cultured hippocampal neurons, defined by stable preformed scaffold complexes associated with neuroligin. A significant proportion of these complexes then recruit STVs to form synapses within 2 hours of their stabilization at the postsynaptic site (Gerrow et al., 2006). (C) In young cortical neurons, glutamatergic synapses can form even faster, on a timescale of several minutes. In these cells, STVs and NMDARs are both found in transport packets that are highly mobile in the axons and dendrites, respectively, before synapse formation. Both STVs and NMDAR transport packets cycle with the membrane during their transport. Contact between an axonal growth cone filopodium and a dendrite (right), or between axon and dendrite shafts (left), leads to the rapid and simultaneous recruitment of STVs and NMDARs at nascent synapses within approximately 7 min of contact (Sabo et al., 2006; Washbourne et al., 2002). Adapted from McAllister, 2007.

Molecular mechanisms of synapse formation

At an early step in synapse formation membrane regions suitable for the formation of a new presynaptic and postsynaptic sites must to be defined and interactions between these regions subsequently lead to accumulation of presynaptic and postsynaptic proteins. While the definitive molecular mechanisms underlying this step remains largely elusive, an increasingly number of molecular signals have been implicated in this process. Trans-synaptic cell adhesion molecules (CAMs) are thought to mediate and stabilize the initial contacts and initiate simultaneous bidirectional signaling in the axon and dendrite for the rapid and simultaneous recruitment of AZ and PSD components (Yamagata et al., 2003).

Molecules that promote synapse formation, called synaptogenic molecules, have been identified based on their ability to promote synapse formation when transfected into cultured neurons. Other lines of evidence were also considered, such as a reduction of synapse number in cultured neurons lacking a particular cell adhesion molecule (CAM) and the presence of a CAM at the dense core vesicles (the vesicles transporting synaptic proteins required for AZ assembly) or at axo-dendritic contacts that later become synapses (Margeta et al., 2008; McAllister, 2007; Sanes and Yamagata, 2009). Homophilic CAMs such as cadherins, synCAMs and NCAM (Biederer et al., 2002; Sara et al., 2005), as well as heterophilic CAMs such as nectins, Neuroligins and Neurexins and SALMs (synaptic adhesion-like molecules), NGLs (netrin-G ligands), and LRRTMs (leucine-rich repeat transmembranes) have all been implicated in initiating synapse formation in various neuronal culture systems (Craig and Kang, 2007; de Wit et al., 2011; Dityatev et al., 2000; Ko et al., 2006; Nam et al., 2011).

With the advancement of genetic knockout techniques, the above-mentioned synaptogenic

CAMs in cultured neurons were subsequently tested *in vivo*. Surprisingly, although animals deficient for these genes did show impaired synaptic transmission, most did not display a reduction of synapse number. For example, a large number of reports demonstrate that the Neurexin-Neuroligin complex is necessary and sufficient for presynaptic and postsynaptic differentiation in cultured neurons. However, mice lacking all three *Neuroligins* (*Nlg1, 2 and 3*) or all three *α-Neurexins* displayed severely impaired synaptic transmission but the number of excitatory synapses appears to be unaffected (Dudanova et al., 2007; Varoqueaux et al., 2006). Thus, Neuroligins and *α-Neurexins* are essential for recruitment of key synaptic components or for maintenance of their function, but they not essential for synapse formation. Genetic redundancy could be one reason to account for the differences between results in cultured neurons and *in vivo*.

Meanwhile, it is important to realize that a culture dish could be an oversimplified environment to study such a complex process, especially considering the complex environment neurons experience in the developing CNS. Combining results in cultured neurons with *in vivo* studies has become crucial in uncovering molecular mechanisms underlying synapse formation. Encouragingly, in recent years a few molecules have been identified to regulate synapse formation *in vivo* in various systems. And a few representative examples are discussed here (summarized in Table 1-1).

The Ephrin axon guidance molecule family has been implicated in synapse formation in vivo. The EphrinB family seems to be especially important for postsynaptic differentiation because knockout of all three EphB receptors dramatically decreases excitatory synapse number in mouse hippocampus *in vivo* (Henkemeyer et al., 2003). In addition, EphB receptor clustering directly regulates NMDAR clustering during synapse formation (Dalva et al., 2000).

In addition to cell-adhesion molecules, some secreted factors have also been shown to be critical for CNS synaptogenesis. For example, a role for the secreted neurotrophin, brain-derived neurotrophic factor (BDNF) to regulate CNS synapse formation was supported by studies both in culture and *in vivo*. BDNF treatment increases numbers of excitatory synapses in cultured neurons (Vicario-Abejon et al., 1998) and the BDNF receptor TrkB knockout mice have decreased numbers of excitatory synapses (Martinez et al., 1998). Recently, TrkB was found to be trafficked in axons in conjunction with SV precursor transport packets (Gomes et al., 2006). Over time, surface TrkB becomes enriched at glutamatergic synapses. Taken together, these results suggest that TrkB directly regulates synapse formation between cortical neurons, possibly by directly influencing the trafficking of co-transported intracellular presynaptic precursors.

Secreted molecules from neighboring glial cells also play a role in glutamatergic synapse formation. This idea was first demonstrated by the synaptogenic effects of glial-derived molecules, such as apolipoprotein E and thrombospondins (TSPs) in cultured neurons (Mauch et al., 2001). Importantly, developing mouse brains deficient in TSP1 and TSP2 form fewer synapses, as shown by staining of a variety of synaptic proteins including PSD95 and Bassoon (Christopherson et al., 2005). Later, the Gabapentin Receptor, α2δ-1, was identified as a neuronal TSP receptor responsible for excitatory CNS synaptogenesis (Eroglu et al., 2009). α2δ-1 is required for TSP-induced synapse formation in cultured neurons and overexpression of α2δ-1 in neurons enhances synapse formation *in vivo*. This evidence supports a synaptogenic role for α2δ-1 as a TSP receptor.

Molecules that inhibit synapse formation (hence synapse-limiting molecules) also play critical roles in regulating synapse formation. In the mouse cortex, major histocompatibility complex I molecules (MHCI), limit synapse number in very young neurons (Glynn et al., 2011).

Knockdown of MHCI expression results in a dramatic increase in synapse number, whereas overexpression of MHCI decreases synapse number in culture. Similarly, glutamatergic synapse density was higher in neurons from $\beta 2m^{-/-}$ (subunit of MHCI) mice throughout development. These results suggest that the number of synapses that a young neuron forms may be both positively and negatively regulated to achieve the appropriate pattern of synapses.

Synaptogenic molecules

Receptor	Ligand	in vivo function
EphB	EphrinB	Positively regulate excitatory synapse number and NMDAR clustering in hippocampal neurons
TrkB	BDNF	Positively regulate excitatory synapse density in hippocampal neurons
α2δ-1	thrombospondins	Positively regulate synase number in mouse cortex

Synapse-limiting molecules

Receptor	Ligand	in vivo function
Major histocompatibility complex class I (MHC1): β2m		Negatively regulate synase density in mouse visual cortex

Table 1-1 Summary of cell-surface receptors and their ligands involved in synapse formation in vivo

Molecular mechanisms of synaptic specificity

In addition to inducing synapse formation in general, cell surface receptors and their ligands are well positioned to mediate recognition between specific synaptic partners and initiate synapse

formation at appropriate locations with specific targets, thus mediating synaptic specificity. Their roles in synaptic specificity have been studied in a variety of neural circuits in different model organisms with different experimental methods. It is therefore difficult and not necessarily informative to simply list all the molecules involved in synaptic specificity here. Instead, through the identification and characterization of these molecules in different systems, a few key strategies have emerged that may account for the establishment of specific synaptic connections during development across all species.

The most straightforward molecular strategy for establishing specific synaptic connections is through direct matching of the cell-surface identities between synaptic partners. Several examples from different systems supported this strategy. One of them involves the conserved, epidermal growth factor (EGF)-repeat-containing transmembrane proteins Teneurins (Figure 1-2A) (Hong et al., 2012). In the *Drosophila* olfactory system, axons of approximately 50 classes of olfactory receptor neurons (ORNs) form one-to-one connections with dendrites of approximately 50 classes of projection neurons (PNs). Luo and collages showed that Ten-m and Ten-a are highly expressed in select PN–ORN matching pairs *in vivo* and Teneurins promote homophilic interactions in vitro. Importantly, Ten-m co-expression in non-partner PNs and ORNs promotes their ectopic connections, suggesting Teneurins match the presynaptic ORNs to postsynaptic PNs through homophilic attractions. However, results from loss-of-function experiments on Teneurins described in the paper did not directly support the homophilic matching model. Further experiments to remove specific Teneurins from specific ORNs or PNs are needed to clarify this issue and fundamentally prove the direct matching model.

Members of the Leucine rich repeat (LRR) containing protein family have also been shown to mediate attractive interactions between synaptic partners *in vivo*. In mouse hippocampus, NGL-2

is specifically localized to the proximal dendrites of CA1 pyramidal neurons and mediates synapse formation with SC axons from CA3 region expressing its ligand Netrin-G2 (DeNardo et al., 2012). In *Ngl-2* null animals, about 30% reduction in dendritic spine density was observed in the proximal dendrites of pyramidal neurons while the spine density in the distal dendrites was not affected. Another LRR containing protein NGL-1 localizes to distal dendrites of CA1 pyramidal neurons and potentially mediates interactions with axons from other regions (Figure 1-2B).

Although the "synapse by matching" strategy is intuitive and widely accepted, it has become increasingly clear that it is not the only strategy to mediate synaptic specificity. Considerable evidence has accumulated that repulsive mechanisms possibly play an equally important role in ensuring synapses form at the appropriate locations and with the correct synaptic partner. For instance, Shen and colleagues have shown that inhibitory signals play an important role in regulating the pattern of synapses formed by DA9 neurons in *C. elegans* (Figure 1-2C). DA9 neurons have processes that run in the anterior-posterior direction both ventrally and dorsally. These processes contact other neurites along their length, but form synapses largely on distal portions of the dorsal axon. This localization is determined by gradients of two secreted molecules Wnt and netrin, originally discovered as a morphogen and guidance factor, respectively (Klassen and Shen, 2007; Poon et al., 2008). UNC-6/netrin is secreted by cells near the ventral midline and present in a ventral-dorsal gradient. LIN-44/Wnt is secreted by cells in the tail and present in a posterior-anterior gradient. Acting through separate receptors (UNC-5/DCC and LIN-17/frizzled, respectively), netrin and Wnt prevent the formation of presynaptic specializations, thereby confining them to the anterior portion of the dorsal process.

Repulsive interactions between prospective synaptic elements can also regulate the correct

composition of synapses. In the visual systems of both vertebrates and invertebrates, neurons form multiple-contact synapses at which a single presynaptic site is apposed to several different postsynaptic sites. *Drosophila* photoreceptor neurons form tetrad synapses, with four distinct postsynaptic elements, one each from lamina neuron L1 and L2 (this pair is invariable), and two elements from other cells apposing each presynaptic site (Meinertzhagen and O'Neil, 1991). Millard and colleagues show that *Drosophila Dscam1* and *Dscam2,* genes encoding homophilic repulsive proteins, act redundantly to ensure the invariable combination of L1 and L2 postsynaptic elements at all postsynaptic tetrads (Figure 1-2D) (Millard et al., 2010). In *Dscam; Dscam2* double mutants, elements from the same cell (two L1 or two L2 elements) were seen within the same postsynaptic tetrad, indicate the strict pairing is lost. Based on these observations, the previously known properties of Dscam, the authors propose that Dscams regulate synaptic specificity by excluding inappropriate partners at multiple-contact synapses. This model was also supported by the developmental characterization of synapse formation process by EM between photoreceptor neurons and L1 and L2 dendrites in *Musca domestica* (Meinertzhagen et al., 2000).

In addition to direct interactions between synaptic partners, establishment of appropriate synaptic connections sometimes require a third cell type. For example, in *C elegans*, a motor neuron called HSNL forms synapses onto VC neurons (VC4 and VC5) and vm2 muscle (Figure 1-2E). Surprisingly, the sites of presynaptic sites within the HSNL axon are not determined by the target neurons (or muscle) or by intrinsic signals within the axon but rather by localized contact with an epithelial cell (called the guidepost cell). This involves two immunoglobulin (Ig) superfamily members SYG1 and SYG2, which are related to the vertebrate Neph and Nephrin (Chao and Shen, 2008; Shen and Bargmann, 2003; Shen et al., 2004). SYG1 is expressed by the HSNL neuron and SYG2 is expressed by guidepost cell, respectively. In mutants lacking *syg1* or *syg2*,

HSNL still forms synapses but now with incorrect partners; conversely, ectopic expression of SYG2 can relocalize HSNL presynaptic specializations to a novel site. Thus, SYG1 and SYG2 act as synaptic recognition molecules that regulate the appropriate locations of synapses.

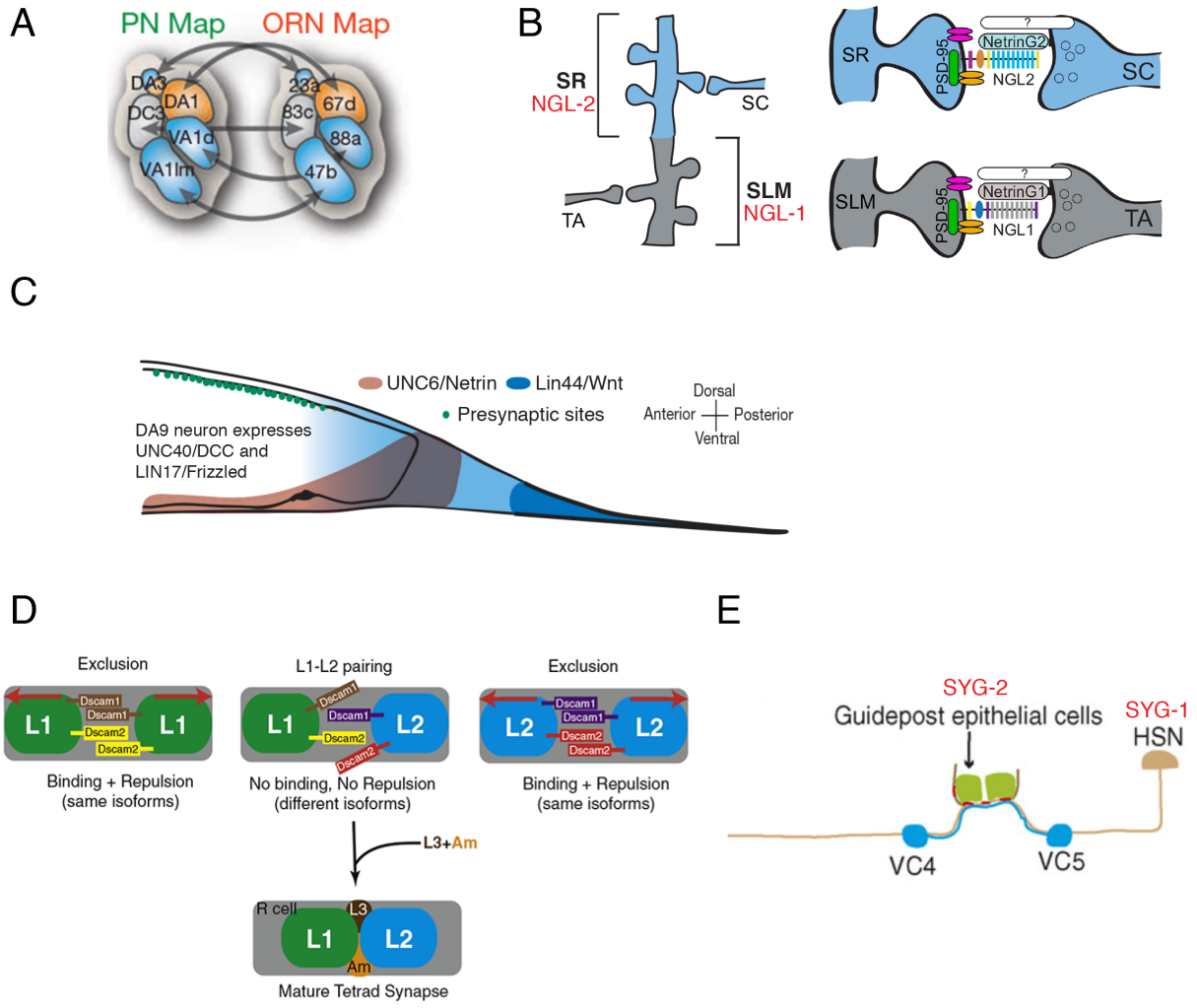

Figure 1-2 Examples of cell-surface receptors and their ligands regulating synaptic specificity in vivo

(A) Combined expression patterns of Teneurin proteins in PNs (left) and ORNs (right). Matching Ten-m or Ten-a expression levels between PNs and ORNs mediates the matching between synaptic partners. Blue: Ten-m high; orange: Ten-a high. Adapted from Hong et al., 2012. (B) NGL-2 regulates input-specific synapse development because it is restricted to the proximal dendrites (SR region) of CA1 pyramidal cells. Its ligand Netrin-G2 is expressed in SC axons, which form synapses with the proximal dendrites. NGL-2 interacts with PSD-95 and may recruit glutamate receptors to the nascent synapse. Distal synapses in CA1 have a complementary set of synaptic proteins, including NGL-1 and Netrin-G1.

Adapted from DeNardo et al., 2012. (C) Model for the roles of UNC-6/netrin and LIN-44/Wnt in subcellular patterning of presynaptic specializations in DA9. Adapted from Poon et al., 2008. (D) Model for synaptic exclusion mediated by Dscam1 and Dscam2. L1 and L2 cells express different sets of Dscam1 proteins and also different Dscam2 proteins or distinct ratios of its two isoforms. When two postsynaptic elements from the same cell encounter each other, Dscam1 and Dscam2 promote self-avoidance (exclusion), preventing L1/L1 or L2/L2 pairs from incorporating into the same tetrad. Red arrows indicate Dscam-mediated homophilic repulsion. Adapted from Millard et al., 2010. (E) Synapse formation between HSNL neurons and its VC targets (VC4 and VC5) is mediated by SYG-1-expressing HSNL cell contact with SYG-2-expressing guidepost epithelial cells. Red puncta represent presynaptic specializations in HSNL. Adapted from Margeta et al., 2008.

The studies and models discussed above provided a framework to explain how the tremendous specificity is achieved within the central nervous system. However, due to experimental limitations within the in vivo model systems, we are still far from completely uncovering the mechanisms underlying synaptic specificity. Among all the roadblocks, one major obstacle to studying the mechanisms of synapse formation has been the lack of methods to efficiently visualize synapses of identified neurons in vivo in the CNS, due to the cellular complexity and the small size of synapses.

Electron Microscopy analyses demonstrate synaptic specificity

Current knowledge of synaptic connectivity in the CNS has been obtained largely by electron microscopy (EM). In the 1980s, connectivity of the nervous system of the adult *C elegans* was mapped by serial-section Transmission Electron Microscopy (SS-TEM), revealing ~7000 synapses in the entire nervous system (White et al., 1986). In this method, a region of the nervous system (in this case, the entire animal) was sectioned into thousands of ultrathin sections and imaged with transmission electron microscope (TEM) individually. Researchers then manually examined the series of electron micrographs and identified each synapse based on certain criteria (mostly the electron dense nature of pre or postsynaptic specializations). Once a synapse was identified, researchers traced the parental processes back to a landmark (e.g. the axon, dendritic or the cell body) that allows the cell type to be identified. This process was

repeated for every synapse identified in that region and the results were reconstructed into a three-dimensional (3D) map containing all neurons in the region and their synaptic connections. Serving as a reference, the worm connectome greatly facilitated the identification of genes that regulate the stereotyped synaptic connectivity and circuits underlying key behaviors as well as synaptic development in worms during the past few decades.

Many efforts have been made to generate connectivity maps for more complex nervous systems. Among those, the visual system of *Drosophila Melanogaster* is perhaps the best characterized. The first and the second optic neuropils (i.e. the lamina and the medulla) of the fly visual system were mapped by several independent SS-TEM studies (Meinertzhagen and O'Neil, 1991; Rivera-Alba et al., 2011; Takemura et al., 2013; Takemura et al., 2008). The lamina neuropil is organized into repeating units called cartridges, with each cartridge consisting of synaptic connections between 6 photoreceptor axons (R1-R6) and the dendrites of lamina monopolar neurons, as well as connections between other neurons (Figure 1-3). In the recent SS-TEM study by Rivera-Alba and colleagues, one lamina cartridge was imaged with TEM and fully reconstructed (Rivera-Alba et al., 2011). Here, 477 presynaptic sites were identified based on the presence of the electron dense T-shaped structures (i.e. T-bars) and a total of 1,407 postsynaptic sites juxtaposing these T-bars were identified. The reconstruction reveals a complex network that displays high level of connecting specificity. For example, the L1 and L2 lamina neurons have similar dendritic morphologies and both lie at the cartridge axis in the center of six photoreceptor axons. They play major roles in motion detection; flies with silenced L1 and L2 neurons are virtually blind to motion. Despite having largely similar synaptic connections with photoreceptor neurons, L1 and L2 display distinct synaptic specificity with another lamina neuron L4. L2 and L4 form reciprocal synapses, meaning that L2 is presynaptic to L4 at some synapses while L4 is

presynaptic to L2 at others. In contrast, L1 and L4 form very few synapses. It remains unclear what mechanisms allow L4 to distinguish between L1 and L2 dendrites when forming synapses, though recent data suggest that the Ig-family cell adhesion molecule Kirre may play a role in this process (Luthy et al., 2014).

The medulla, the second visual neuropil of *Drosophila*, is much more complex compared to the lamina in terms of the number of cell types and their connectivity. Like the lamina, it consists of hundreds of repeating units called columns (Figure 1-3). In a recent study, Chklovskii and colleagues developed a state-of-the-art semi-automated pipeline to reconstruct a connectome of 379 neurons including all the synaptic connections among neurons within a single reference column, as well as all the connections between the reference column and some neurons within six nearest-neighbor columns (Takemura et al., 2013). This newly completed connectome again uncovered highly specific synaptic connections. In addition to the vertical repeating columns, medulla is also organized into 10 horizontal layers. Specific cell types target their axons or elaborate dendrites within one or more specific layers. For instance, R7 photoreceptor axons specifically terminate at the M6 layer. It has been suggested that layer specificity is equivalent to synaptic specificity. For instance, once an R7 axon correctly targets to the M6 layer, it form synapses with all the nearby processes in that layer. The medulla EM connectome greatly challenges this assumption. More than 20 cell types elaborate processes in the M6 layer and many of them directly contact R7 axons. R7 axons, however, selectively form synapses with only 5 target cell types and the vast majority of the synaptic connections are with one dominant partner Dm8. These data reveal a high level of wiring specificity at the synapse level that potentially contributes to specific functions.

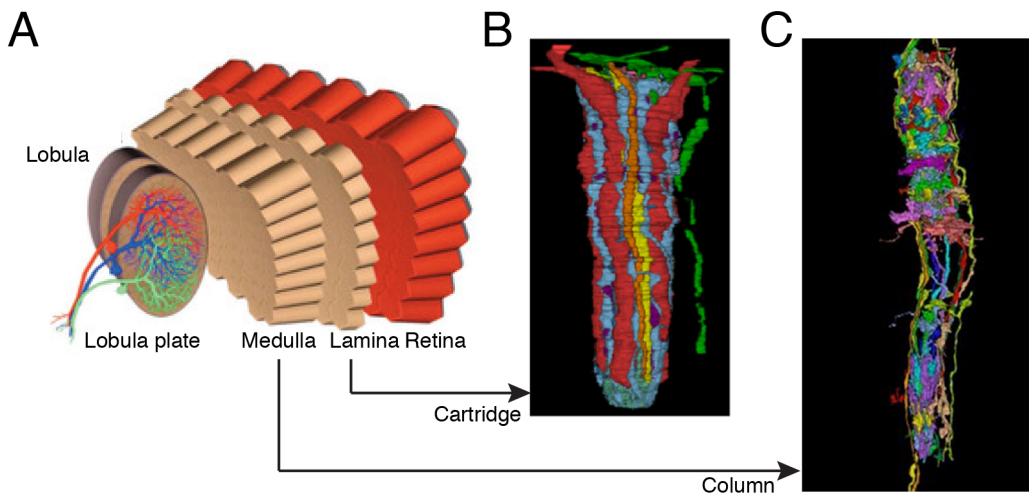

Figure 1-3 Three dimension SSEM reconstruction of the lamina cartridge and the medulla column

(A) Repetitive organization of the fly visual system, including the retina, the lamina and the medulla. (B-C) 3D SSEM reconstruction of one lamina cartridge (B) and one medulla column (C). Different colors represent neuronal processes of different cell types. Adapted from Matthews et al., 2003, Rivera-Alba et al., 2011 and Takemura et al., 2013.

EM studies have also demonstrated synaptic specificity in the mammalian nervous system. For example, combining serial block-face scanning electron microscopy (SB-SEM) and two-photon calcium imaging, Briggman and colleagues showed that in the direction-selectivity circuit of the mouse retina, the dendrites of mouse starburst amacrine cells (SACs) make highly specific synapses with direction-selective ganglion cells depending on the ganglion cell's preferred direction (Briggman et al., 2011). This work indicates that a wiring asymmetry contributes to the computation of direction selectivity.

The major limitation of the EM-based methods is that they are extremely time-consuming and labor-intensive. For instance, the state-of-the-art semi-automated pipeline developed by Chklovskii and colleagues to reconstruct the fly medulla connectome required ~14,400 person-hours in total in the steps of manually refining the SSEM dataset (Takemura et al., 2013). As a consequence, assessing variations of synaptic connections among cells of the same cell type and

between animals is problematic with EM. EM analysis of synaptic patterns at multiple developmental stages, in various mutant backgrounds or under different activity-modulated conditions is not feasible in most instances. In addition, the many steps of sample and data processing could introduce many artifacts into SS-TEM data, making it less biologically relevant to study dynamic processes like activity-dependent synaptic changes. These limitations have driven researchers to find more efficient ways to visualize synapses.

Two general directions have been taken to improve the efficiency of synapse visualization. The first direction is to further improve EM-based methods focusing on the efficiency.

The SB-SEM method used in the study of the mouse direction-selective circuit is one example of efforts towards this direction (Briggman and Bock, 2012). In this method, volume information equivalent to that from reconstructing thin serial sections is obtained when the sections are imaged before being cut, that is, by repeatedly imaging the block face using a scanning electron microscope (SEM). An automated microtome is used to shave off a 50nm-thick slice in between imaging sessions. This method does not provide resolution as high as SS-TEM because the slice thickness that a microtome can reliably cut without distorting the new surface for imaging is limited. Though it may not be sufficient yet to generate detailed connectomes, it did however allow a large enough volume to be imaged at sufficient resolution, which made it possible to study the directionality of presynaptic SAC dendrites and possibly other wiring problems in the CNS.

Along the same line, the focused ion beam with scanning electron microscopy (FIB-SEM) provides a solution to increase resolution (Kizilyaprak et al., 2014). A focused ion beam (a fine atomic beam with <10-nm diameter), instead of a microtome, is used to polish the surface of

biological samples. A sequence of fine polishing steps of 10 nm or less, each followed by imaging of each new surface, can give a stack of 3D data with isotropic resolution. Such continuous milling/imaging also gives excellent registration and avoids many of the defects, such as tears and folds associated with cutting the thin sections required for SS-TEM. However, this comes at the cost of slower imaging speeds. In addition, FIB-SEM technology has a smaller field of view when compared to SS-TEM, meaning a smaller volume can be imaged each time. Encouragingly, researchers at Janelia Research Campus have made improvements to the scalability of FIB-SEM, which allowed them to generate datasets encompassing more than 7 complete medulla columns with isotropic resolution and minimal imaging artifacts (personal communication).

Progress in synapse visualization with light microscopy

The second direction to improve the efficiency of synapse visualization is to develop tools that allow synapses be to imaged with light microscopy. This direction includes two aspects: the development of synaptic markers and the improvement of the microscopes.

Two approaches have been developed to label synapses with fluorescent molecules. The first involves targeted expression of fluorescently tagged synaptic proteins to label presynaptic and/or postsynaptic sites (Nonet, 1999; Wagh et al., 2006; Yeh et al., 2005; Zhang et al., 2002). This method is widely used across all systems, form worms to mammals. The tagged synaptic proteins are under the control of an enhancer/promoter sequence that ensures cell-type specific expression. Alternatively, the tagged synaptic proteins are under the control of a constitutive promoter but delivered to specific tissue by microinjection. These markers often serve as probes to detect changes in various aspects of synapse biology. For instance, Shen and colleagues employed a

cohort of fluorescently tagged synaptic proteins including Rab3::mCherry and SNB::YFP , specifically expressed in motor neuron DA9 in *C elegans* to demonstrate that Netrin/DCC and Wnt/Frizzled signaling negatively regulate the location of presynaptic sites in this neuron (Klassen and Shen, 2007; Poon et al., 2008). Time-lapse imaging of multiple tagged synaptic proteins co-expressed in developing neurons also provides important results regarding synapse assembly. The key observations described in the previous section of this introduction were only possible because of these tools. One major caveat of these tagged synaptic markers is that they are not typically expressed under the endogenous regulatory elements of the corresponding synaptic genes (i.e., enhancers, promoters, introns and 5' and 3' regions). As a result, the tagged synaptic proteins are often overexpressed and may accumulate non-specifically outside of actual synapses, causing labeling artifacts. In addition, exogenous regulatory elements do not reproduce the natural developmental expression of synaptic proteins and as a result, the observations made with these markers regarding the timing of synapse formation and the accumulation of key synaptic components might not accurately reflect the real sequence of events *in vivo*.

The second way to fluorescently label synapses relies on visualizing protein interactions across the synaptic cleft. In GFP Reconstitution Across Synaptic Partners (GRASP), these interactions are observed through the reconstitution of GFP fluorescence (Feinberg et al., 2008) (see Chapter 2). In this method, two complementary GFP fragments are fused to general or synaptically localized transmembrane proteins and expressed on the membrane of different neurons. The fragments can self-assemble into a fluorophore when in close vicinity to detect inter-neuronal contacts or synapses. This method has been used in worms, flies and mice for rapid detection of inter-neuronal contacts including synapses, which is particularly useful in circuit mapping (see

Chapter 2 for details) (Feinberg et al., 2008; Gordon and Scott, 2009; Kim et al., 2012; Yamagata and Sanes, 2012). However, in all organisms where GRASP is used, GRASP components are not expressed at the endogenous levels of the corresponding synaptic transmembrane proteins. In certain mature neurons, exogenous regulatory elements may be sufficient to produce fusion proteins (GRASP components) localized to synapses. In other cases, overexpressed split GFP fragments may accumulate in inappropriate intracellular locations and thus might not accurately reflect the location of synapses. It also may not be appropriate to use GRASP to follow synapse formation during development, as the timing of expression for each split GFP fragment was artificially determined by the expression drivers.

In addition to the development of fluorescent synaptic markers, innovations in optics and microscopy have also contributed tremendously to the visualization of synapses at the light level. Among those, the invention and application of super-resolution microscopy has been most exciting to the study of synapse biology.

Due to the diffraction of light, the resolution of conventional light microscopy is limited. A modern microscope with high numerical aperture usually reaches a resolution of ~250 nm, which is several times larger than the dimension of a chemical synapse. Super-resolution microscopy techniques use clever experimental techniques and known limitations on the matter being imaged to reconstruct a super-resolution image, thus allowing the capture of images with a higher resolution than the diffraction limit. Among the super resolution methods, stimulated emission depletion (STED) microscopy and stochastic optical reconstruction microscopy (STORM) have broad applications in synapse biology and their design principle and applications will be discussed here.

STED microscopy is a process that provides super resolution by selectively deactivating fluorophores to enhance the imaging in that area (Figure 1-4A and B) (Klar et al., 2000). In addition to the conventional laser beam that excites the fluorophores, a donut-shaped depletion laser beam is used to de-excite the peripheral fluorescence through stimulated emission, and thus only fluorescence emission from the sub-diffraction-limited center is left out to be collected. The resolution achieved by STED microscope in biological samples can reach 30-50nm. Stephan Sigrist and colleagues pioneered the work of using STED microscopy to study synapse assembly. Using antibodies against various synaptic proteins, Sigrist and colleagues analyzed the subcellular localization of several presynaptic proteins and subunits of the neurotransmitter receptors at the *Drosophila* neuromuscular junction (NMJ) (Fouquet et al., 2009). With resolution that was sufficient not only to resolve two different proteins at the same presynaptic site (e.g., BRP and Cac1 in Figure 1-4C) but also to resolve the N- and C-terminus of the same protein (e.g., BRP in Figure 1-4D), they successfully uncovered the molecular architecture of presynaptic sites at *Drosophila* NMJ.

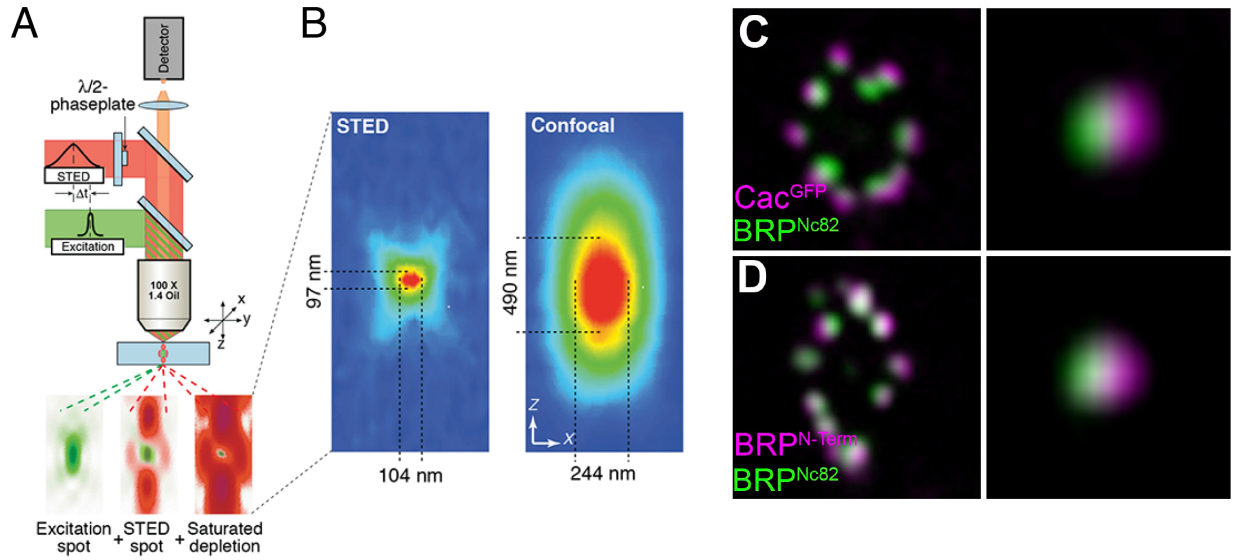

Figure 1-4 Design principles of STED Microscopy and using STED to dissect synapse composition

(A) Sketch of a point-scanning STED microscope. Excitation and STED are accomplished with synchronized laser pulses focused by a lens into the sample, sketched as green and red beams, respectively. Fluorescence is registered by a detector. Below, note the panels outlining the corresponding spots at the focal plane: the excitation spot (left) is overlapped with the STED spot featuring a central naught (center). Saturated depletion by the STED beam reduces the region of excited molecules (right) to the very zero point, leaving a fluorescent spot of subdiffraction dimensions shown in panel B. (B) Fluorescent spot in the STED and in the confocal microscope. The reduction in dimensions (x,y,z) yields an ultra small volume of subdiffraction size, corresponding to 6% of its confocal counterpart. (A-B) are adapted from Hell 2003. (C) Spatial relationship between presynaptic protein Bruchpilot (BRP) and Ca^{2+} channel (Cac1) at individual synapses is uncovered by STED imaging at *Drosophila* NMJ. Magenta, Cac^{GFP}; green, BRP recognized by C-terminus antibody Nc82. (D) Topology of the presynaptic protein BRP is uncovered by STED imaging using two BRP antibodies that recognize the N-terminus and C-terminus of this protein respectively. Magenta, $BRP^{N\text{-}term}$ (N-terminus); green, BRP^{Nc82} (C-terminus). (C-D) are adapted from Fouquet et al., 2009.

STORM acquires its high resolution based on single-molecule imaging of photo-switchable fluorescent probes (Rust et al., 2006). A typical STORM imaging experiment is often comprised of many imaging cycles (Figure 1-5). Within each cycle, only a sparse subset of fluorophores are activated, imaged and deactivated. The low density of the activated fluorophores allows the images of these fluorophores to be readily separated from each other. As a result, the position of each individual fluorophore can be determined to a precision substantially beyond the

diffraction-limited resolution. Iterating this procedure to obtain the localizations of many fluorophores then allows the reconstruction of a sub-diffraction-limit image from these localization points. Xiaowei Zhuang's group pioneered the work of using STORM to study synapses *in vivo*. Zhuang and colleagues have developed the multi-color 3D STORM technique and used it to determine key parameters, such as the axial positions, the orientation and radial (lateral) distribution of various synaptic proteins, in the molecular architecture of chemical synapses at mouse olfactory bulb (Dani et al., 2010). They were also able to use STORM to analyze the neurotransmitter receptor composition and plasticity within individual postsynaptic sites.

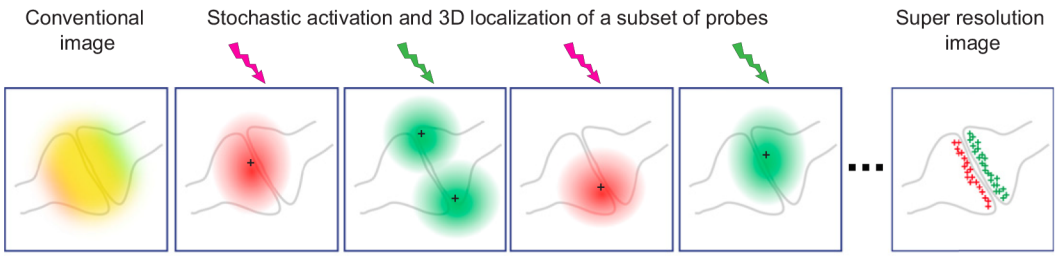

Figure 1-5 Schematic of three dimensional STORM

For molecules that give overlapping images (represented by the colored region in the left panel), STORM resolves these molecules by stochastically activating them at different times during image acquisition. At any time, only a sparse, optically resolvable subset of molecules are activated, allowing their images (represented by the red and green ellipsoids in the middle panels) to be separated from each other and their 3D positions (represented by the crosses in the middle panels) to be precisely determined from the centroid positions and ellipiticities of these images. Iteration of this process allows the positions of many molecules to be determined and a superresolution image to be reconstructed from these positions. Adapted from Dani et al., 2010.

STED microscopy and STORM have distinct advantages and limitations (Hell, 2003). STED offers very fast time resolution when imaging a small area. Impressive video-rate imaging has been achieved with STED, making it a particularly powerful approach for probing fast dynamics in small brain structures, such as a dendritic spine. As a point-scanning approach, the image

acquisition time of STED increases linearly with the sample volume. On the other hand, the single-molecule-localization based STORM is a wide-field imaging method that does not require scanning even for 3D imaging. This allows a large volume to be imaged in a short amount of time and enables relatively high-throughput analysis, though the imaging speed of STORM does not increase with decreasing sample volume as rapidly as STED. Second, unlike STORM, STED microscopy is a purely optical method that does not require any mathematical manipulation or image processing (which is necessary for STORM). It also requires minimal sample preparation and can even be used to image live cells. A drawback of STED microscopy is photobleaching, because in order to achieve high resolution, the power of the depletion laser beam is extremely high and causes more photobleaching.

At the current stage and in the near future, combining fluorescent synaptic markers and super-resolution fluorescence approaches like STED, STORM and others will provide powerful options for imaging synaptic structures in the brain with high resolution.

References

Biederer, T., Sara, Y., Mozhayeva, M., Atasoy, D., Liu, X., Kavalali, E.T., and Sudhof, T.C. (2002). SynCAM, a synaptic adhesion molecule that drives synapse assembly. Science 297, 1525-1531.

Briggman, K.L., and Bock, D.D. (2012). Volume electron microscopy for neuronal circuit reconstruction. Curr Opin Neurobiol 22, 154-161.

Briggman, K.L., Helmstaedter, M., and Denk, W. (2011). Wiring specificity in the direction-selectivity circuit of the retina. Nature 471, 183-188.

Chao, D.L., and Shen, K. (2008). Functional dissection of SYG-1 and SYG-2, cell adhesion molecules required for selective synaptogenesis in C. elegans. Mol Cell Neurosci 39, 248-257.

Christopherson, K.S., Ullian, E.M., Stokes, C.C., Mullowney, C.E., Hell, J.W., Agah, A., Lawler, J., Mosher, D.F., Bornstein, P., and Barres, B.A. (2005). Thrombospondins are astrocyte-secreted proteins that promote CNS synaptogenesis. Cell 120, 421-433.

Craig, A.M., and Kang, Y. (2007). Neurexin-neuroligin signaling in synapse development. Curr Opin Neurobiol 17, 43-52.

Dalva, M.B., Takasu, M.A., Lin, M.Z., Shamah, S.M., Hu, L., Gale, N.W., and Greenberg, M.E. (2000). EphB receptors interact with NMDA receptors and regulate excitatory synapse formation. Cell 103, 945-956.

Dani, A., Huang, B., Bergan, J., Dulac, C., and Zhuang, X. (2010). Superresolution imaging of chemical synapses in the brain. Neuron 68, 843-856.

de Wit, J., Hong, W., Luo, L., and Ghosh, A. (2011). Role of leucine-rich repeat proteins in the development and function of neural circuits. Annu Rev Cell Dev Biol 27, 697-729.

DeNardo, L.A., de Wit, J., Otto-Hitt, S., and Ghosh, A. (2012). NGL-2 regulates input-specific synapse development in CA1 pyramidal neurons. Neuron 76, 762-775.

Dityatev, A., Dityateva, G., and Schachner, M. (2000). Synaptic strength as a function of post- versus presynaptic expression of the neural cell adhesion molecule NCAM. Neuron 26, 207-217.

Dudanova, I., Tabuchi, K., Rohlmann, A., Sudhof, T.C., and Missler, M. (2007). Deletion of alpha-neurexins does not cause a major impairment of axonal pathfinding or synapse formation. J Comp Neurol 502, 261-274.

Eroglu, C., Allen, N.J., Susman, M.W., O'Rourke, N.A., Park, C.Y., Ozkan, E., Chakraborty, C., Mulinyawe, S.B., Annis, D.S., Huberman, A.D., *et al*. (2009). Gabapentin receptor alpha2delta-1

is a neuronal thrombospondin receptor responsible for excitatory CNS synaptogenesis. Cell 139, 380-392.

Feinberg, E.H., Vanhoven, M.K., Bendesky, A., Wang, G., Fetter, R.D., Shen, K., and Bargmann, C.I. (2008). GFP Reconstitution Across Synaptic Partners (GRASP) defines cell contacts and synapses in living nervous systems. Neuron 57, 353-363.

Fouquet, W., Owald, D., Wichmann, C., Mertel, S., Depner, H., Dyba, M., Hallermann, S., Kittel, R.J., Eimer, S., and Sigrist, S.J. (2009). Maturation of active zone assembly by Drosophila Bruchpilot. J Cell Biol 186, 129-145.

Friedman, H.V., Bresler, T., Garner, C.C., and Ziv, N.E. (2000). Assembly of new individual excitatory synapses: time course and temporal order of synaptic molecule recruitment. Neuron 27, 57-69.

Gerrow, K., Romorini, S., Nabi, S.M., Colicos, M.A., Sala, C., and El-Husseini, A. (2006). A preformed complex of postsynaptic proteins is involved in excitatory synapse development. Neuron 49, 547-562.

Glynn, M.W., Elmer, B.M., Garay, P.A., Liu, X.B., Needleman, L.A., El-Sabeawy, F., and McAllister, A.K. (2011). MHCI negatively regulates synapse density during the establishment of cortical connections. Nat Neurosci 14, 442-451.

Gomes, R.A., Hampton, C., El-Sabeawy, F., Sabo, S.L., and McAllister, A.K. (2006). The dynamic distribution of TrkB receptors before, during, and after synapse formation between cortical neurons. J Neurosci 26, 11487-11500.

Gordon, M.D., and Scott, K. (2009). Motor control in a Drosophila taste circuit. Neuron 61, 373-384.

Hell, S.W. (2003). Toward fluorescence nanoscopy. Nat Biotechnol 21, 1347-1355.

Henkemeyer, M., Itkis, O.S., Ngo, M., Hickmott, P.W., and Ethell, I.M. (2003). Multiple EphB receptor tyrosine kinases shape dendritic spines in the hippocampus. J Cell Biol 163, 1313-1326.

Hong, W., Mosca, T.J., and Luo, L. (2012). Teneurins instruct synaptic partner matching in an olfactory map. Nature 484, 201-207.

Kim, J., Zhao, T., Petralia, R.S., Yu, Y., Peng, H., Myers, E., and Magee, J.C. (2012). mGRASP enables mapping mammalian synaptic connectivity with light microscopy. Nature methods 9, 96-102.

Kizilyaprak, C., Daraspe, J., and Humbel, B.M. (2014). Focused ion beam scanning electron microscopy in biology. Journal of microscopy.

Klar, T.A., Jakobs, S., Dyba, M., Egner, A., and Hell, S.W. (2000). Fluorescence microscopy with diffraction resolution barrier broken by stimulated emission. Proc Natl Acad Sci U S A 97, 8206-8210.

Klassen, M.P., and Shen, K. (2007). Wnt signaling positions neuromuscular connectivity by inhibiting synapse formation in C. elegans. Cell 130, 704-716.

Ko, J., Kim, S., Chung, H.S., Kim, K., Han, K., Kim, H., Jun, H., Kaang, B.K., and Kim, E. (2006). SALM synaptic cell adhesion-like molecules regulate the differentiation of excitatory synapses. Neuron 50, 233-245.

Luthy, K., Ahrens, B., Rawal, S., Lu, Z., Tarnogorska, D., Meinertzhagen, I.A., and Fischbach, K.F. (2014). The irre Cell Recognition Module (IRM) Protein Kirre Is Required to Form the Reciprocal Synaptic Network of L4 Neurons in the Drosophila Lamina. J Neurogenet.

Margeta, M.A., Shen, K., and Grill, B. (2008). Building a synapse: lessons on synaptic specificity and presynaptic assembly from the nematode C. elegans. Curr Opin Neurobiol 18, 69-76.

Martinez, A., Alcantara, S., Borrell, V., Del Rio, J.A., Blasi, J., Otal, R., Campos, N., Boronat, A., Barbacid, M., Silos-Santiago, I., and Soriano, E. (1998). TrkB and TrkC signaling are required for maturation and synaptogenesis of hippocampal connections. J Neurosci 18, 7336-7350.

Mauch, D.H., Nagler, K., Schumacher, S., Goritz, C., Muller, E.C., Otto, A., and Pfrieger, F.W. (2001). CNS synaptogenesis promoted by glia-derived cholesterol. Science 294, 1354-1357.

McAllister, A.K. (2007). Dynamic aspects of CNS synapse formation. Annu Rev Neurosci 30, 425-450.

Meinertzhagen, I.A., and O'Neil, S.D. (1991). Synaptic organization of columnar elements in the lamina of the wild type in Drosophila melanogaster. J Comp Neurol 305, 232-263.

Meinertzhagen, I.A., Piper, S.T., Sun, X.-J., and Frohlich, A. (2000). Neurites morphogenesis of identified visual interneurons and its relationship to photoreceptor synaptogenesis in the flies, *Musca domestica* and *Drosophila melanogaster*. Euro J Neuro 2000, 1342-1356.

Millard, S.S., Lu, Z., Zipursky, S.L., and Meinertzhagen, I.A. (2010). Drosophila dscam proteins regulate postsynaptic specificity at multiple-contact synapses. Neuron 67, 761-768.

Nam, J., Mah, W., and Kim, E. (2011). The SALM/Lrfn family of leucine-rich repeat-containing cell adhesion molecules. Semin Cell Dev Biol 22, 492-498.

Nonet, M.L. (1999). Visualization of synaptic specializations in live C. elegans with synaptic vesicle protein-GFP fusions. J Neurosci Methods 89, 33-40.

Poon, V.Y., Klassen, M.P., and Shen, K. (2008). UNC-6/netrin and its receptor UNC-5 locally exclude presynaptic components from dendrites. Nature 455, 669-673.

Rivera-Alba, M., Vitaladevuni, S.N., Mishchenko, Y., Lu, Z., Takemura, S.Y., Scheffer, L., Meinertzhagen, I.A., Chklovskii, D.B., and de Polavieja, G.G. (2011). Wiring economy and

volume exclusion determine neuronal placement in the Drosophila brain. Curr Biol 21, 2000-2005.

Rust, M.J., Bates, M., and Zhuang, X. (2006). Sub-diffraction-limit imaging by stochastic optical reconstruction microscopy (STORM). Nature methods 3, 793-795.

Sabo, S.L., Gomes, R.A., and McAllister, A.K. (2006). Formation of presynaptic terminals at predefined sites along axons. J Neurosci 26, 10813-10825.

Sanes, J.R., and Yamagata, M. (2009). Many paths to synaptic specificity. Annu Rev Cell Dev Biol 25, 161-195.

Sara, Y., Biederer, T., Atasoy, D., Chubykin, A., Mozhayeva, M.G., Sudhof, T.C., and Kavalali, E.T. (2005). Selective capability of SynCAM and neuroligin for functional synapse assembly. J Neurosci 25, 260-270.

Shen, K., and Bargmann, C.I. (2003). The immunoglobulin superfamily protein SYG-1 determines the location of specific synapses in C. elegans. Cell 112, 619-630.

Shen, K., Fetter, R.D., and Bargmann, C.I. (2004). Synaptic specificity is generated by the synaptic guidepost protein SYG-2 and its receptor, SYG-1. Cell 116, 869-881.

Takemura, S.Y., Bharioke, A., Lu, Z., Nern, A., Vitaladevuni, S., Rivlin, P.K., Katz, W.T., Olbris, D.J., Plaza, S.M., Winston, P., *et al*. (2013). A visual motion detection circuit suggested by Drosophila connectomics. Nature 500, 175-181.

Takemura, S.Y., Lu, Z., and Meinertzhagen, I.A. (2008). Synaptic circuits of the Drosophila optic lobe: the input terminals to the medulla. J Comp Neurol 509, 493-513.

Varoqueaux, F., Aramuni, G., Rawson, R.L., Mohrmann, R., Missler, M., Gottmann, K., Zhang, W., Sudhof, T.C., and Brose, N. (2006). Neuroligins determine synapse maturation and function. Neuron 51, 741-754.

Vicario-Abejon, C., Collin, C., McKay, R.D., and Segal, M. (1998). Neurotrophins induce formation of functional excitatory and inhibitory synapses between cultured hippocampal neurons. J Neurosci 18, 7256-7271.

Wagh, D.A., Rasse, T.M., Asan, E., Hofbauer, A., Schwenkert, I., Durrbeck, H., Buchner, S., Dabauvalle, M.C., Schmidt, M., Qin, G., *et al*. (2006). Bruchpilot, a protein with homology to ELKS/CAST, is required for structural integrity and function of synaptic active zones in Drosophila. Neuron 49, 833-844.

Washbourne, P., Bennett, J.E., and McAllister, A.K. (2002). Rapid recruitment of NMDA receptor transport packets to nascent synapses. Nat Neurosci 5, 751-759.

White, J.G., Southgate, E., Thomson, J.N., and Brenner, S. (1986). The structure of the nervous system of the nematode Caenorhabditis elegans. Philos Trans R Soc Lond B Biol Sci 314, 1-340.

Yamagata, M., and Sanes, J.R. (2012). Transgenic strategy for identifying synaptic connections in mice by fluorescence complementation (GRASP). Frontiers in molecular neuroscience 5, 18.

Yamagata, M., Sanes, J.R., and Weiner, J.A. (2003). Synaptic adhesion molecules. Curr Opin Cell Biol 15, 621-632.

Yeh, E., Kawano, T., Weimer, R.M., Bessereau, J.L., and Zhen, M. (2005). Identification of genes involved in synaptogenesis using a fluorescent active zone marker in Caenorhabditis elegans. J Neurosci 25, 3833-3841.

Zhang, Y.Q., Rodesch, C.K., and Broadie, K. (2002). Living synaptic vesicle marker: synaptotagmin-GFP. Genesis 34, 142-145.

Chapter 2 Adapting GFP Reconstitution Across Synaptic Partners (GRASP) in *Drosophila melanogaster*

Abstract

The "GFP reconstitution across synaptic partners" (GRASP) method was originally developed in *C elegans*. In this method, non-fluorescent fragments of GFP are expressed in two different cells; the fragments self-assemble at cell-cell contact between the two to form a fluorophore. Using transmembrane synaptic proteins to localize GFP fragments to presynaptic and/or postsynaptic sites, GRASP has proven useful for light microscopic identification of synapses in *C elegans* and mice, but has not yet been fully applied to *Drosophila melanogaster*, which is a great model system to test gene function. I adapted GRASP to mark synapses in *Drosophila* by optimizing transmembrane split-GFP carriers for *Drosophila* synapses. I demonstrate that the modified GRASP can mark synaptic connections between synaptic partners in the fly visual system. This adapted GRASP system was also used to successfully map neuronal connections in the circuit underlying fly mating behavior. While the adapted GRASP in *Drosophila* is useful in certain contexts, the intrinsic caveat originated from the overexpression of GRASP components has limited its applications.

Introduction

The "GFP reconstitution across synaptic partners" (GRASP) method was first developed in *C elegans* by Bargmann and colleagues to mark synapses between partner neurons (Feinberg et al., 2008). It is based on the proximity of the presynaptic and the postsynaptic plasma membranes. In CNS synapses, the membranes of two synaptic partners are typically

separated by less than 100 nm of extracellular space, a distance that can be spanned by transmembrane proteins expressed by the two cells. Proximity of two opposing membranes is detected by the stable, extracellular assembly of the GFP from two complementary fragments (i.e. spGFP1-10 and spGFP11) expressed on different cells, in the context of transmembrane protein carriers that are either broadly distributed on the plasma membrane or narrowly localized to synaptic regions. The large spGFP1-10 fragment contains the first 214 residues or 10 of the 11 strands of the beta-barrel structure of the exceptionally stable 'superfolder' GFP protein (Pedelacq et al., 2006). The small spGFP11 fragment consists of just 16 residues, which make up the 11th strand of the GFP beta-barrel. Each of these fragments is soluble, nonfluorescent, and relatively inert in the absence of its complementary fragment but the two fragments can self-assemble into a full-length GFP that fluoresce when in close proximity. Human T-cell protein CD4 is used as the general membrane carrier for spGFP fragments to detect cell-cell contacts. PTP3A, a member of the LAR/receptor tyrosine phosphatase family, is used as a carrier to localize the spGFP fragment to presynaptic sites while Neuroligin is used as the carrier to localize the spGFP fragments to both presynaptic and postsynaptic sites (Figure 2-1). Using these different carriers, GRASP can be used to assess nearest neighbors across the cell membrane or the nearest neighbors at a synapse.

Bargmann and colleagues demonstrated the effectiveness of GRASP *in vivo* using the defined connectivity of the *C elegans* nervous system as a guide and demonstrated that GRASP could detect synapses between known synaptic partners, identify synaptic defects in mutants where normal synaptic connections were disrupted, and uncover previously uncharacterized details of synaptic locations.

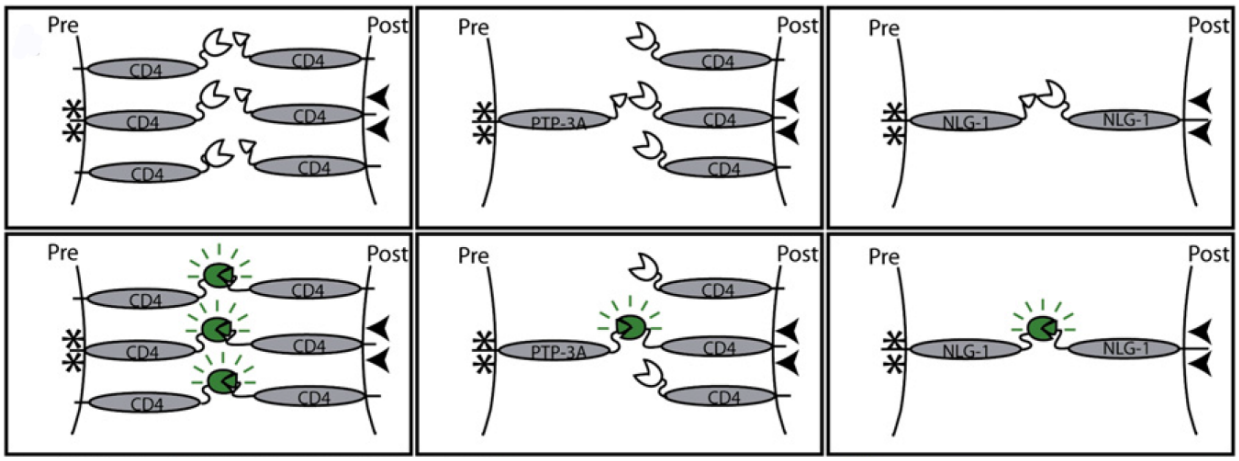

Figure 2-1 Schematic diagram of GRASP in C elegans

GRASP with delocalized CD4 tethers (left), presynaptically localized PTP- 3A and a delocalized CD4 tether (center), and pre- and postsynaptically localized NLG-1 tethers (right). Asterisk symbolizes presynaptic site; arrowhead, postsynaptic site (Adapted from Feinberg et al., 2008).

The design principal of GRASP is generalizable and it has been adapted to other model organisms. Two groups implemented GRASP in mice (hence named mGRASP) using slightly different genetic methods. Both groups found that mouse Neurexin (Nrx) and Neuroligin (Nlg) were effective tethers for the splitGFP fragments in presynaptic and postsynaptic cells, respectively. Yamagata and Sanes used a transgenic strategy to express the split GFP fragments and demonstrated that mGRASP could label rod photoreceptor synapses in the outer plexiform layer of the mouse retina (Yamagata and Sanes, 2012). In the other study, Kim et al used a viral strategy to achieve targeted expression of mGRASP components in selected presynaptic and postsynaptic neurons in the mouse hippocampus (Kim et al., 2012). Importantly, they accessed mGRASP signal both between a pair of synaptic partners and between a pair of neurons that form non-synaptic axo-dendritic contacts. And the results indicated that mGRASP detected synapses rather than neurite touches in this system. A major advantage of the viral strategy is that it provides more

temporal and spatial control on the expression of mGRASP components compared to the transgenic strategy, but at the same time it is technically difficult and invasive to the animals.

The adaptation of GRASP to *Drosophila* turned out to be surprisingly difficult, despite that many genetic tools are available in this model organism. Gordon and Scott first adapted GRASP into *Drosophila* using Gal4-UAS and LexA-LexAoP systems for targeted expression of two split GFP fragments in distinct cell populations (Gordon and Scott, 2009). In their work, both split GFP fragments were tethered to general transmembrane protein CD4. As a result, this version of fly GRASP does not selectively detect synapses but detects any cell-cell contacts. Despite of its limitations, this method still provided useful information regarding potential neuronal connections in certain circuits; such as the circuits underlying fly taste preference (Gordon and Scott, 2009). However, due to the lack of well-characterized transmembrane molecules that specifically localized to synapses as carriers for spGFP fragments, the implementation of GRASP in flies to selectively label synapses remains unsatisfying. Thus in this study, we adapted GRASP to *Drosophila* to label synapses between specific neurons by using different synaptically localized transmembrane proteins as carriers for the spGFP fragments. We demonstrated that the adapted GRASP could label synapses between synaptic partners in the fly visual system. The adapted GRASP also facilitated mapping of the neural circuit underlying interspecies mating. However, in certain circuits of the visual system, the adapted GRASP failed to distinguish synapses from general cell-cell contacts possibly due to the overexpression nature of this labeling method.

Results

Generation of presynaptic GRASP components in *Drosophila*

To generate a GRASP system that selectively marks synapses in *Drosophila*, at least one of the two spGFP-tethering proteins should be localized to synaptic regions. In order to specifically target spGFP1-10 to presynaptic sites, a few presynaptic transmembrane molecules were tested as "tethers". These "tethers" include true transmembrane molecules Neurexin1 (Nrx1) and Lar, as well as an artificial "fusion" transmembrane molecule RIM-TM (Figure 2-2).

Neurexins (Nrxs) have been proposed to regulate the differentiation and function of presynaptic sites in both vertebrates and flies, through the trans-synaptic interaction with their binding partner Neuroligins (Li et al., 2007; Zeng et al., 2007). spGFP 1-10::Nrx1 was generated by inserting the large spGFP1-10 fragment immediately after the signal peptide from the *C elegans pat3* gene followed by full-length Nrx1 minus the first 57 amino acids, which encodes the endogenous signal peptide of Nrx1. Similarly, receptor protein tyrosine phosphatase Lar has also been shown to regulate presynaptic development in a few model organisms including *Drosophila* (Kaufmann et al., 2002). spGFP1-10::Lar was generated in a similar fashion as spGFP1-10::Nrx1 with the full-length Lar minus the endogenous signal peptide.

RIM is a conserved cytosolic protein that has been shown to localize to presynaptic sites at *Drosophila* neuromuscular junction and recruit other synaptic components during synapse assembly (Graf et al., 2012). I generated the artificial transmembrane molecule RIM-TM by fusing full-length RIM with the transmembrane domain and the first two extra-cellular Ig domains of the CD4 protein. The RIM-TM fragment was then inserted downstream of the pat3 signal peptide followed by spGFP1-10, resulting in spGFP1-10::RIM-TM.

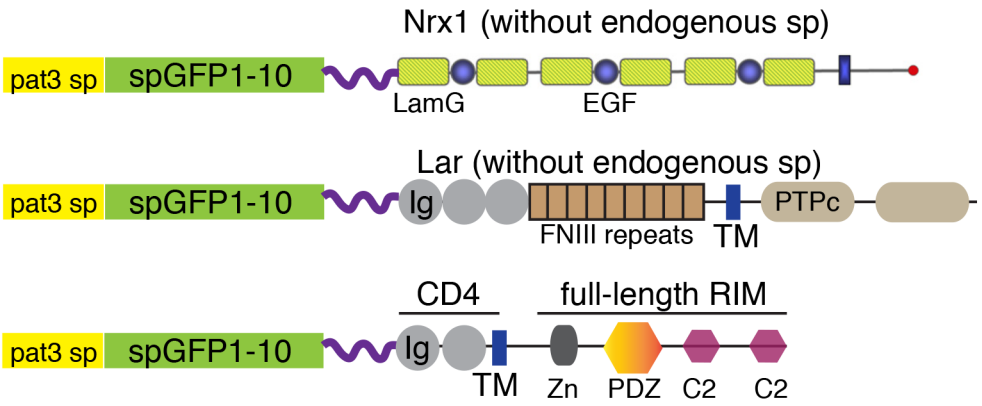

Figure 2-2 Generating presynaptic GRASP components in Drosophila

Representative domains for Nrx1, Lar and RIM-TM are indicated. sp, signal peptide; purple curve, Glycine-Serine linker.

All three potential presynaptic GRASP components were then placed under the control of the UAS sequence, which allows them to be expressed in specific neurons using cell-type specific Gal4 drivers. These three UAS constructs were first transfected into *Drosophila* Schneider 2 (S2) cells to confirm their cell surface expression with an antibody (Ab290) that recognizes fragment spGFP1-10 (Gordon and Scott, 2009). All three constructs and the positive control (UAS-spGFP1-10::CD4) were expressed on the S2 cell surface determined by the positive Ab290 staining without membrane permeablization (Figure 2-3). These constructs were then introduced into fly genome as transgenes.

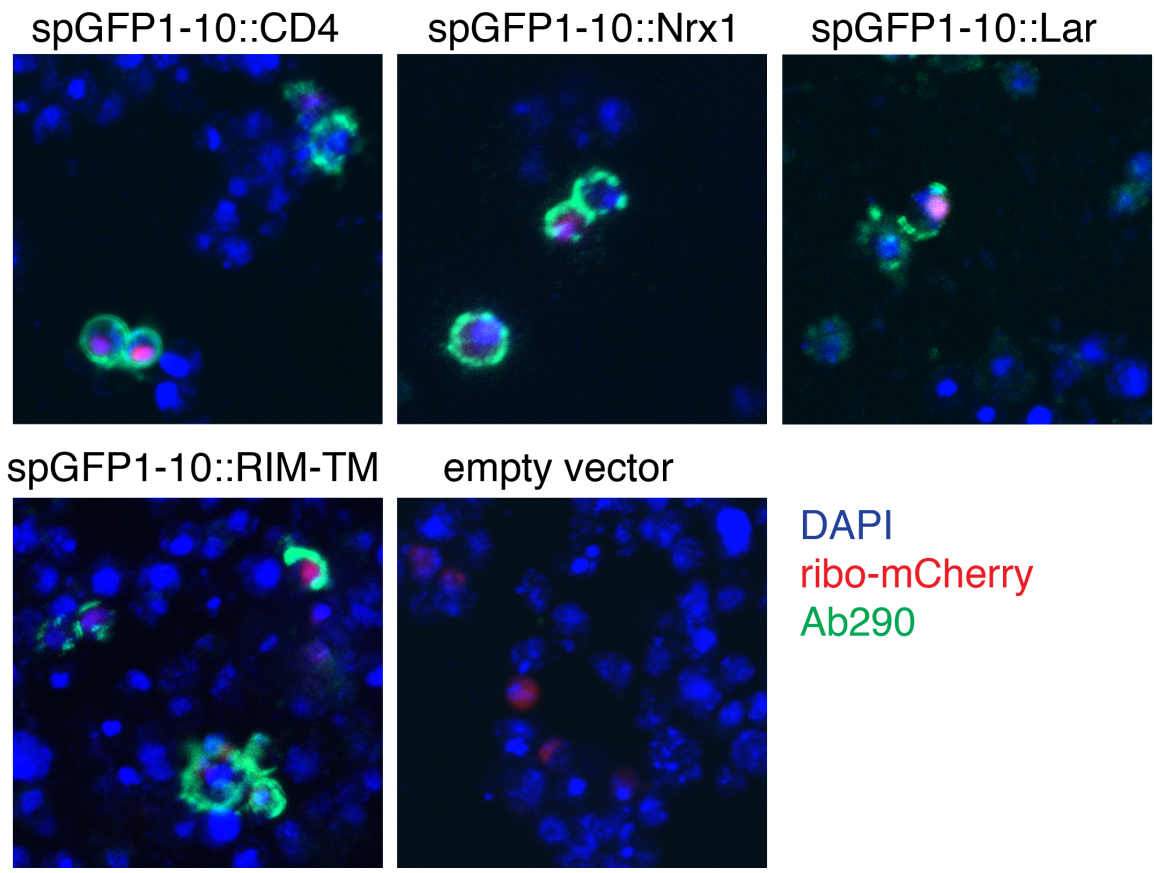

Figure 2-3 Testing the expression of GRASP components in S2 cells

In all panels, the corresponding GRASP construct was co-transfected into S2 cells with a ribosomal marker (ribo-mCherry) and a Cu^{2+}-inducible Gal4 construct that activates the expression of the corresponding GRASP component under UAS control.

GRASP with Nrx1 and CD4 specifically marks synapses between synaptic partners

The initial GRASP study in *C elegans* has shown that localizing one spGFP fragment to the presynaptic sites was sufficient to selectively mark synapses between synaptic partners even when the other spGFP fragment was uniformly localized on the postsynaptic cell surface (Feinberg et al., 2008).

Therefore, we paired the spGFP1-10 tethered to the three different carriers (Nrx1, Lar and

RIM-TM) in presynaptic neurons with the spGFP11::CD4 in the postsynaptic neurons and assess if they can selectively label synapses between synaptic partners, respectively. The spGFP1-10::Nrx1/Lar/RIM-TM was expressed in presynaptic neurons via Gal4-UAS system, while the spGFP11::CD4 was expressed in postsynaptic neurons via LexA-LexAoP system.

We first tested these pairs between presynaptic L3 neurons and postsynaptic Tm9 neurons. Axons of the L3 lamina monopolar neurons specifically target to the M3 layer in the medulla and form synapses onto dendrites of Tm9 neurons in that layer (Figure 2-4A). Dendrites of Tm9 neurons span several layers (M2-M4), but only receive L3 inputs in M3. When we expressed spGFP1-10::Nrx1 or spGFP1-10::RIM-TM in L3 and spGFP11::CD4 in Tm9, respectively, we observed reconstituted native GFP fluorescence only in the M3 layer, suggesting these GRASP pairs selectively label L3-Tm9 synapses (Figure 2-4B). When we expressed spGFP1-10::Lar in L3 and spGFP11::CD4 in Tm9, reconstituted native GFP fluorescence was observed in the M3 layer but in a stochastic fashion (Figure 2-4B). The stochastic pattern of reconstituted GFP suggests that spGFP1-10::Lar may not reliably localize to the presynaptic sites in all the L3 neurons, therefore we decided to instead focus on spGFP1-10:: Nrx1 and spGFP1-10::RIM-TM in subsequent experiments.

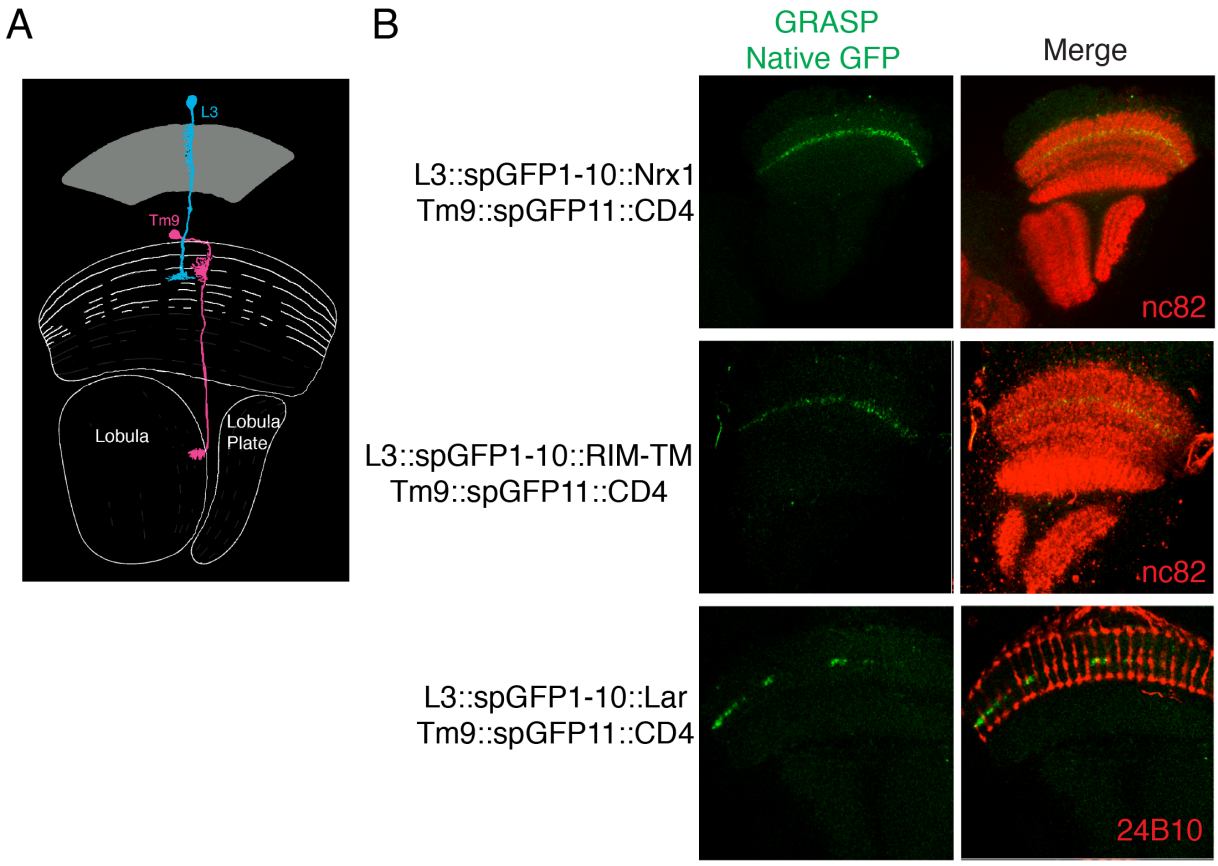

Figure 2-4 GRASP with Nrx1/RIM-TM and CD4 mark synapses between L3 and Tm9 neurons

(A) Schematic showing a single L3 neuron and a single Tm9 neuron. Note that there are approximately 800 pairs of L3 and Tm9 in the medulla but only one pair is shown in this schematic. (B) GRASP between L3 and Tm9 with three different presynaptic components. The reconstituted GFP fluorescence was concentrated in a single band in the M3 layer in the medulla.

In addition to L3 neurons, photoreceptor neurons R8 have also been reported to form synapses onto Tm9 dendrites in the medulla, though the number of synapses is far fewer than L3-Tm9 synapses (Gao et al., 2008). We tested if our GRASP system with Nrx1 or RIM-TM could detect synapses between R8 axons and Tm9 dendrites. As a negative control, we expressed the GRASP components in R7 axons and Tm9 dendrites, respectively (Figure 2-5). According to SS-TEM studies, R7 axons do not form synapses with Tm9 dendrites, though they do have membrane contacts (Takemura et al., 2013). If our GRASP system specifically detects synapses, we would expect to observe robust GFP fluorescence between the R8-Tm9

pair but little or no fluorescence between the R7-Tm9 pair. And this was indeed the case for Nrx1. In the R8-Tm9 pair, many GFP fluorescent puncta were detected in the M2 and M3 layer of the medulla. In contrast, few GFP fluorescent puncta were seen between R7-Tm9 pairs, supporting the labeling specificity of our GRASP system. To confirm that these two pairs of neurons have similar general membrane contacts, we used the GRASP system in which both spGFP fragments were tethered to CD4 in these two pairs. Indeed, similar intensity and area of GFP fluorescence was observed between the R8-Tm9 pair and the R7-Tm9 pair. Together, these results suggest that the GRASP system with Nrx1 can specifically label synaptic contacts between synaptic partners.

In contrast, when the spGFP1-10::RIM-TM was expressed in R7 neurons and spGFP11::CD4 was expressed in Tm9 neurons, substantial GFP fluorescence was detected in the medulla(Figure 2-5). This indicated that the GRASP system with RIM-TM marked non-synaptic cell-cell contacts and thus failed to specifically mark synapses between synaptic partners.

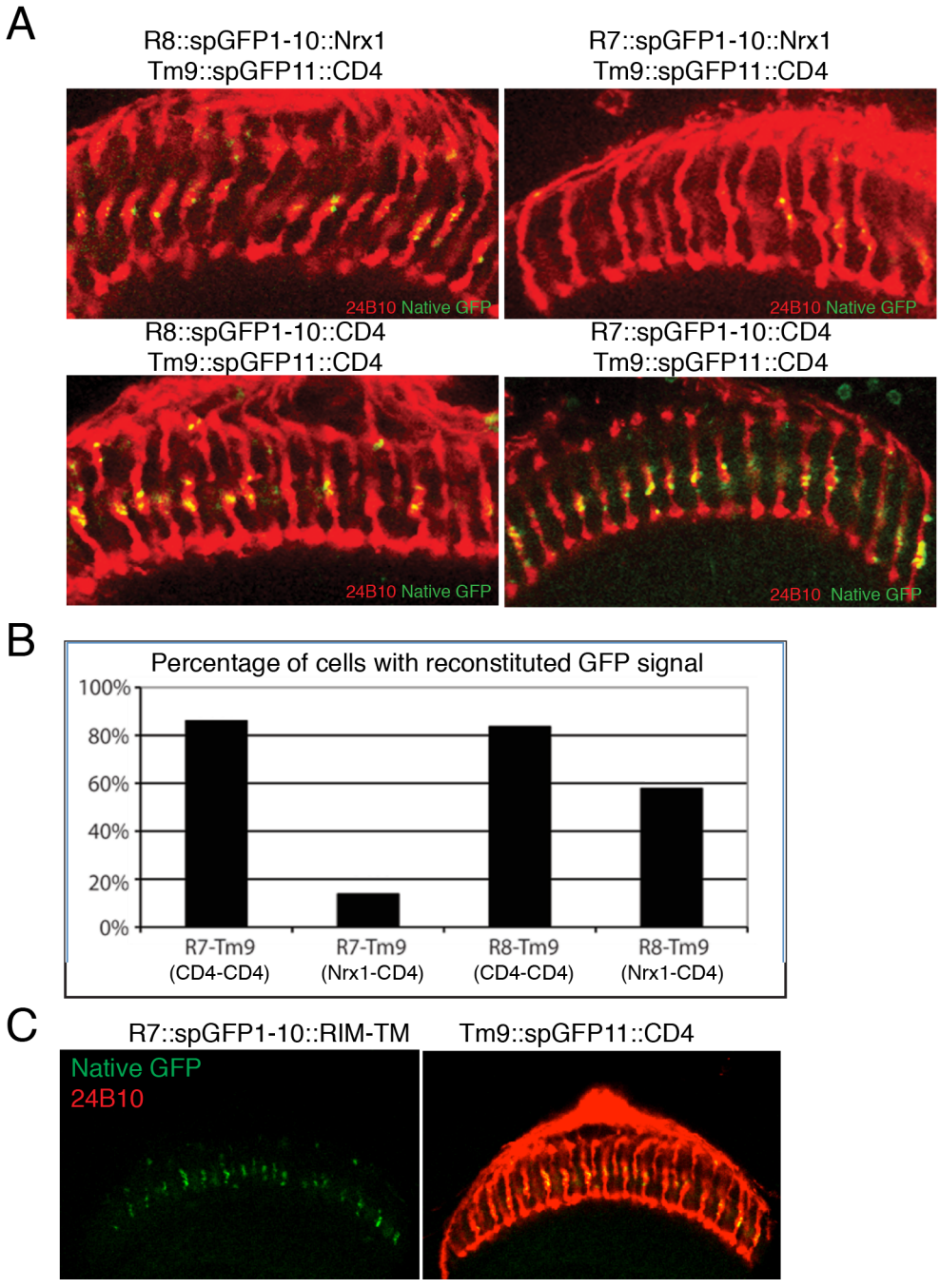

Figure 2-5 GRASP with Nrx1-CD4 specifically mark synapses between synaptic partners

(A) GRASP with Nrx1 and CD4 selectively label synapses between R8-Tm9 neurons but not between non-synaptic pair R7-Tm9. GRASP with CD4-CD4 does not distinguish R8-Tm9 and R7-Tm9. (B) Percentage of the R7-Tm9 or R8-Tm9 pairs labeled by Nrx1-CD4 GRASP and CD4-CD4 GRASP. GRASP with Nrx1-CD4 preferentially labels synaptic partners. (C) Significant reconstituted GFP is observed between non-synaptic pair R7-Tm9 when the presynaptic GRASP carrier is RIM-TM.

Mapping the neural circuit underlying *Drosophila* mating behavior using GRASP

A species can be defined as a set of organisms that share a gene pool and breed with each other (Dobzhansky, 1937; Mayr et al., 1988). The lack of interspecies breeding results from mechanisms that promote breeding with conspecifics and those that interpose a reproductive barrier between species (Coyne and Orr, 1998). Despite the prevalence of behavioral reproductive isolation and its importance to evolution, the neural pathways that suppress interspecies courtship are poorly understood.

In a recent study, Shah and colleagues sought to identify male *D. melanogaster* sensory structures that inhibit courtship with other drosophilids (Fan et al., 2013). They find that the chemoreceptor Gr32a inhibits male *D. melanogaster* from courting diverse fruit fly species. Gr32a recognizes nonvolatile aversive cues present on these reproductively dead-end targets, and activity of Gr32a neurons is necessary and sufficient to inhibit interspecies courtship. Male-specific Fruitless (FruM), a master regulator of courtship, also inhibits interspecies courtship.

Since Gr32a and FruM are not co-expressed in the same neuronal populations, it is likely that FruM neurons and Gr32a neurons are in a shared neural circuit that inhibit interspecies courtship. To test this hypothesis, through a collaborative effort, we tested whether Gr32a neurons might contact FruM neurons using GRASP with Nrx1. spGFP1-10::Nrx1 was expressed in Gr32a neurons using Gr32a-Gal4 and spGFP11::CD4 was expressed in FruM neurons using Fru-LexA. In the experimental flies, native GFP fluorescence in the ventral nerve cord (VNC) and the subesophageal ganglion (SOG) was observed (Figure 2-6), locations at which tarsal sensory neurons synapse with central neurons (Dunipace et al.,

2001; Scott et al., 2001; Stocker, 1994). Such GRASP signal suggests synaptic contact between Gr32a and FruM neurons though further verification with EM is needed. Removal of foreleg tarsi eliminated native GFP fluorescence in the VNC and the vertical limb of innervation in the SOG (Figure 2-6), demonstrating that these contacts with FruM neurons emanated from foreleg Gr32a neurons (Wang et al., 2004). The residual GRASP fluorescence in the SOG is consistent with projections of proboscis Gr32a neurons. These results are consistent with the notion that Gr32a and FruM function within a shared neural circuit to inhibit interspecies courtship. This example demonstrates that GRASP with Nrx1 can facilitate circuit mapping.

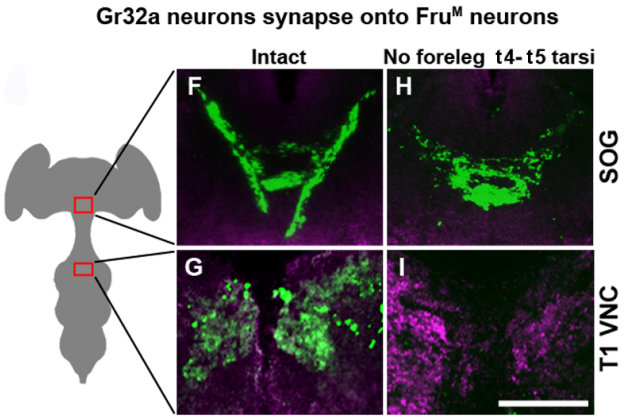

Figure 2-6 GRASP shows that FruM neurons connect with Gr32a neurons to inhibit interspecies courtship

Left, Schematic of the fly central nervous system shows the location of the SOG and first thoracic segment (T1) VNC (red boxes). Right, native GRASP fluorescence (green) in the vertical limb of the SOG and the T1 VNC in *D. melanogaster* males (Gr32a:spGFP1-10::Nrx, frulex:spGFP11::CD4) is lost upon T1 tarsectomy. The neuropil (magenta) is immuno-labeled with nc82. Adapted from Fan et al., 2013.

GRASP with Nrx1 still labels non-synaptic contacts in some contexts

To test if the GRASP system with Nrx1 can be used as a universal tool to detect synaptic

contacts throughout the visual system, we tested it in more pairs of neurons including both synaptic partners and non-partners and characterized its labeling accuracy.

One good circuit to test the labeling specificity of GRASP is the L1-L2-L4 circuit in the lamina. Lamina monopolar neuron L1 and L2 are the major second-order neurons receiving direct synaptic inputs from R1-R6 photoreceptor neurons (Rivera-Alba et al., 2011). The dendrites of L1 and L2 are virtually indistinguishable in terms of morphology and location within each lamina cartridge (Figure 2-7A). Intriguingly, L2 dendrites form reciprocal synapses with L4 dendrites, meaning that L2 dendrites is presynaptic to L4 dendrites and vice versa. In sharp contrast, L1 dendrites form few synapses with L4, according to the SS-TEM studies (Figure 2-7A). Although the molecular basis for the differences in synaptic specificity between L2-L4 and L1-L4 has not been fully characterized, it provides an excellent and stringent test for the labeling specificity of GRASP with Nrx1-CD4.

We first confirmed that both L2-L4 and L1-L4 had large area of membrane contact using the GRASP system with CD4-CD4 (Figure 2-7B). Next, we expressed spGFP1-10::Nrx1 in L4 neurons with L4-Gal4, and spGFP11::CD4 in L1 or L2 neurons with L1- or L2-LexA respectively and compared the reconstituted GFP fluorescence between these two pairs. To our disappointment, although the fluorescent intensity is lower between the L1-L4 pair compared to the L2-L4 pair, there was still significant reconstituted GFP fluorescence between L1 and L4, suggesting that the GRASP system with Nrx1 labeled non-synaptic contacts (background) in addition to synaptic contacts (Figure 2-7C).

Several reasons could account for this non-specific labeling problem. The most likely reason is that the spGFP1-10::Nrx1 is over-expressed in L4 neurons. High expression level is

common for the Gal4-UAS mediated expression. When spGFP1-10::Nrx1 is expressed at much higher level than the endogenous Nrx1 in L4 neurons, excessive spGFP1-10::Nrx1 becomes mislocalized outside of presynaptic sites. These non-synaptic spGFP1-10:Nrx1 reconstitutes with the spGFP11::CD4 distributed uniformly on the postsynaptic neuron, causing GFP fluorescence to be detected outside of synapses. While the expression level of spGFP1-10::Nrx1 depends on the strength of the Gal4 driver, the issue of non-specific labeling also varies among different cells. This is possibly why GRASP with Nrx1 showed decent labeling specificity between L3-Tm9 and R8-Tm9 pairs but not between L1-L4.

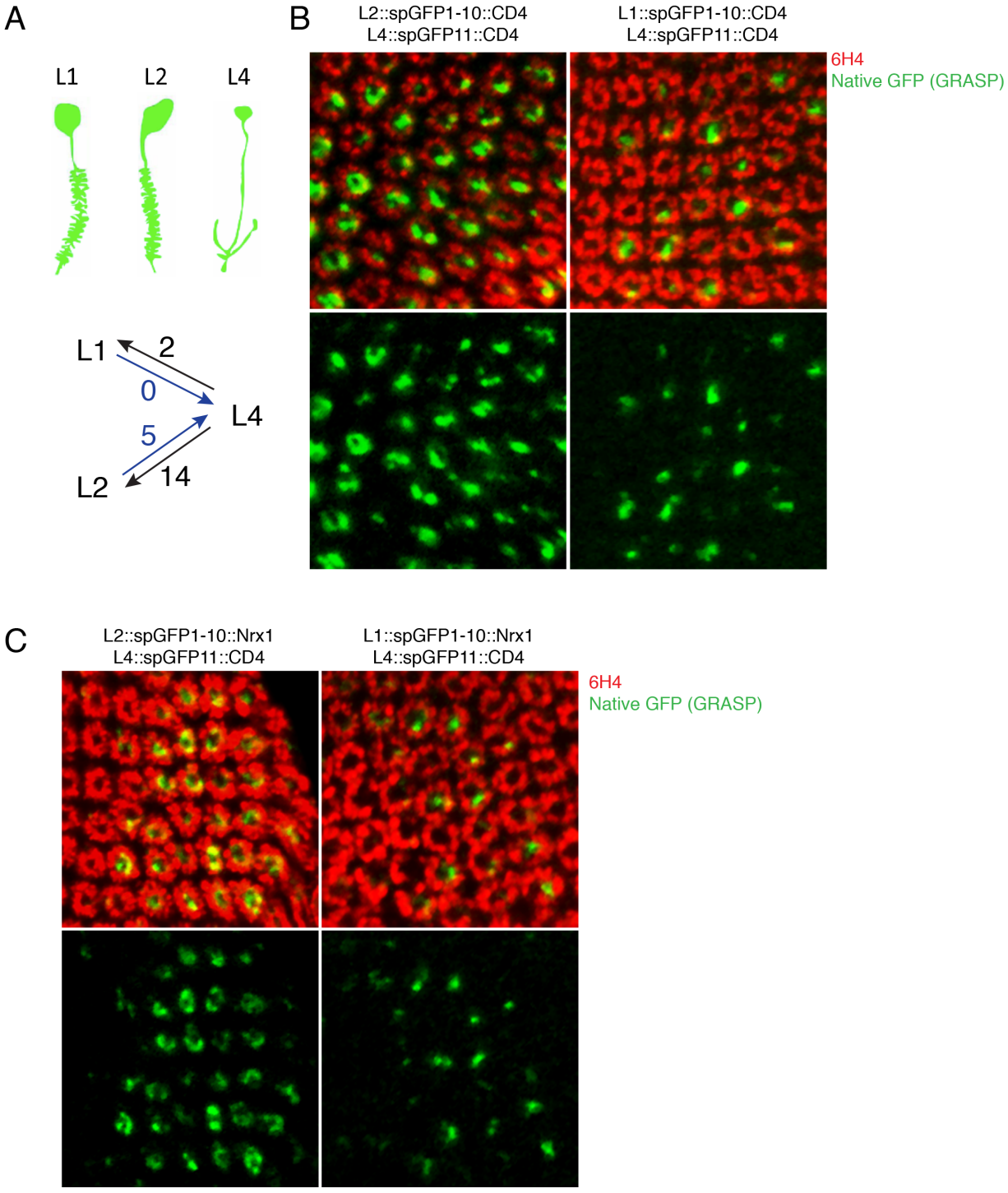

Figure 2-7 GRASP with Nrx1-CD4 fail to distinguish synapses from non-synaptic contacts in the L1-L2-L4 circuit

(A) Schematic showing the morphology of L1, L2 and L4 neurons in the lamina (top) and number of synapses between each pair (bottom). Each arrow points from presynaptic cell to postsynaptic cell. The number on the arrow indicates number of synapses mapped by the most recent EM study

(Rivera-Alba et al., 2011). (B) GRASP with CD4-CD4 detects membrane contacts between each pair (L2-L4 and L1-L4). Images show the cross-section view of the lamina. Green, reconstituted GRASP fluorescence; red, 6H4 antibody labels lamina cartridges. (C) GRASP with Nrx1-CD4 shows significant reconstituted GFP fluorescence between synaptic pair L2-L4 but also between non-synaptic pair L1-L4. Images show the cross-section view of the lamina. Green, reconstituted GRASP fluorescence; red, 6H4 antibody labels lamina cartridges.

Generating a postsynaptic GRASP component to increase labeling specificity

One way to increase labeling specificity of GRASP is to also restrict the spGFP11 fragment to postsynaptic sites in addition to the presynaptically restricted spGFP1-10. One obvious candidate transmembrane tether to attach to spGFP11 is Neuroligin (Nlg), the trans-synaptic binding partner of Nrx1. There are two characterized Neuroligins in *Drosophila*, Nlg1 and Nlg2. Both of them have been shown to play a role in regulating synapse maturation and function through binding with Nrx1 at larval neuromuscular junction (Banovic et al., 2010; Sun et al., 2011). Only Nlg2 is expressed in the fly CNS, according to results of in situ hybridization analysis (Banovic et al., 2010). Therefore, I focused on Nlg2 and generated a postsynaptic GRASP component by inserting the spGFP11 tag immediately after the pat3 signal peptide followed by full-length Nlg2 minus the first 34 amino acids (Nlg2 endogenous signal peptide) (Figure 2-8A). The *spGFP11::Nlg2* fusion sequence was then placed downstream of the LexAoP element.

We first tested whether the combination of spGFP1-10::Nrx1 and spGFP11::Nlg2 can label synapses between L3-Tm9 synaptic pairs. To our surprise, no reconstituted GFP fluorescence was detected with this combination (data not shown). The same results were seen in other synaptic partner pairs. We suspected that the LexAoP-spGFP11::Nlg2 was not expressed properly in the postsynaptic neurons. However, due to a lack of Nlg2 antibody and antibody that recognizes the small GFP fragment spGFP11, we were not able to confirm our suspicion.

Alternative transmembrane tethers for the spGFP11 fragment in the postsynaptic neurons are the neurotransmitter receptors. Different cell types utilized different neurotransmitters and their postsynaptic partners express the corresponding neurotransmitter receptors. It is therefore not possible to use one receptor as the universal carrier for spGFP proteins in all postsynaptic neurons. To start, we focused on the photoreceptor synapses, which are histaminergic. Therefore, histamine receptors are good candidates to localize spGFP11 to the postsynaptic sites in photoreceptor target neurons. Two genes encode histamine receptors in *Drosophila*, *HisCl1* (*Ort*) and *HisCl2*, and both are histamine-gated chloride channels (Pantazis et al., 2008). In situ hybridization analysis has shown that Ort is expressed in the neurons while HisCl2 is expressed in the glia (Witte et al., 2002). Function rescue experiments have demonstrated that *Ort* encodes the functional histamine receptor that is both necessary and sufficient in neurons to mediate synaptic transmission in the visual system (Gao et al., 2008). We therefore generated a postsynaptic GRASP component by inserting the spGFP11 fragment immediately after the pat3 signal peptide followed by full-length Ort minus the first 36 amino acids (Ort endogenous signal peptide) (Figure 2-8A). This fusion sequence was placed under LexAoP sequence so that it can be expressed in cells of interest using different LexA drivers.

Next we tested GRASP with spGFP11::Ort and spGFP1-10::Nrx1 in synaptic partners R7 and Dm8 neurons. Photoreceptor neuron R7 axons specifically target to the M6 layer of the medulla and form presynaptic outputs onto processes of Dm8 neurons (Gao et al., 2008). Using an R7-Gal4 and a Dm8-LexA, we observed reconstituted GFP fluorescence specifically in the M6 layer of the medulla (Figure 2-8B). In contrast, little or no GFP fluorescence was observed between L1 and Dm8, which are not synaptic partners based on

EM though L1 axons also target to the M6 layer and form membrane contacts with Dm8 processes (Takemura et al., 2013). These results suggest that by restricting the localization of GRASP components on both sides of synapse, labeling specificity of GRASP could be improved. One caveat of this method is that for each type of synapses with a different neurotransmitter, a new postsynaptic GRASP component needs to be generated. And it is difficult to use this version of GRASP to detect synapses with unidentified neurotransmitters.

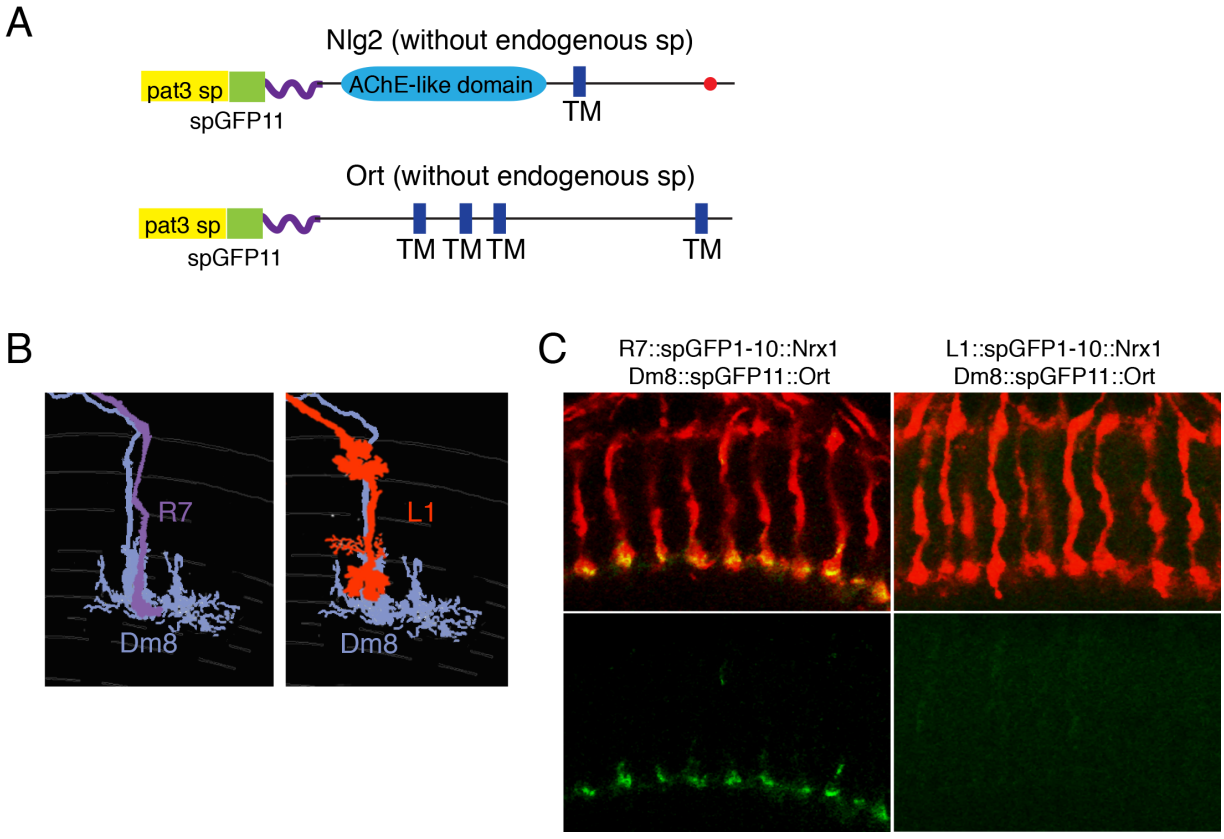

Figure 2-8 Generating postsynaptic GRASP components in Drosophila

(A) Schematic showing the construction of postsynaptic GRASP components with Nlg2 and Ort. sp, signal peptide; TM, transmembrane domain. Red dot, PDZ binding motif in Nlg2; purple curve, Glycine-Serine linker. (B) Schematics showing R7 and Dm8 in the same medulla column (left) and L1 and Dm8 in the same column (right). (C) GRASP with Nrx1-Ort detects synapses between R7 and Dm8 but not contacts between non-synaptic pair L1 and Dm8.

Discussion

GRASP is the first example of detecting synapses with protein-protein interactions across the synaptic cleft. It provides an elegant way to detect general and synaptic connections across organisms, from worms to mice. One major problem with this technique is the issue of labeling specificity. In all organisms where GRASP was used, the GRASP components are not under the control of the endogenous regulatory mechanisms of the corresponding synaptic proteins and are likely to be overexpressed in many cases. In those cases, overexpressed split GFP fragments may accumulate at inappropriate intracellular locations and thus might not accurately reflect the location of synapses (the L1-L4 case). This also made GRASP not suitable for studying synapse formation during development, as the expression timing for each split GFP fragment was artificially determined by the cell-type specific drivers rather than the endogenous expression timing of synaptic proteins. The possibility of inducing ectopic contacts by overexpression trans-synaptic cell adhesion proteins during development also needs to be considered. This is why current GRASP methods have more success in mapping mature neural circuits (e.g., the *Drosophila* mating circuit) than in studying synapse formation during development and identification of molecules that regulate synaptic specificity.

Even with those limitations, GRASP is by no means a dead-end technique. Modifications and improvements can be made to the system to overcome the limitations and expand its applicability. For example, in a recent publication, Lee and colleagues placed one of the spGFP fragments under an inducible promoter and only express this spGFP fragment in specific neurons in adult flies to avoid mislocalization of the spGFP proteins during development (Karuppudurai et al., 2014). It is also possible to generate an enhanced variant

of the GRASP system with each split GFP component expressed from the endogenous locus of the corresponding transmembrane synaptic protein using the same design strategy discussed in the next chapter of this thesis. This would increase the labeling specificity of GRASP in mature animals and make it suitable for studying the formation of synaptic contacts during development.

Experimental Procedures

Generation of GRASP constructs

The Nrx1, Lar, RIM, Nlg2 and Ort fragments were PCR amplified from cDNA library generated from total RNAs of the fly brain based on sequence information from *flybase.org*. The RIM-TM fragment was constructed as the following; the first two Ig domain and transmembrane domain of CD4 was PCR amplified from the worm GRASP construct kindly provided by Dr. Cori Bargmann and cloned into pBluescript vector via XbaI and XmaI sites. Full length RIM cDNA was also cloned into the resulting vector via XmaI site.

The pat33 signal peptide followed by the spGFP1-10 was PCR amplified from the worm GRASP construct kindly provided by Dr. Cori Bargmann and cloned into the pUAST-attB vector via EcoRI and NotI sites to create pUAST-attB-spGFP1-10. The Nrx1, Lar and RIM-TM were then cloned into pUAST-attB-spGFP1-10 via the NotI site to create (a) pUAST-attB-spGFP11::Nrx1; (b) pUAST-attB-spGFP11::Lar; (c) pUAST-attB-spGFP11::RIM-TM.

The pat33 signal peptide followed by the spGFP11 was PCR amplified from the worm GRASP construct kindly provided by Dr. Cori Bargmann and cloned into the pLH-attB vector via EcoRI and NotI sites to create pLH-attB-spGFP11. The Nlg2 and Ort were then

cloned into pLH-attB-spGFP11 via NotI site to generate (d) pLH-attB-spGFP11::Nlg2; and (e) pLH-attB-spGFP11::Ort.

S2 cell transfection and staining

Plasmids were transfected into S2 cells with Effectene Transfection Kit from Qiagen in glass-bottom plates and followed the protocol in the kit. A day after tranfection, cells were fixed with 2% PFA in PBS for 20min at room temperature, washed 3x with PBS and blocked with 10% Normal Goat Serum in PBS for 40min. After blocking, the cells were incubated in primary antibody Ab290 for 1.5hrs at room temperature, washed 3x with PBS and incubated in secondary antibody for 1.5hrs and washed 3x with PBS. Lastly, the cells were stained with DAPI for 15min at room temperature and again washed 2x with PBS. The cells were directly imaged in the glass-bottom plates with confocal microscope.

***Drosophila* stocks**

Flies were reared at 25° on standard cornmeal/molasses food. The following stocks were used: (1) UAS-spGFP1-10::CD4 (2) LexAop-spGFP11::CD4; (3) R14B07(L3)-Gal4; (4) R24C08 (Tm9)-LexA; (5) PanR7-Gal4; (6) Rh6-Gal4; (7) Fru^{M}-LexA; (8) Gr32a-Gal4; (9) R27G06 (L1)-Gal4; (10) R19D03 (L2)-Gal4; (11) R31C06 (L4)-LexA; (12) R24F06 (Dm8)-LexA

Histology

Histology was performed as described previously with minor modifications. Fly brains were fixed with PBL (4% paraformaldehyde, 75 mM lysine, 37 mM sodium phosphate buffer pH 7.4) for 25min at room temperature. After multiple rinses in PBS with 0.5% Triton X-100

(PBT), brains were blocked in 10% normal goat serum in PBT (blocking solution) for 1hr. Brains were incubated with primary and secondary antibodies for 2 days each at 4° with multiple rinses in blocking solution in between and afterwards. Brains were mounted in Slow Fade Gold anti-Fade Reagent (Life technologies). To observe native GRASP GFP fluorescence, no GFP antibody was used.

The following primary antibodies were used: nc82, 24B10 and 6H4 (1:10, Developmental Studies Hybridoma Bank), rabbit-anti-GFP (1:200, Abcam, Ab290 to recognize spGFP1-10). The following secondary antibodies were used: Alexa Fluor 647 Goat-anti-mouse, Alexa Fluor 488 Goat-anti-rabbit (all at 1:500, Life technologies A21235 and A11008).

Microscopy and image analysis

Confocal images were acquired with Zeiss LSM510 confocal microscope. The staining patterns were reproducible between samples but overall fluorescence signal and noise unavoidably shows some variation between sections and samples. Some adjustments of laser power, gain and black level settings were therefore made to obtain similar overall fluorescence signals. Single plane or maximum intensity projection confocal images were exported into TIF files using LSM Image Browser (ZEISS).

References

Banovic, D., Khorramshahi, O., Owald, D., Wichmann, C., Riedt, T., Fouquet, W., Tian, R., Sigrist, S.J., and Aberle, H. (2010). Drosophila neuroligin 1 promotes growth and postsynaptic differentiation at glutamatergic neuromuscular junctions. Neuron 66, 724-738.

Coyne, J.A., and Orr, H.A. (1998). The evolutionary genetics of speciation. Philos Trans R Soc Lond B Biol Sci 353, 287-305.

Dobzhansky, T. (1937). Further Data on the Variation of the Y Chromosome in Drosophila Pseudoobscura. Genetics 22, 340-346.

Dunipace, L., Meister, S., McNealy, C., and Amrein, H. (2001). Spatially restricted expression of candidate taste receptors in the Drosophila gustatory system. Curr Biol 11, 822-835.

Fan, P., Manoli, D.S., Ahmed, O.M., Chen, Y., Agarwal, N., Kwong, S., Cai, A.G., Neitz, J., Renslo, A., Baker, B.S., and Shah, N.M. (2013). Genetic and neural mechanisms that inhibit Drosophila from mating with other species. Cell 154, 89-102.

Feinberg, E.H., Vanhoven, M.K., Bendesky, A., Wang, G., Fetter, R.D., Shen, K., and Bargmann, C.I. (2008). GFP Reconstitution Across Synaptic Partners (GRASP) defines cell contacts and synapses in living nervous systems. Neuron 57, 353-363.

Gao, S., Takemura, S.Y., Ting, C.Y., Huang, S., Lu, Z., Luan, H., Rister, J., Thum, A.S., Yang, M., Hong, S.T., *et al*. (2008). The neural substrate of spectral preference in Drosophila. Neuron 60, 328-342.

Gordon, M.D., and Scott, K. (2009). Motor control in a Drosophila taste circuit. Neuron 61, 373-384.

Graf, E.R., Valakh, V., Wright, C.M., Wu, C., Liu, Z., Zhang, Y.Q., and DiAntonio, A. (2012). RIM promotes calcium channel accumulation at active zones of the Drosophila neuromuscular junction. J Neurosci 32, 16586-16596.

Karuppudurai, T., Lin, T.Y., Ting, C.Y., Pursley, R., Melnattur, K.V., Diao, F., White, B.H., Macpherson, L.J., Gallio, M., Pohida, T., and Lee, C.H. (2014). A hard-wired glutamatergic

circuit pools and relays UV signals to mediate spectral preference in Drosophila. Neuron 81, 603-615.

Kaufmann, N., DeProto, J., Ranjan, R., Wan, H., and Van Vactor, D. (2002). Drosophila liprin-alpha and the receptor phosphatase Dlar control synapse morphogenesis. Neuron 34, 27-38.

Kim, J., Zhao, T., Petralia, R.S., Yu, Y., Peng, H., Myers, E., and Magee, J.C. (2012). mGRASP enables mapping mammalian synaptic connectivity with light microscopy. Nature methods 9, 96-102.

Li, J., Ashley, J., Budnik, V., and Bhat, M.A. (2007). Crucial role of Drosophila neurexin in proper active zone apposition to postsynaptic densities, synaptic growth, and synaptic transmission. Neuron 55, 741-755.

Mayr, B., Kalat, M., and Rab, P. (1988). Heterochromatins and band karyotypes in three species of salmonids. TAG Theoretical and applied genetics Theoretische und angewandte Genetik 76, 45-53.

Pantazis, A., Segaran, A., Liu, C.H., Nikolaev, A., Rister, J., Thum, A.S., Roeder, T., Semenov, E., Juusola, M., and Hardie, R.C. (2008). Distinct roles for two histamine receptors (hclA and hclB) at the Drosophila photoreceptor synapse. J Neurosci 28, 7250-7259.

Pedelacq, J.D., Cabantous, S., Tran, T., Terwilliger, T.C., and Waldo, G.S. (2006). Engineering and characterization of a superfolder green fluorescent protein. Nat Biotechnol 24, 79-88.

Rivera-Alba, M., Vitaladevuni, S.N., Mishchenko, Y., Lu, Z., Takemura, S.Y., Scheffer, L., Meinertzhagen, I.A., Chklovskii, D.B., and de Polavieja, G.G. (2011). Wiring economy and

volume exclusion determine neuronal placement in the Drosophila brain. Curr Biol 21, 2000-2005.

Scott, K., Brady, R., Jr., Cravchik, A., Morozov, P., Rzhetsky, A., Zuker, C., and Axel, R. (2001). A chemosensory gene family encoding candidate gustatory and olfactory receptors in Drosophila. Cell 104, 661-673.

Stocker, R.F. (1994). The organization of the chemosensory system in Drosophila melanogaster: a review. Cell Tissue Res 275, 3-26.

Sun, M., Xing, G., Yuan, L., Gan, G., Knight, D., With, S.I., He, C., Han, J., Zeng, X., Fang, M., *et al*. (2011). Neuroligin 2 is required for synapse development and function at the Drosophila neuromuscular junction. J Neurosci 31, 687-699.

Takemura, S.Y., Bharioke, A., Lu, Z., Nern, A., Vitaladevuni, S., Rivlin, P.K., Katz, W.T., Olbris, D.J., Plaza, S.M., Winston, P., *et al*. (2013). A visual motion detection circuit suggested by Drosophila connectomics. Nature 500, 175-181.

Wang, Z., Singhvi, A., Kong, P., and Scott, K. (2004). Taste representations in the Drosophila brain. Cell 117, 981-991.

Witte, I., Kreienkamp, H.J., Gewecke, M., and Roeder, T. (2002). Putative histamine-gated chloride channel subunits of the insect visual system and thoracic ganglion. J Neurochem 83, 504-514.

Yamagata, M., and Sanes, J.R. (2012). Transgenic strategy for identifying synaptic connections in mice by fluorescence complementation (GRASP). Frontiers in molecular neuroscience 5, 18.

Zeng, X., Sun, M., Liu, L., Chen, F., Wei, L., and Xie, W. (2007). Neurexin-1 is required for synapse formation and larvae associative learning in Drosophila. FEBS Lett 581, 2509-2516.

Chapter 3 Cell-type Specific Labeling of Synapses in vivo through Synaptic Tagging with Recombination

This chapter is adapted from the following publication with minor changes.

Chen, Y., Akin, O., Nern, A., Tsui, C.Y., Pecot, M.Y., and Zipursky, S.L. (2014). Cell-type-specific labeling of synapses in vivo through synaptic tagging with recombination. Neuron 81, 280-293.

Summary

The study of synaptic specificity and plasticity in the Central Nervous System (CNS) is limited by the inability to efficiently visualize synapses in identified neurons using light microscopy. Here we describe **S**ynaptic **Ta**gging with **R**ecombination (STaR), a method for labeling endogenous presynaptic and postsynaptic proteins in a cell-type specific fashion. We modified genomic loci encoding synaptic proteins within Bacterial Artificial Chromosomes such that these proteins, expressed at endogenous levels and with normal spatiotemporal patterns, were labeled in an inducible fashion in specific neurons through targeted expression of site-specific recombinases. Within the *Drosophila* visual system, the number and distribution of synapses correlate with Electron Microscopy studies. Using two different recombination systems, presynaptic and postsynaptic specializations of synaptic pairs can be co-labeled. STaR also allows synapses within the CNS to be studied in live animals non-invasively. In principle, STaR can be adapted to the mammalian nervous system.

Introduction

The lack of methods to efficiently visualize synapses of identified neurons in the central nervous system (CNS) remains a major obstacle to studying mechanisms of synaptic specificity and plasticity. Due to the cellular complexity of the CNS and the small size of synapses, maps of synaptic connectivity have relied on Serial Section Electron Microscopy (SSEM). A comprehensive map of the synaptic connections between neurons in *Caenorhabditis elegans* was determined by SSEM in the 1980s (White et al., 1986). In *Drosophila melanogaster*, detailed maps of synaptic connectivity in the visual system have been determined by several SSEM studies (Meinertzhagen and O'Neil, 1991; Rivera-Alba et al., 2011; Takemura et al., 2013; Takemura et al., 2008). These studies reveal complex and highly specific patterns of connections and provide a foundation for studying the molecular mechanisms of circuit assembly.

SSEM analysis is extremely time-consuming. For instance, Chklovskii and colleagues developed a state-of-the-art semi-automated pipeline to reconstruct a connectome of 379 neurons in the fly visual system (Takemura et al., 2013). In this study, the steps of manually refining the SSEM dataset required ~14400 person-hours in total. As a consequence, assessing variations of synaptic connections among cells of the same cell type and between animals is problematic with Electron Microscopy (EM). In addition, EM analysis of synaptic patterns at multiple developmental stages, in various mutant backgrounds or under different activity-modulated conditions is not feasible in most instances. These limitations have driven researchers to find ways to visualize synapses by light microscopy.

Two approaches have been developed to study synapses using light microscopy. The first involves targeted expression of tagged synaptic proteins to label presynaptic and/or postsynaptic

sites (Nonet, 1999; Wagh et al., 2006; Yeh et al., 2005; Zhang et al., 2002). The second relies on visualizing protein interactions across the synaptic cleft. In GFP Reconstitution Across Synaptic Partners (GRASP), these interactions are observed through the reconstitution of GFP fluorescence (Feinberg et al., 2008). In both methods, the modified synaptic proteins are not typically expressed under their endogenous regulatory elements. As a result, the tagged proteins are often over-expressed and may accumulate in inappropriate intracellular locations and thus may not accurately reflect synaptic pairs and the location of synapses (see *Results and Discussion*). The ideal tool to faithfully label synapses with light microscopy would ensure targeted expression of modified synaptic proteins to only discrete subsets of neurons under the control of their endogenous regulatory mechanisms.

Here we describe Synaptic Tagging with Recombination (STaR), a genetic approach to label synapses in identified neurons with light microscopy. We modified the endogenous genomic loci encoding synaptic proteins within Bacterial Artificial Chromosomes (BACs) to generate inducible presynaptic and postsynaptic markers expressed in a cell-type specific manner, under the control of their endogenous regulatory mechanisms. Here, as a proof-of-principle study, we show that these markers allow the development and distribution of synapses in specific neurons of the fly visual system to be studied in detail in both fixed brain samples and in live animals.

Results

Cell-type Specific Labeling of Presynaptic Sites with the STaR Method

The presynaptic active zones in *Drosophila* are commonly marked by T-shaped electron dense structures (i.e. T-bars) visualized by Transmission Electron Microscopy (TEM). Similar to the

presynaptic ribbons at vertebrate synapses, T-bars are thought to serve as platforms for synaptic vesicle release. They are present at many synapses in *Drosophila*, including the vast majority, if not all, of the synapses in the visual system, as well as many synapses in the central brain (Butcher et al., 2012; Prokop and Meinertzhagen, 2006; Yasuyama et al., 2003). T-bars are used as the key criterion for synapse identification, as postsynaptic densities are poorly resolved using TEM in flies. T-bars comprise clusters of Bruchpilot (BRP) protein, the single CAST/ERC family member in *Drosophila* (Fouquet et al., 2009; Kittel et al., 2006; Wagh et al., 2006). By confocal microscopy these clusters appear as fluorescent puncta when stained with BRP antibody, and each punctum correlates with one presynaptic active zone (Fouquet et al., 2009; Hamanaka and Meinertzhagen, 2010). Since BRP protein is broadly expressed in the fly CNS, it is generally not possible to assign BRP puncta to processes of specific cell types, due to the small size of processes and the density of BRP puncta within the neuropil (e.g. see Figure1B).

To visualize presynaptic sites in specific cell types, we devised a genetic strategy, **S**ynaptic **Ta**gging with **R**ecombination (STaR), to label endogenous BRP protein only in processes of identified cells (Figure 1A). We modified the endogenous *brp* sequence in a BAC by inserting a V5 tag into the *brp* coding region downstream from transcriptional and translational stop sequences flanked by *FRT* recombination sites (Golic and Lindquist, 1989; Southern et al., 1991; Venken et al., 2006; Warming et al., 2005). In the absence of FLP recombinase, the BAC encoded BRP protein is not tagged. By contrast, cell-type specific expression of FLP recombinase induces recombination between the two *FRT* sites to excises the stop sequence, allowing the expression of V5-tagged-BRP only in cells of interest.

To visualize the morphology of cells expressing tagged BRP, and thus to associate BRP puncta with specific neuronal processes, we inserted a *2A-LexA* cassette downstream of the V5 tag; the

2A peptide allows for co-translation of LexA which, in turn, drives expression of, for example, myristoylated-tandem-Tomato (myr-tdTomato) from the LexAoP enhancer (Lai and Lee, 2006; Ryan and Drew, 1994). The modified BAC was introduced into flies as a transgene (Groth et al., 2004). When combined with various cell-type specific FLP recombinases, V5-tagged BRP puncta can be detected in identified neurons marking individual presynaptic sites (Figures 1A, 2, 3 and S3). In order to label presynaptic sites in live animals without relying on immuno-staining, we also prepared a GFP-tagged version of the BRP BAC construct with a similar design (see *Experimental Procedures* and Figure 8).

The BAC-encoded modified BRP proteins were expressed in the same manner as the unmodified protein from the endogenous locus. In transgenic flies carrying a BAC encoding the constitutively tagged BRP (i.e. *brp-FRT-V5-2A-LexA or brp-FRT-GFP*), the tagged BRP expression pattern was indistinguishable from BRP expression pattern in the wild type flies both at adult stage and during development (Figure 1B, S1A and S2A). These BACs also rescued lethality completely in *brp* mutants. In addition, the BRP expression pattern did not change with gene dosage, as it remained the same in flies carrying one to four copies of the *brp* gene (Figure S1B and S1C).

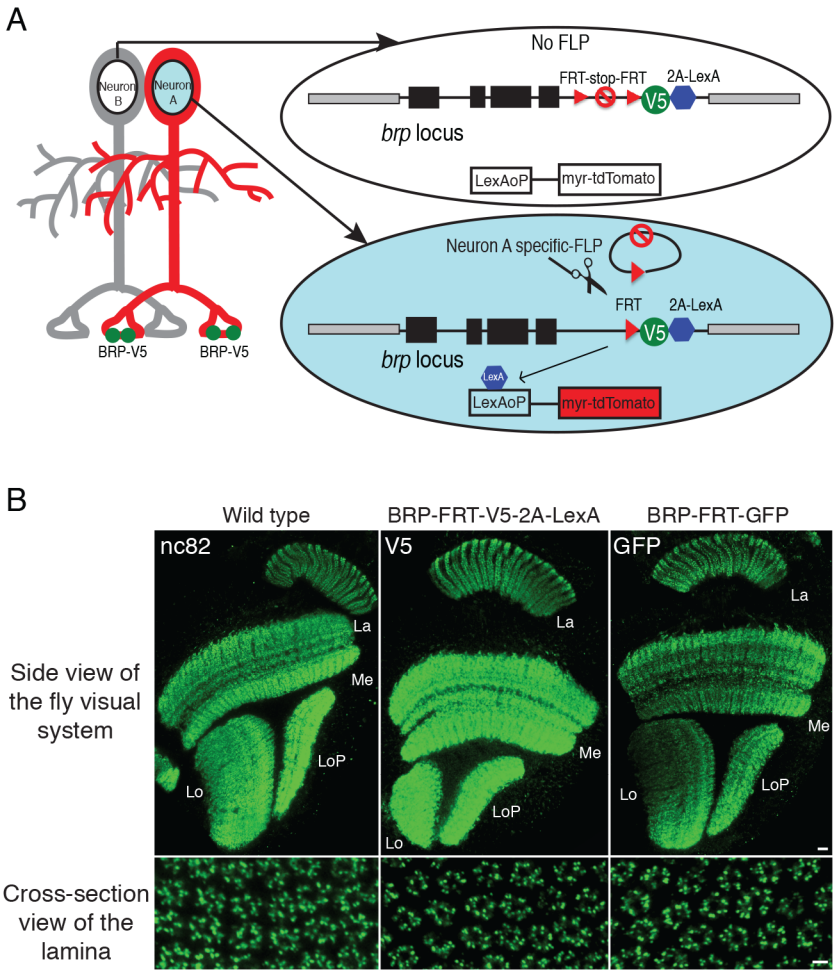

Figure 3-1 Cell-type specific tagging of the active zone protein BRP using STaR

(A) Schematic diagram for STaR. BRP protein is tagged selectively in Neuron A by targeted expression of FLP recombinase to remove the FRT-Stop-FRT cassette. Black boxes, *brp* exons; black lines, *brp* introns; gray boxes, neighboring genes. (B) The expression pattern of BRP proteins tagged via STaR detected with anti-V5 (middle panels) or with anti-GFP (right panels) is indistinguishable from the endogenous BRP protein detected with an anti-BRP antibody (nc82) (left panels). Scale bars, 10µm (top panels) and 2µm (bottom panels). La, lamina; Me, medulla; Lo, lobula; and LoP, lobula plate.

BRP Puncta in Light Microscopy Match T-bars Visualized by EM

To address whether the BRP marker reliably marks presynaptic sites, we assessed the distribution of BRP puncta in a variety of cell types in the visual system, using various cell-type specific drivers to express FLP recombinase in identified neurons (Figure 2 and S3). As in EM

studies, BRP puncta in lamina monopolar neurons L1-L5 were predominantly localized to their axonal terminals in the medulla neuropil (Figure 2B), while L2 and L4, also, elaborated a small number of presynaptic sites in proximal regions of their processes within the lamina neuropil (arrowheads in Figure 2B) (Meinertzhagen and O'Neil, 1991; Rivera-Alba et al., 2011; Takemura et al., 2013; Takemura et al., 2008). In transmedulla neuron Tm9, the vast majority of BRP puncta were observed at their axon terminals in the lobula neuropil (arrows in Figure 2C), while very few BRP puncta were seen in their dendrites in the medulla (arrowheads in Figure 2C). This distribution is consistent with results from EM analysis (Takemura et al., 2013). In addition, we were able to label the presynaptic sites in large interneurons like Dm6 and Dm8 (Figure 2D and S2D). Determining the distribution of synapses in these neurons is difficult at the EM level, due the large volume of neuropil their branches span. In summary, the BRP marker accurately reflects the distribution of presynaptic sites in specific neurons as determined by EM.

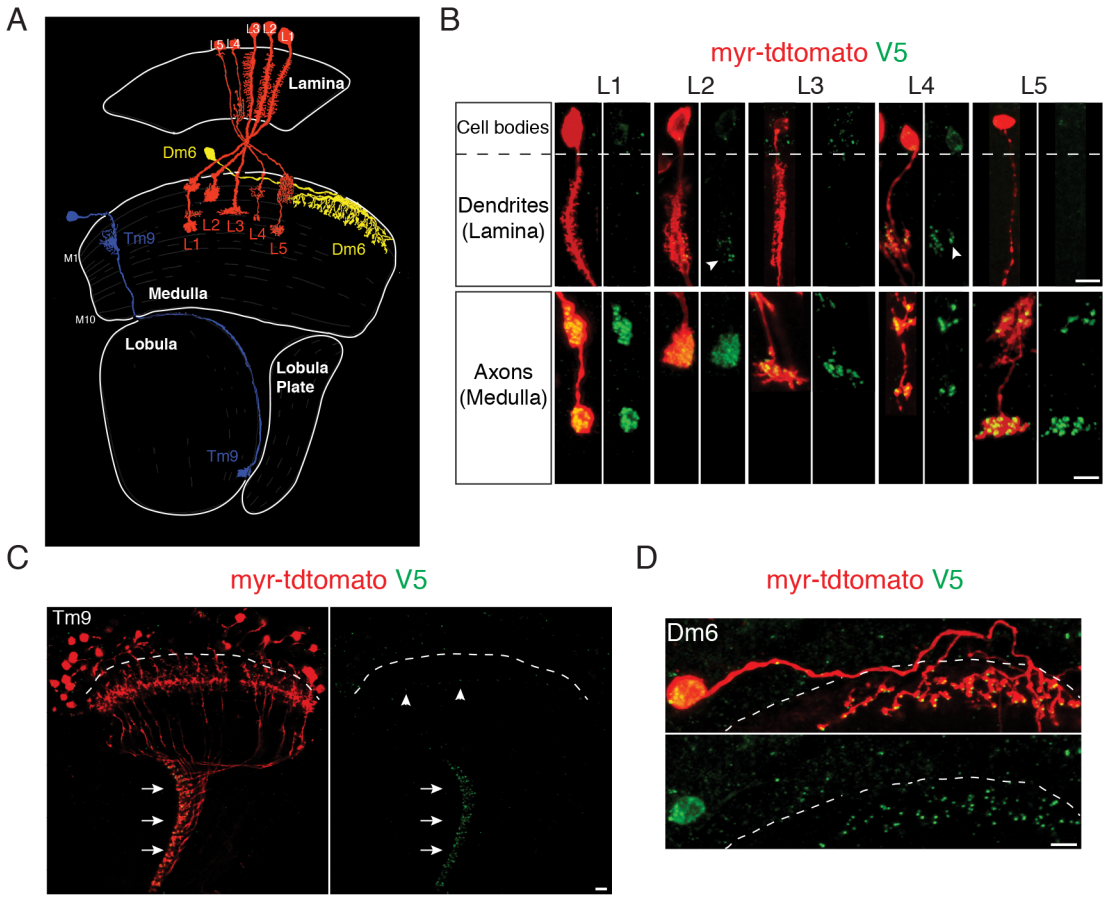

Figure 3-2 STaR labeling of presynaptic sites in various neurons in the fly visual system

(A) Schematic drawing of the *Drosophila* visual system with neurons shown in this figure: Lamina monopolar neurons L1-L5, Transmedullary neuron Tm9 and Distal medulla neuron Dm6. Adapted from (Fischbach and Dittrich, 1989). (B-D) Presynaptic sites in various neurons labeled with STaR. Red, myr-tdTomato outlining the neurons expressing the marker; Green, V5 staining labels BRP at presynaptic sites. The dashed lines separate the cortex region comprising the cell bodies (above the line) and the neuropil region comprising neuronal processes (below the line). The V5 antibody shows non-specific background in the cortex, but is specific in the neuropil. Scale bars, 5μm. (B) Presynaptic sites in L1-L5. Top, L1-L5 dendrites in the lamina neuropil; Bottom, L1-L5 axons in the medulla neuropil. Arrowheads, BRP-V5 puncta in L2 and L4 processes in the lamina. (C) Presynaptic sites in Tm9. Many Tm9 neurons were labeled. The vast majority of V5 signal was detected at the Tm9 axon terminals in the innermost layer of the lobula neuropil (arrows), while a very small number of puncta was detected in the Tm9 dendrites in the medulla (arrowheads). (D) Presynaptic sites in Dm6.

We next assessed whether the BRP marker could be used to quantify the number of presynaptic sites in specific neurons. Initially, we compared the number and distribution of BRP puncta with

that of T-bars in photoreceptor neurons, as assessed by EM. The fly compound eye contains some 750 ommatidia, each comprising 8 photoreceptor neurons falling into 3 classes: R1-R6, R7 and R8 (Clandinin and Zipursky, 2002). The R1-R6 neurons terminate within the lamina neuropil and are primarily presynaptic to lamina neurons (Figure 3A) (Meinertzhagen and O'Neil, 1991; Rivera-Alba et al., 2011). R7 and R8 axons innervate the medulla neuropil and are primarily presynaptic to specific medulla neurons (Gao et al., 2008; Takemura et al., 2013; Takemura et al., 2008). To assess the number of BRP puncta in R1-R6, we used a pan-photoreceptor FLP (panPR-FLP) to activate the BRP marker in all photoreceptor neurons and assessed the number and distribution of presynaptic sites in the lamina (Figure 3). Two FLP recombinases, expressed selectively in R7 or R8 neurons respectively, were used to examine the presynaptic sites along the length of R7 or R8 axons in the medulla (Figure 3D).

BRP puncta in different classes of photoreceptor neurons were quantified by taking stacks of cross-section images of the axons (right panels in Figure 3B and bottom panels in Figure 3D). BRP puncta were distributed uniformly along the entire length of R1-R6 axons within the lamina neuropil (Figure 3B and C). The number of BRP puncta was remarkably similar to T-bars assessed using EM (Table 1) (Meinertzhagen and O'Neil, 1991; Meinertzhagen and Sorra, 2001; Rivera-Alba et al., 2011). R7 and R8 axons span the outer 6 and outer 3 layers of the medulla neuropil (i.e. layer M1-M6 and layer M1-M3), respectively. As in the EM reconstruction studies (Takemura et al., 2013; Takemura et al., 2008), each R8 axon elaborates presynaptic sites along its length spanning layers M1-M3. By contrast, the presynaptic sites in R7 axons preferentially localize to the M4-M6 layers (Figure 3D and E). As with R1-R6 neurons, the number and distribution of BRP puncta in R7 and R8 neurons was very similar to that of T-bars assessed by EM (Table 1 and Figure 3E) (Takemura et al., 2013; Takemura et al., 2008). Thus, STaR

provides an efficient means of quantifying synapses by light microscopy.

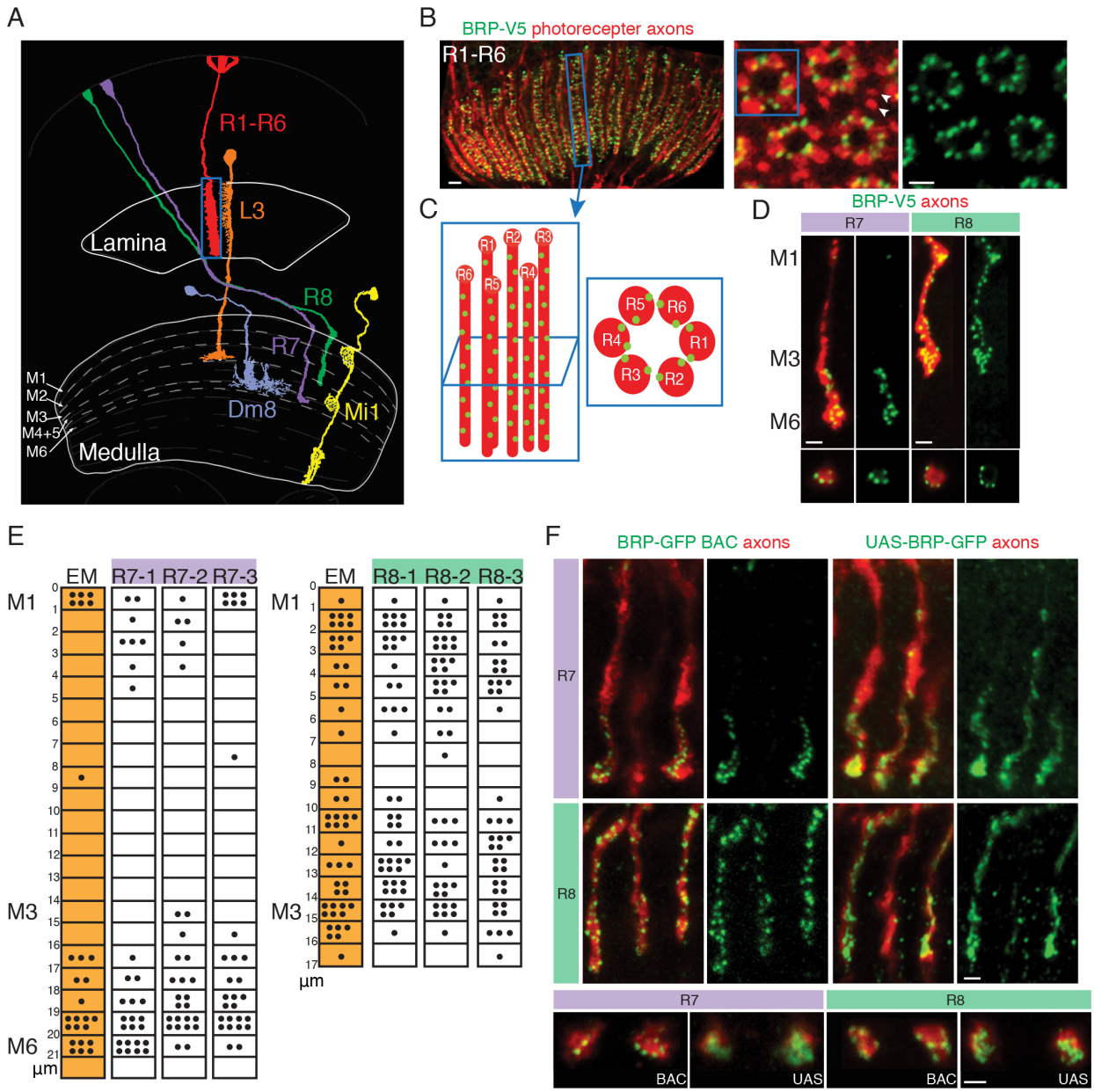

Figure 3-3 STaR labeling of presynaptic sites facilitates quantification in photoreceptor neurons

(A) Schematic drawing of three classes of photoreceptor neurons (R1-R6, R7 and R8) and examples of their postsynaptic partners: L3 for R1-R6, Dm8 for R7 and Mi1 for R8. Only one of the ~750 R1-R6, R7 and R8 neurons is depicted. Adapted from (Fischbach and Dittrich, 1989). (B) Side view (left panel) and cross-section views (center and right panels) of presynaptic sites in R1-R6 axons in the lamina labeled using STaR. Red, myr-tdTomato labels photoreceptor axons; Green, V5 staining labels presynaptic sites. Arrowheads mark R7 and R8 axons outside of the R1-R6 axon "rosette". Scale bars, 2µm. (C) Schematic

diagram of one set of R1-R6 axons in a single lamina cartridge from the side view (left) and the cross-section view (right). Red, R1-R6 axons; Green dots, presynaptic sites. (D) Presynaptic sites in R7 and R8 axons in the medulla labeled with STaR. Top panels, side view; Bottom panels, cross-section view. Red, myr-tdTomato labels R7 and R8 axons, respectively; Green, V5 staining labels BRP at presynaptic sites. Scale bars, 2μm. (E) The distribution of presynaptic sites in R7 and R8 axons mapped with STaR corresponds well with EM reconstruction results. The numbers on the left represents the distance (in μm) from the top of the medulla (designated "0"). Each black dot represents one presynaptic T-bar (EM data from Takemura et al., 2013; shown as orange shaded columns) or one BRP-V5 punctum (white columns). Each column represents one R7 or R8 axon. (F). Comparison between STaR labeling of BRP and the Gal4-driven UAS-BRP-GFP marker in R7 and R8 neurons. Only subsets of the axons are labeled with STaR (BRP-GFP BAC) or the UAS-BRP-GFP marker. Top panels, side view; Bottom panels, cross-section view. Red, photoreceptor axons marked with myr-tdTomato (left panels) or 24B10 (right panels); Green, GFP staining. Scale bars, 2μm.

Quantification of BRP puncta for several other neuronal classes also correlated well with T-bars analyzed by EM (Table 1) (Meinertzhagen and O'Neil, 1991; Meinertzhagen and Sorra, 2001; Rivera-Alba et al., 2011; Takemura et al., 2008; Takemura et al., 2013). The high correlation between the two methods suggests that the number of presynaptic sites in each cell type is largely stereotyped. In addition, we were able to observe small variations in the number of presynaptic sites among individual neurons of the same class and among individual animals (see Standard Deviations in Table 1 and data not shown). Thus, comparison between STaR and SSEM provides a rapid means of verifying SSEM and conversely the large number of different cells analyzed by STaR permits an assessment of the variability in synapse number not readily achieved by EM.

To assess the importance of using synaptic markers expressed at endogenous levels for mapping synapses, we compared the GFP-tagged BRP STaR marker to the Gal4-driven UAS-BRP-GFP marker in R7 and R8 neurons, respectively (Brand and Perrimon, 1993; Wagh et al., 2006). The protein encoded by UAS-BRP-GFP accumulated in a diffuse pattern within the R7 and R8 axon terminals and thus failed to mark individual presynaptic sites, in sharp contrast to the endogenous STaR marker (Figure 3F and S4). Thus, it is not possible to quantify synapses using

a GAL4/UAS version of tagged BRP in these neurons. Similar results were observed with another commonly used presynaptic marker UAS-synaptotagmin-GFP (Figure S4C). Thus, the STaR method, but not GAL4 mediated expression of tagged presynaptic markers, facilitates quantification of synapses within the CNS.

Lamina	Neuron	Meinertzhagen and Sorra, 2001	Rivera-Alba et al., 2011	BRP Marker (counter #1)	BRP Marker (counter #2)
	R1-R6	283 (n=1)	264 (n=1)	262±34 (n=15)	250±23 (n=15)
	L2	8 (n=1)	7 (n=1)	9±1 (n=25)	10±2 (n=25)
	L4 (L4+L4x+L4y)	23 (n=1)	21 (n=1)	24±3 (n=30)	26±4 (n=30)
	C2	16 (n=1)	8 (n=1)	9±1 (n=30)	9±1 (n=30)
Medulla	Neuron	Takemura et al., 2008	Takemura et al., 2013	BRP Marker (counter #1)	BRP Marker (counter #2)
	R7	20±2 (n=3)	26 (n=1)	27±5 (n=30)	24±6 (n=30)
	R8	35±1 (n=3)	50 (n=1)	46±5 (n=30)	47±7 (n=30)
	L4	22±2 (n=3)	26 (n=1)	26±4 (n=30)	26±5 (n=30)

Table 3-1 Number of presynaptic sites in various neurons mapped by EM and the inducible BRP marker

The number of cells quantified for each cell type (n) is shown in the table. Number of presynaptic sites is represented as Mean ± Standard Deviation for each cell type. For L4, the total number of BRP puncta in a single lamina cartridge innervated by three L4 dendrites is shown here, one from the home cartridge (L4) and two from neighboring cartridges (L4x and L4y).

Cell-type Specific Labeling of Postsynaptic Sites with the STaR Method

We sought to generate an endogenous marker that selectively marks postsynaptic sites in specific neurons. In contrast to BRP that marks virtually all presynaptic sites, a complementary marker for postsynaptic sites in flies is not known. As an alternative, we chose to tag neurotransmitter receptors in an inducible fashion to demarcate postsynaptic sites. As a proof-of-principle example, we tagged the histamine-gated chloride channel 2 (Ort), the histamine receptor expressed in the postsynaptic partners of the histaminergic photoreceptor neurons, to demonstrate the feasibility of this approach (Gao et al., 2008; Gengs et al., 2002; Pantazis et al., 2008; Stuart et al., 2007).

We modified the endogenous *ort* sequence in a genomic construct to encode a different inducible epitope tag named OLLAS (Figure 4A) (Park et al., 2008). The OLLAS tag was inserted immediately downstream of the Ort signal sequence (i.e. at the N-terminus of the mature protein). The modified Ort protein is expressed in the same spatiotemporal fashion and at the same level as the unmodified protein from the endogenous locus (Figure S2B and S5). To achieve cell-type-specific expression, an FRT-flanked stop cassette was inserted into the first intron upstream of the translational start. This cassette included a splice acceptor (SA) upstream of the translational and transcriptional stop sequences in the cassette that prevented expression of the *ort* gene. When combined with a cell-type specific FLP recombinase, the stop cassette was removed,

allowing the OLLAS-tagged Ort protein to be expressed in target neurons marking the postsynaptic sites. As insertion of the *2A-LexA* sequence at the 3' end of the *ort* open reading frame disrupted Ort protein expression, it was not possible to use this strategy to independently assess the morphology of the cell (see *Discussion*). Nevertheless, by using highly cell-type specific enhancers to drive the FLP recombinase, we were able to reliably label histamine receptors in identified neurons (see Figure 4).

Cell-type specific FLPs were used to selectively activate the Ort marker in L3 neurons (postsynaptic to R1-R6 neurons) and Dm8 neurons (postsynaptic to R7 neurons) (Figure 4B-G) (Gao et al., 2008; Rivera-Alba et al., 2011). L3 neurons extend multiple primary dendrites from the axon shaft with short spike-like secondary dendrites extending between neighboring R1-R6 axons, as shown by the targeted expression of the dendritic marker Denmark via the Gal4-UAS system (Figure 4B and C) (Brand and Perrimon, 1993; Nicolai et al., 2010). OLLAS-tagged Ort in L3 preferentially localized to secondary dendrites (arrowheads in Figure 4D), although some signal was observed along the primary dendrites and the proximal region of the axon shaft (Figure 4D). When we compared the expression pattern of the Ort marker to a general membrane marker (i.e. myr-GFP) expressed in the same L3 neurons, a clear difference in intensity at specific subcellular locations was observed, supporting that the preferential localization of OLLAS-Ort to L3 secondary dendrites is not due to the overall lower expression level of the endogenous construct (Figure S5B).

Dm8 neurons extend a single axon to the M6 layer and arborize extensively within this layer (Figure 4E and E') (Gao et al., 2008). OLLAS-labeled puncta decorated Dm8 processes and overlapped extensively with the presynaptic R7 terminals (Figure 4F-G'). Taken together, these results demonstrate that the Ort marker is selectively enriched in regions in close proximity to

presynaptic terminals of photoreceptor axons.

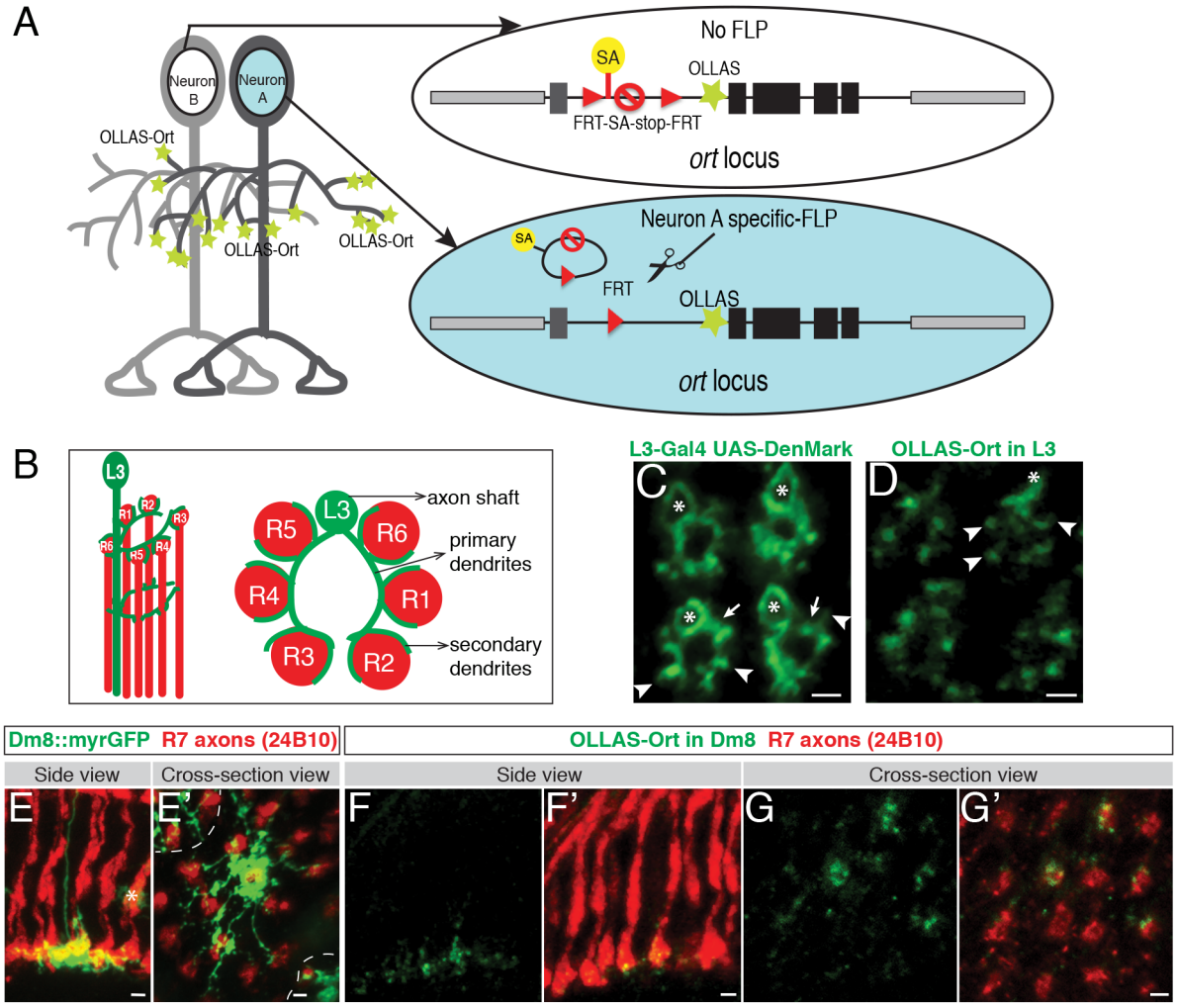

Figure 3-4 Labeling postsynaptic sites in specific cell types using STaR

(A) Schematic diagram of the cell-type specific postsynaptic marker, the histamine receptor Ort. SA, Splicing Acceptor sequence; OLLAS, an epitope tag; black boxes, *ort* coding exons; dark gray box, *ort* non-coding exon; black lines, *ort* introns; and light gray boxes, neighboring genes. (B) Schematic drawing of one L3 neuron from the side (left) and in cross-section view (right). (C) Cross-section view of L3 neurons labeled with the dendritic marker UAS-DenMark. (D) Postsynaptic sites in L3 neurons labeled with STaR. In (C) and (D): asterisks, axon shaft; arrows, primary dendrites; and arrowheads, secondary dendrites. Scale bars, 2µm. (E and E') Side view (E) and cross-section view (E') of processes of a single Dm8 neuron labeled with myristoylated GFP (myrGFP). The asterisk in (E) marks processes of a non-Dm8 neuron in the background. The dashed lines in (E') separate processes of a single Dm8 neuron from processes of its neighbors. Scale bars, 2µm. (F-G') Side views (F and F') and cross-section views (G and G') of Ort in the Dm8 neurons labeled with STaR. More than one Dm8 neuron is labeled in (G and G'). Red, 24B10 antibody staining labeling axons of R7 and R8 neurons; Green, OLLAS staining. Scale bars, 2µm.

Co-labeling Presynaptic and Postsynaptic Sites with STaR using Two Different Recombination Systems

In order to simultaneously label presynaptic and postsynaptic sites in partner neurons, we incorporated two non-overlapping recombination systems in the same animal (Figure 5) (Nern et al., 2011). The major output synapses of R1-R6 photoreceptor neurons are tetrads (i.e. one presynaptic site opposing four postsynaptic elements); L1 and L2 lamina neurons are postsynaptic at all tetrads and L3 is only postsynaptic at a subset of these with the remainder of the postsynaptic elements provided by amacrine cells or glia (Figure 5A) (Meinertzhagen and O'Neil, 1991; Rivera-Alba et al., 2011). Endogenous Ort is expressed in lamina neurons L1- L3, but neither in L4 nor L5 (Gao et al., 2008). To tag Ort in L1-L3, FLP recombinase was expressed in all lamina neurons. To co-label the presynaptic sites we generated a new version of the BRP marker by replacing the *FRT* sites with R recombinase recognition sites (*RSRT*) (Nern et al., 2011). R recombinase was then expressed in all photoreceptor neurons to induce V5 labeling of BRP in R1-R6 neurons (Figure 5A). Combining the two labeling systems in the same animal resulted in matching of V5 puncta with concentrated OLLAS staining in synaptic partners (Figure 5B). This matching was not observed when we co-expressed the BRP marker in R1-R6 neurons and a general membrane marker (myr-tdTomato) in L1-L3 neurons (Figure S6).

Using a similar scheme, we labeled V5-tagged BRP in the presynaptic R7 neurons and OLLAS-tagged Ort in the postsynaptic Dm8 neurons in the medulla (Figure 5C). The juxtaposition of V5 puncta and concentrated OLLAS staining shows that STaR allows co-labeling of presynaptic and postsynaptic sites simultaneously in synaptic partners in a complex neuropil.

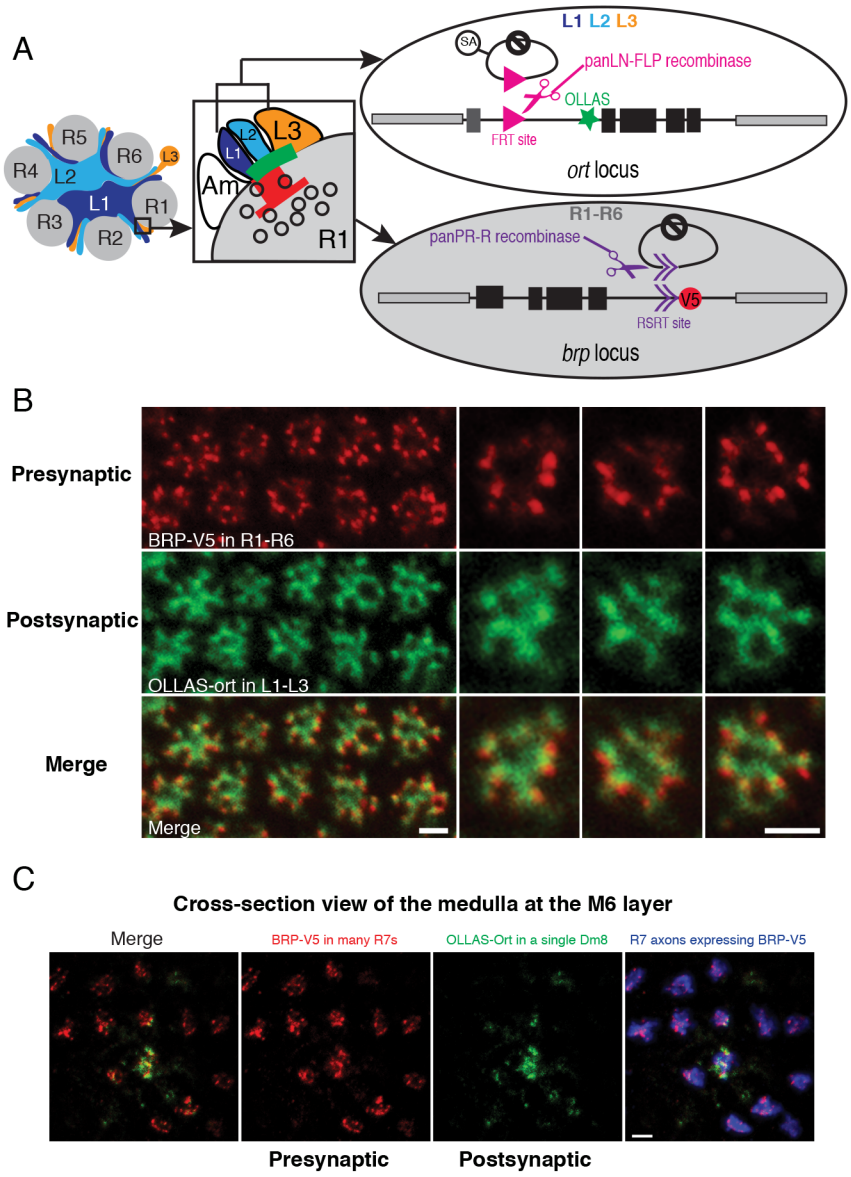

Figure 3-5 Co-labeling of presynaptic and postsynaptic sites in partner neurons with different recombination systems using STaR

(A) Schematic for STaR co-labeling the presynaptic and postsynaptic sites in partner neurons (i.e. R1-R6 neurons synapsing onto L1-L3 neurons). Left: R1-R6 axons and dendrites of L1, L2 and L3 neurons in a single lamina cartridge. Center: a tetrad synapse between a single presynaptic R1 cell and four postsynaptic elements one each from an L1, L2, L3 and amacrine cell (Am). Red, presynaptic T-bar; Green, postsynaptic neurotransmitter receptors. Open circles, synaptic vesicles. Right: the R-RSRT and FLP-FRT recombination systems independently activate the inducible presynaptic marker and postsynaptic marker in R1-R6 neurons and L1-L3 neurons, respectively. Black boxes, coding exons; dark gray box, the non-coding exon; black lines, introns; and light gray boxes, neighboring genes. (B) Co-labeling presynaptic sites in R1-R6 neurons and postsynaptic sites in L1-L3 neurons using STaR. Each BRP-V5 punctum (red) appears in juxtaposition to concentrated OLLAS-Ort staining (green). Scale bars, 2μm.(C) Co-labeling presynaptic sites in R7 neurons and postsynaptic sites in Dm8 neurons using STaR.

The R7 axons expressing BRP-V5 (red) are simultaneously labeled by myr-tdTomato (blue). Only a subset of R7 neurons is labeled with V5. Scale bar, 2μm.

Formation of Presynaptic Sites in Developing Neurons

The extraordinary density of axonal and dendritic processes of many different neuronal cell types in the developing neuropil hinders the study of synapse formation in the CNS. Here, we took advantage of cell-type specific labeling of presynaptic and postsynaptic sites during development to follow the time course of synapse formation in all three classes of photoreceptor neurons.

During synapse formation, synaptic proteins are trafficked to specific locations and assembled into presynaptic structures (Owald and Sigrist, 2009). As the tagged BRP protein is expressed via its endogenous regulatory mechanisms, the appearance of BRP puncta provides a marker for active zone assembly (Fouquet et al., 2009). We analyzed presynaptic development in photoreceptor neurons by assessing the spatiotemporal accumulation of BRP puncta within them at different times during development.

R1-R6 neurons extend axons into the lamina during the 3rd instar larval and early pupal stages with their growth cones terminating in the developing lamina (Figure 6A). These growth cones rearrange within the lamina between 30 and 40 hours after puparium formation (hAPF) forming nascent lamina cartridges comprising the growth cones of six R1-R6 axons from six different ommatidia. These axons then extend some 20 microns deeper forming the full depth of the lamina neuropil (Clandinin and Zipursky, 2002). Selective tagging of BRP in photoreceptor neurons revealed a few BRP puncta within R1-R6 growth cones at 40hAPF, just prior to extension (Figure 6B and C). By 45hAPF, R1-R6 axons extend an additional 5 microns as they become morphologically transformed from motile growth cones with filopodia to cylindrically

shaped axon terminals. As these axons extend, BRP puncta appear at the borders between neighboring axons suggesting that initial presynaptic sites have formed (arrowheads in Figure 6C). Although terminal extension is complete by 65 hAPF, BRP puncta continue to accumulate through the remaining 30 hours of pupal development (Figure 6B, C, H and I).

A similar time course of BRP accumulation was observed in R7 and R8 terminals. Prior to 40hAPF, R7 and R8 growth cones extend into the developing optic lobes in birth order and terminate in intermediate targets (Figure 6D). R8 growth cones reside at the distal edge of the medulla and R7 growth cones occupy a characteristic position proximal to R8 growth cones. At 40hAPF each R8 growth cone harbors 1-3 bright BRP puncta roughly in the center of the growth cone; a small number of BRP puncta were also seen in R7 growth cones (Figure 6E, F and H). Commencing just after 40hAPF, R7 and R8 growth cones extend into deeper layers of the medulla in a synchronous fashion (Nern et al., 2005; Timofeev et al., 2012; Ting et al., 2005). Coincident with this synchronous extension, BRP puncta begin to accumulate in the newly extended R7 and R8 axon terminals also in a synchronous fashion (Figure 6E, F, H and I). This process is very similar to the presynaptic development in R1-R6 neurons in the lamina.

Together, despite differences in their targeting regions and synaptic partners, the time course of presynaptic development for all three classes of photoreceptor neurons is highly similar: the formation of presynaptic sites initiates in the same time window between 40h-53hAPF and is coincident with the extension of the axons marking the transition from growth cones to synaptic terminals. Importantly, when the UAS-BRP-GFP marker was expressed in R7 neurons via Gal4-mediated expression at these developmental stages, strong GFP signal was observed throughout the terminals at both 40hAPF and 53hAPF, failing to reveal the transition of these growth cones to synaptic terminals (Figure 6G and S4). Thus, STaR facilitates analysis of synaptic

development at the level of single identified cells in the context of a complex neuropil.

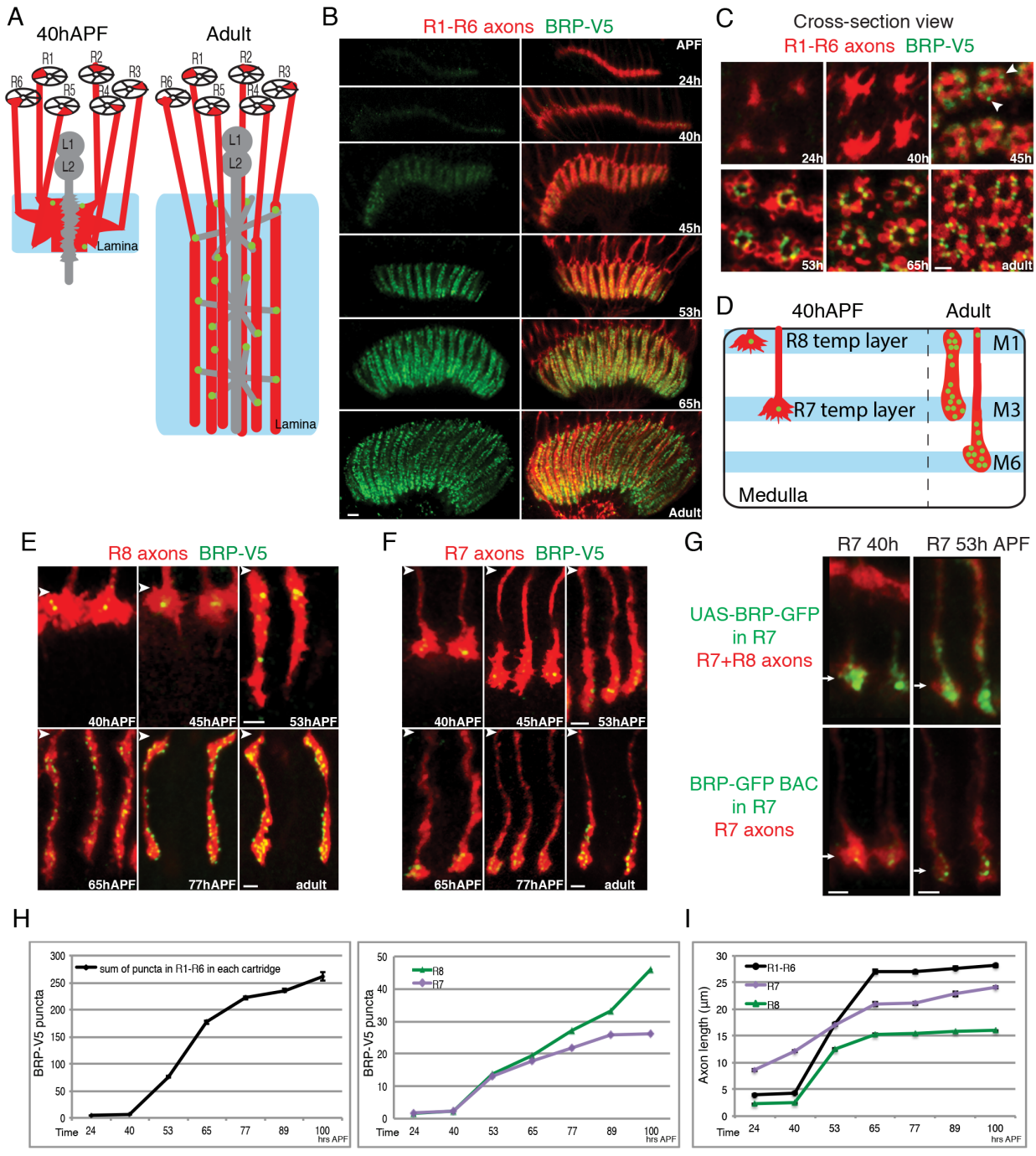

Figure 3-6 STaR labeling of presynaptic sites in the developing photoreceptor axons

(A) Schematic drawing of R1-R6 axons in the lamina before (left) and after (right) synapse formation. (B

and C) Presynaptic sites in R1-R6 axons labeled with STaR at different developmental times viewed from the side (B) and in cross-section (C) of the lamina. Scale bars, 5μm in (B) and 2μm in (C). Red, R1-R6 axons labeled with myr-tdTomato; Green, V5 staining. Arrowheads point to the initial BRP puncta at 45hAPF. (D) Schematic drawing of R7 and R8 axons in the medulla before and after synapse formation. (E and F) Presynaptic sites in R8 (E) and R7 (F) axons labeled with STaR at different developmental times. The arrowheads indicate the top of the medulla neuropil in each image. Scale bars, 2μm. (G) Comparison between the GFP-tagged BRP endogenous marker and the Gal4-driven UAS-BRP-GFP marker in R7 neurons during development. Arrows point to R7 terminals. Red, photoreceptor axons marked with MAb24B10 (top panels) or myr-tdTomato (bottom panels); Green, GFP staining. Scale bars, 2μm. (H) Number of BRP-V5 puncta in R1-R6 axons within each lamina cartridge (left) and R7 and R8 axons (right) at different developmental times. The numbers in the left panel refer to the sum of puncta in all 6 axons within the same lamina cartridge. Error bars, Standard Error. (I) Approximate length of photoreceptor axons at different developmental times. The length is measured from the top of the corresponding neuropil (lamina for R1-R6, medulla for R7 and R8) to the end of the axons marked with myr-tdTomato. Error bars, Standard Error.

Accumulation of Neurotransmitter Receptors at Postsynaptic Sites

We next followed postsynaptic development of targets of photoreceptor neurons. For this, we focused on L3 neurons in the lamina using targeted expression of Denmark to label L3 dendrites and accumulation of OLLAS-tagged Ort through STaR to label postsynaptic sites. At 24hAPF, filopodia-like dendritic structures extend from the proximal region of the L3 axon (Figure 7A). Between 40-45hAPF, these processes extend into the center of the lamina cartridge between the inner cluster of L1 and L2 axons and the surrounding rosette of R1-R6 axons (Figure 7A and data not shown). By this stage of development, a significant number of presynaptic sites in the R1-R6 axons have formed (Figure 6B, C and H). By 53hAPF, short spike-like secondary dendrites extend out from the primary dendrites and intercalate between the R1-R6 axons. Curiously, these secondary dendrites continue to elongate and surround individual photoreceptor axons at 65hAPF, but later retract (arrowheads in Figure 7A). By 77hAPF, the retraction is complete and the dendrites look morphologically indistinguishable from those of adult L3 neurons. OLLAS-tagged Ort begins to accumulate in L3 dendrites at 77hAPF (Figure 7B), after L3 dendrites have adopted their mature morphology and long after the onset of BRP puncta

accumulation in the presynaptic photoreceptor axons.

The late localization of Ort to dendrites, after the appearance of BRP puncta also occurred in the other postsynaptic partners of R1-R6 neurons including L1, L2 and Am cells, as well as in the Ort-expressing cells in the medulla postsynaptic to R7 and R8 terminals (Figure S2B). These findings suggest a common timeline for synapse formation in all three classes of photoreceptor neurons (Figure 7C). Presynaptic sites start to form in the photoreceptor axons in close temporal association with dendritogenesis in target neurons. Dendritic processes of postsynaptic neurons go through dynamic morphological changes. It is only after they adopt their mature morphology, some 30 hours after the onset of dendritogenesis, that neurotransmitter receptors become localized to these postsynaptic sites.

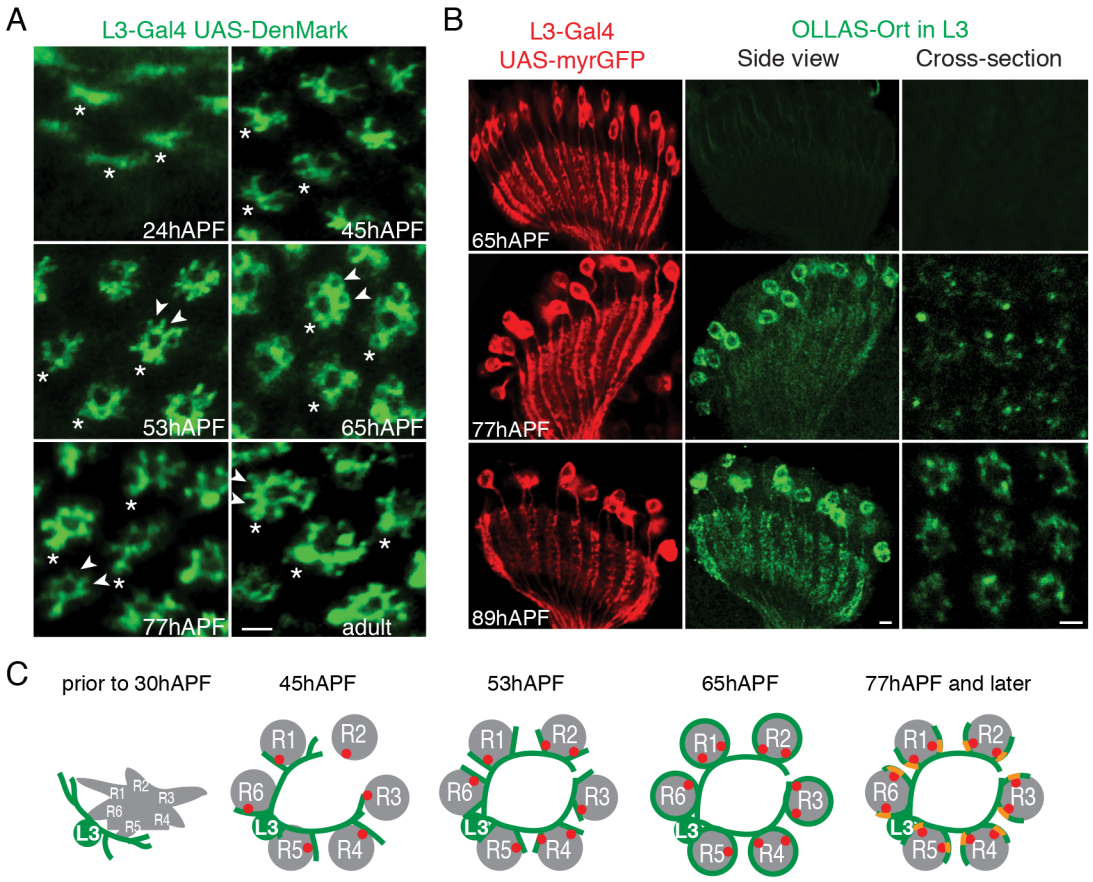

Figure 3-7 Accumulation of neurotransmitter receptors labeled with STaR in developing L3 neurons

(A) Cross-section view showing the development of L3 dendrites at different developmental times marked by L3-specific expression of Denmark. Asterisks indicate the axon shafts; arrowheads at 53, 77hAPF and adult stage highlight the cup-shaped staining indicating L3 secondary dendrites only partially surround R cell axons at these times; arrowheads at 65hAPF point to the overgrown secondary dendrites completely surrounding R cell axons (R cell axons are not labeled in these images). Scale bar, 2μm. (B) Accumulation of Ort in L3 dendrites marked by STaR. Left: Side view showing L3 cell bodies and dendrites marked with myr-GFP. Center: side view showing Ort accumulation in L3 cell bodies and dendrites. Scale bars, 5μm. Right: cross-section view showing Ort accumulation in L3 dendrites. Scale bars, 2μm. (C) Schematic diagrams summarizing synapse formation between R1-R6 cells and L3 neurons. Presynaptic sites (red dots) form prior to dendritogenesis. Dendrites (green) go through dynamic morphological changes extending beyond their targets followed by retraction to them. These morphological changes occur prior to expression of the neurotransmitter receptors (yellow) within dendrites.

Following the Formation of Presynaptic Sites in Live Animals

The ability to image synapses in real-time in live animals is crucial to reveal dynamic changes during synapse formation as well as changes in synaptic organization as a consequence of activity. To test the utility of the STaR strategy in visualizing synapse formation in live animals, we used an R8-specific FLP recombinase to selectively tag BRP with GFP in R8 neurons and followed the dynamics of this marker during the time window of initial synapse formation (i.e. 42-55hAPF) in live, developing pupae with two-photon microscopy (O.A. and S.L.Z., unpublished data). Gal4-mediated expression of UAS-myr-tdTomato was used in parallel to mark R8 axons. After the pupal case surrounding the head was gently removed, each pupa was mounted on a slide with one eye contacting the coverslip. The objective lens was placed against the eye under the coverslip and the dynamics of the developing R8 terminals were visualized directly through the retina in the underlying optic lobe. This is a non-invasive procedure; fertile flies emerge after pupal development with no morphological defects in the visual system.

Consistent with our observation with the fixed samples, after targeting to the distal edge of the medulla, R8 growth cones remain there until 40hAPF with weak GFP signal localized to the center of the growth cone (Figure 8). After 40hAPF, each R8 growth cone starts targeting to the M3 layer first with the rapid extension of a very thin process (Figure 8, red channel, 42-45hAPF). Once this leading process reaches the M3 target layer, it thickens from the top down and the R8 growth cone begins its transformation into a mature axon terminal with the appearance of many BRP puncta along its length (Figure 8B, 45-52hAPF). Live imaging revealed that stable BRP puncta are largely absent from the leading thin process but rapidly populate the thickening terminal. When individual puncta were tracked between successive time points, we found that stable puncta appear from the proximal to distal locations along the length of the extending terminal (data not shown). In summary, STaR allows imaging of synapse formation in specific

neurons in real-time within the CNS non-invasively in intact animals.

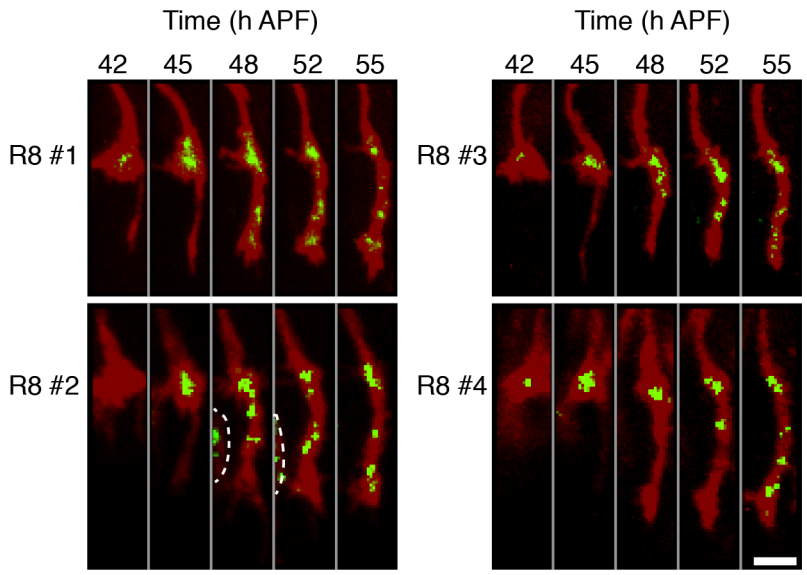

Figure 3-8 Following presynaptic development in R8 axons in live animals using STaR

Snap-shot images of the axons (red) and the presynaptic sites (green) in four developing R8 neurons in the live pupa labeled with STaR using two photon microscopy. The resolution of these images is lower than the images of the stained samples (Figure 6E), due to the lower intensity of the native fluorescence and the suboptimal orientation of the live pupa (compared to the dissected brain) relatively to the objective lens. Dashed line in R8 #2 separates a neighboring R8 axon. Scale bar, 5μm.

Discussion

In this study, we describe STaR, a method for marking synapses in defined populations of neurons in both the developing and adult fly nervous system. First, we show that the number and distribution of presynaptic sites labeled by the presynaptic marker correspond well with SSEM studies. Second, by using two independent recombination systems in the same animal, we labeled matching presynaptic and postsynaptic sites simultaneously in synaptic partners. Third, we show that these markers can be used to study synapse formation in identified cells types within the complex CNS in both fixed samples and in live animals.

STaR was inspired by the GRASP method developed by Bargmann and colleagues for studies of neural circuits in *C. elegans* (Feinberg et al., 2008), and limitations we encountered in using it to study synapse formation in the fly visual system. The initial adaptation of GRASP to *Drosophila* used the general transmembrane protein CD4 to tether the two split GFP fragments (spGFP1-10 and spGFP11) and was used to detect cell-cell contacts (Gordon and Scott, 2009). We generated synapse-specific GRASP by fusing spGFP1-10 to Neurexin-1 (Nrx-1), a transmembrane protein involved in synapse formation and maturation (Fan et al., 2013; Li et al., 2007; Zeng et al., 2007). This construct (Nrx-1::spGFP1-10) in combination with CD4::spGFP11 detected synaptic connections between neurons in the fly visual system, previously defined by EM reconstruction (e.g. L3-Tm9; L2-L4; R7-Dm8 etc.) (Fan et al., 2013; Takemura et al., 2013) (Y.C. and S.L.Z., unpublished). We also observed GFP signal, however, between pairs of neurons which, though in close association, do not form synaptic contacts (e.g. L1-L2 and L1-L4) (Rivera-Alba et al., 2011)(Y.C. and S.L.Z., unpublished). Thus, signals detected by this method may not strictly reflect synaptic contacts, presumably due to localization artifacts arising from over-expression.

The STaR method facilitates rapid comparisons of the pattern and number of synapses in specific neurons at multiple developmental stages, in various mutant backgrounds or under different activity-modulated conditions. The synaptic markers can be readily integrated into genetic schemes, such as RNA-interference and Mosaic Analysis with a Repressible Cell Marker (MARCM) to study the molecular mechanisms underlying synaptic specificity (Dietzl et al., 2007; Lee and Luo, 2001; Ni et al., 2009). These markers can also detect the modulation of synapse number and structure by activity. Indeed, after exposing fruit flies reared in the darkness to light for 15 minutes, we observed a 15% increase in the number of BRP puncta in R1-R6 photoreceptor axons with STaR (Figure S7), similar to results of previous EM studies on the

houseflies *Musca domestica* (Rybak and Meinertzhagen, 1997). In live animals, the intensity of BRP-GFP fluorescence is lower than GFP or V5 antibody staining on the fixed samples but we did not observe differences in BRP localization. Together with the fact that the number and pattern of V5-tagged BRP puncta correlates very well with EM studies in adult flies, we believe that our fixation and immuno-staining conditions introduced minimal, if any, artifacts, which may have influenced the interpretations of our observations in mature and developing animals.

In many neurons presynaptic sites are relatively sparse (see Table 1 and Figure 2 and 3) and, hence, quantification of BRP puncta is not limited by the resolution of light microscopy (i.e. neighboring presynaptic sites are easily separable). By contrast, for some lamina neuron terminals in the medulla (e.g. L2 in Figure 2B) quantification is hindered by increased density of presynaptic sites even when imaged from the optimal orientation to resolve neighboring puncta. Preliminary studies indicate that STaR is suitable for super-resolution techniques, such as Stochastic Optical Reconstruction Microscopy (STORM), which would facilitate accurate mapping and quantification of the number of presynaptic sites in neurons with particularly high density of synapses (data not shown) (Rust et al., 2006).

STaR can be extended readily to studies in other regions of the fly nervous system. Although the application of the STaR was greatly facilitated by the large collection of cell-type-specific enhancer/promoters available in the fly visual system (Gohl et al., 2011; Jenett et al., 2012; Pfeiffer et al., 2008), similar reagents are rapidly becoming available for many other regions of the fly nervous system and thus labeling presynaptic sites of vast numbers of different neurons will become straight forward. Although the Ort postsynaptic marker is limited to the histaminergic neurons, the same design principle can be applied to other types of

neurotransmitter receptors to expand our postsynaptic marker tool kit to label different types of postsynaptic sites. In future studies inclusion of the GAL80 repressor within the stop cassette will facilitate the use of the GAL4-UAS system to label the neurotransmitter receptor-expressing cells without inserting the 2A-LexA cassette to the C-terminus (Ma and Ptashne, 1987), which may disrupt the expression of tagged receptors as it did for Ort.

The STaR strategy can be expanded to generate markers for other types of communication within neural circuits not readily accessible to EM analysis. Gap junctions, for instance, are widely used in the fly nervous system yet are difficult to identify by EM (Shaw et al., 1989; Shimohigashi and Meinertzhagen, 1998). Cell-type specific tagging of gap junction components, the innexin family proteins (Bauer et al., 2005), may provide an entry point to study these structures. In a similar fashion, different neuromodulatory and neuropeptide receptors can be labeled in an inducible fashion. The use of different recombination systems, such as the FLP, R, B2, B3 and KD (Nern et al., 2011), allows different tagged synaptic proteins to be visualized in combination to characterize the molecular properties of identified synapses and other structures in the brain.

While we used BAC recombineering techniques to modify genomic loci of synaptic proteins (Venken et al., 2006), a variety of additional methods are available to generate STaR-based markers, such as Minos-mediated integration cassette (MiMIC) insertions (Venken et al., 2011), and site-specific recombination through cassette exchange (Pecot et al., 2013; Weng et al., 2009). In principle, the STaR method can be extended to the mouse and zebrafish through knock-in and BAC transgenic techniques and through the use of multiple recombination systems (e.g. Cre-Lox and the B3 and KD systems) (Capecchi, 2005; Nern et al., 2011; Stuart et al., 1988).

In summary, we have developed STaR, a cell-type specific synaptic tagging method for light microscopy in fixed and live preparations. We anticipate that this methodology will be useful to investigators examining the architecture, development, dynamics and function of synapses in a wide variety of neural circuits.

Experimental procedures

Generation of the BRP presynaptic marker and Ort postsynaptic marker

See Supplemental Experimental Procedures for detailed information regarding the generation these markers.

Drosophila stocks

Specific fly genotypes in each experiment are described in supplementary methods. Flies were reared at 25° on standard cornmeal/molasses food. Pupal staging was performed by counting the number of hours at 25° after selecting pre-pupa (i.e. 0 hAPF). For instance, 24hrs after the pre-white pupal stage at 25° is 24hAPF.

In addition to the STaR markers presented in this study, we used the following lines: (1) 9-9 Gal4 (L3); (2) Dac-FLP 20 (Pecot et al., 2013); (3) MH56 Gal4 (L3) (Timofeev et al., 2012); (4) Rh4-Gal4 (R7); (5) Rh6-Gal4 (R8) (Tahayato et al., 2003); (6) GMR-FLP (PanPR-FLP) (Pignoni et al., 1997); (7) UAS-FLP (Duffy et al., 1998; Nern et al., 2011); (8) GMR-Gal4 (PanPR-Gal4) (Wernet et al., 2003); (9) UAS-Denmark (Nicolai et al., 2010); (10) UAS-BRP-GFP (Wagh et al., 2006); (11) 20C11(R7)-FLP; (12) Senseless (R8)-FLP; (13) LexAoP-myr-tdTomato in su(Hw)attP2 and su(Hw)attP5; (14) GMR>stop>Gal4; (15) UAS>stop>myr-tdTomato in su(Hw)attP2; (16) UAS-R in attP2 (Nern et al., 2011); (17) UAS-myr-GFP in

attP40 (18) UAS-myr-tdTomato in su(Hw)attP2 (Pfeiffer et al., 2010); (19) R27G05-FLP2::PEST in attp40 (PanLN-FLP); (20) R20C11-Gal4 (R7); (21) R24C08-Gal4 (Tm9); (22) R53C12-Gal4 (Mi1); (23) R20G06-Gal4 (Dm6); (24) w; R20C11-AD; R25B02-DBD (C2); (25) w; R26H02-AD; R29G11-DBD (C3); and (26) w; R55F02-AD; R69A01-DBD (Dm8) (Pfeiffer et al., 2008; Tuthill et al., 2013). Stock (4)-(10) were acquired from Bloomington *Drosophila* Stock Center. Stock (11)-(15) were generated in this study. Stocks (24)-(26) are split GAL4 stocks.

Histology

Histology was performed as described previously with minor modification (Pecot et al., 2013). Fly brains were fixed with PBL (4% paraformaldehyde, 75 mM lysine, 37 mM sodium phosphate buffer pH 7.4) for 25min at room temperature. After multiple rinses in PBS with 0.5% Triton X-100 (PBT), brains were blocked in 10% normal goat serum in PBT (blocking solution) for 1hr. Brains were incubated with primary and secondary antibodies for 2 days each at 4° with multiple rinses in blocking solution in between and afterwards. Brains were mounted in Slow Fade Gold anti-Fade Reagent (Life technologies).

See Supplementary Experimental Procedures for a complete list of primary and secondary antibodies used in this study.

Microscopy and image analysis

Confocal images were acquired with Zeiss LSM780 confocal microscope. The staining patterns were reproducible between samples but overall fluorescence signal and noise unavoidably shows some variation between sections and samples. Some adjustments of laser power, gain and black

level settings were therefore made to obtain similar overall fluorescence signals. Single plane or maximum intensity projection confocal images were exported into TIF files using LSM Image Browser (ZEISS).

For quantification of the BRP-V5 puncta, confocal stack images were taken from the optimal orientation (cross-section of the axon axes) to cover the entire axon length. For each cell type, several Z-step values were tested out to find an optimal value (normally between 0.8-1.5μm) to avoid imaging the same puncta redundantly in adjacent sections or missing puncta. The number of BRP-V5 puncta were then scored by two counters (counter #1 and #2 in Table 1) independently by going through the stack images section by section with LSM Image Browser. Counter #2 was an undergraduate student who was unfamiliar with synapses in the fly visual system. Five optic lobes from five animals were imaged and quantified for each cell type. For R1-R6 neurons, three cartridges in each optic lobe were scored, giving a total of 15 cartridges or R1-R6 sets. For L2 neurons, five cells in each optic lobe were scored, giving a total of 25 cells. For the other cell types, six cells in each optic lobe were scored, giving a total of 30 cells for each cell type.

Live imaging of *Drosophila* pupae

Live *Drosophila* pupae were staged and mounted on slides at around 36hAPF with one eye contacting the coverslip. Stack images of the R8 axons were taken directly through the retina into the underlying optic lobe every 15 minutes for the next 24hrs with custom 2-photon microscope. These stack images were then reconstructed and aligned to generate maximum-intensity projection images shown in Figure 8. (O.A. and S.L.Z., unpublished data). Detailed information regarding the 2-photon microscope, the imaging set-up and data processing are available upon

request.

Supplemental information

Supplemental Figures and legends

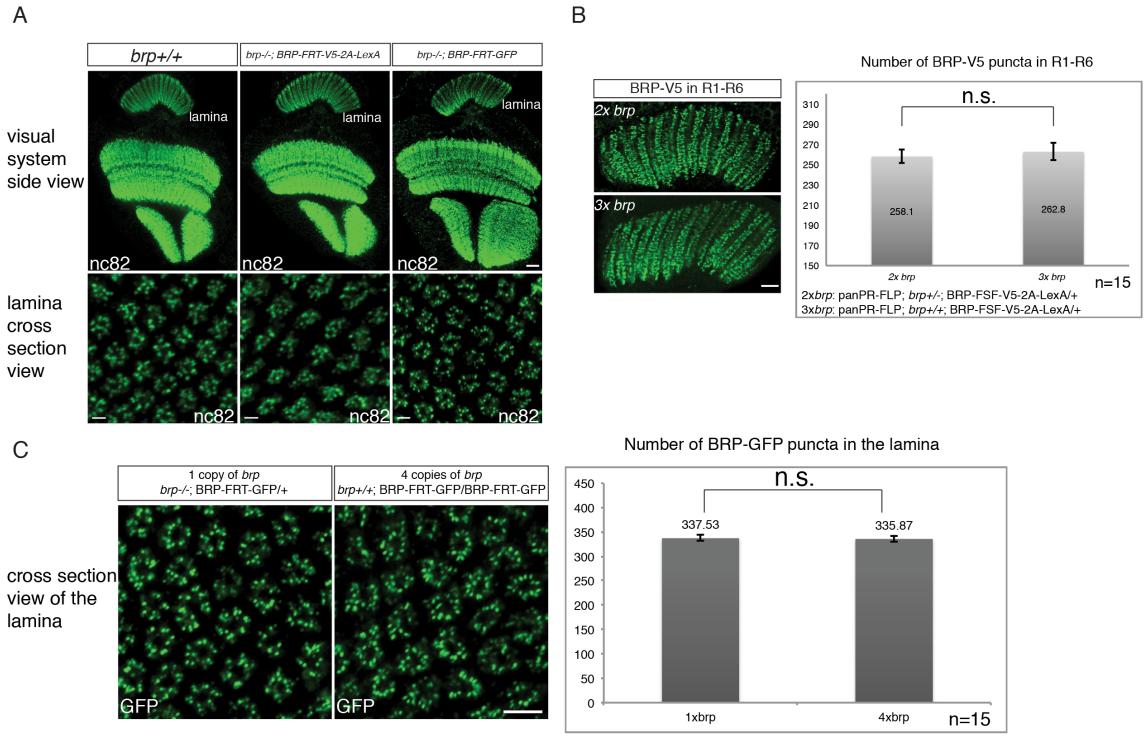

Figure S3-1 BRP BAC rescues *brp* mutation and effects of the BRP BAC transgene. Related to Figure 1. (A) The BAC restores the expression pattern of endogenous BRP shown by nc82 staining. Left, wild type animal; Middle and Right, rescue animals, where the only source of BRP are the BAC transgenes. Scale bars, 10μm (top) and 2μm (bottom). (B) Presence of the *brp* BAC transgene does not change the distribution or the number of presynaptic sites in R1-R6 neurons. Distribution (Left, scale bar 5μm) and number of presynaptic sites in R1-R6 neurons in *brp* wild type (*3xbrp*) and heterozygous (*2xbrp*) animals, each carrying one copy of the *brp* BAC transgene. Error bars represent standard error. n.s., not statistically significant according to student t test. (C) The number of BRP-GFP puncta is not sensitive to the gene dosage effects. Distribution (Left, scale bar 2μm) and number of BRP-GFP puncta in the lamina (not just in R1-R6 neurons) in flies carrying only 1 copy of the *brp* gene and 4 copies of the *brp* gene. Error bars represent standard error.

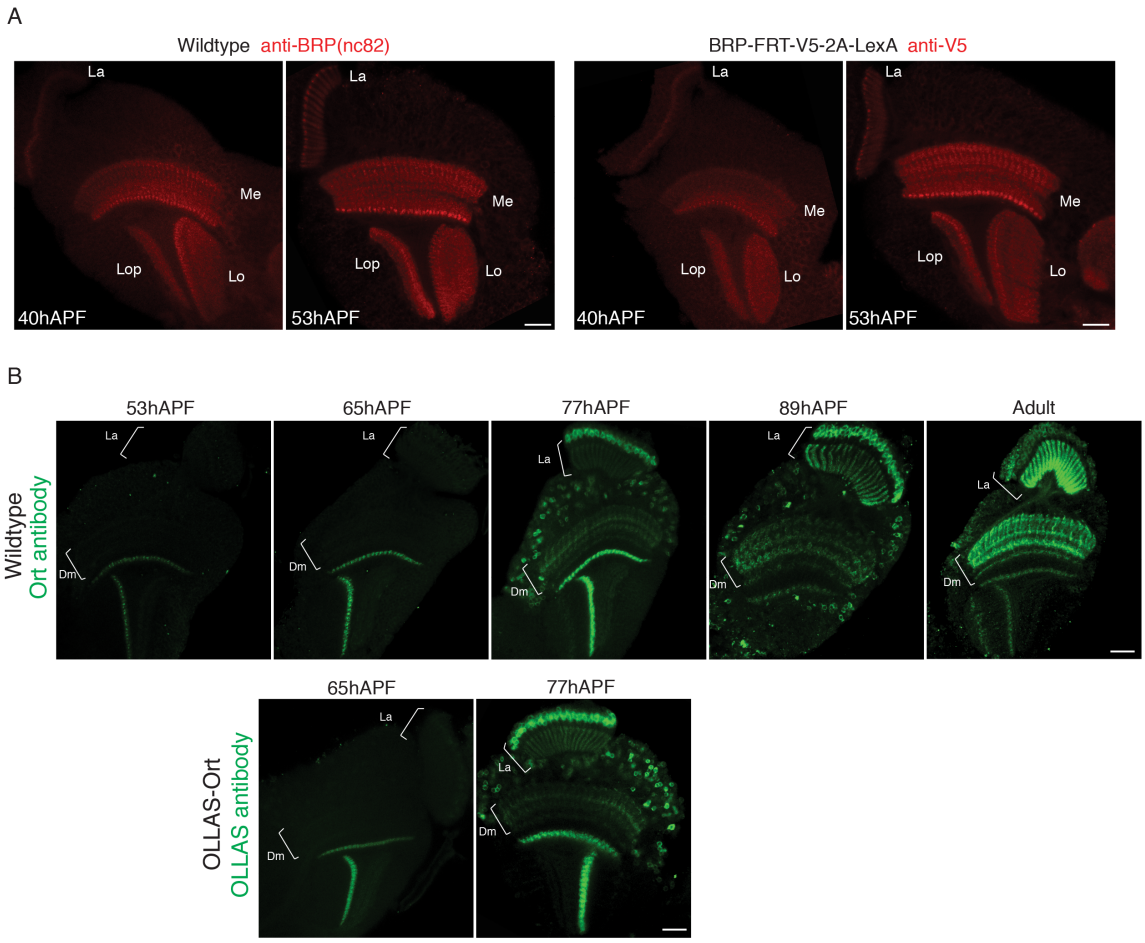

Figure S3-2 The BRP and Ort markers resemble endogenous BRP and Ort expression pattern throughout development. Related to Figure 1, 4, 6 and 7. Scale bars, 20μm. (A) The V5-tagged BRP resembles endogenous BRP expression pattern before and after the upregulation of BRP expression in the lamina (La, 40hAPF and 53hAPF, respectively). (B) Ort staining was not detected prior to 77hAPF in the lamina (La) with processes postsynaptic to R1-R6 neurons or in the distal medulla (Dm) with processes postsynaptic to R7 and R8 neurons, suggesting that the late accumulation of Ort proteins at processes of synaptic partners to photoreceptors is a common feature. The Ort staining in the proximal medulla and lobula neuropil originates from unknown cell types expressing Ort from early pupal stage. The OLLAS-tagged Ort resembles endogenous Ort expression pattern before and after the upregulation of Ort expression in the lamina and the distal medulla (65hAPF and 77hAPF, respectively).

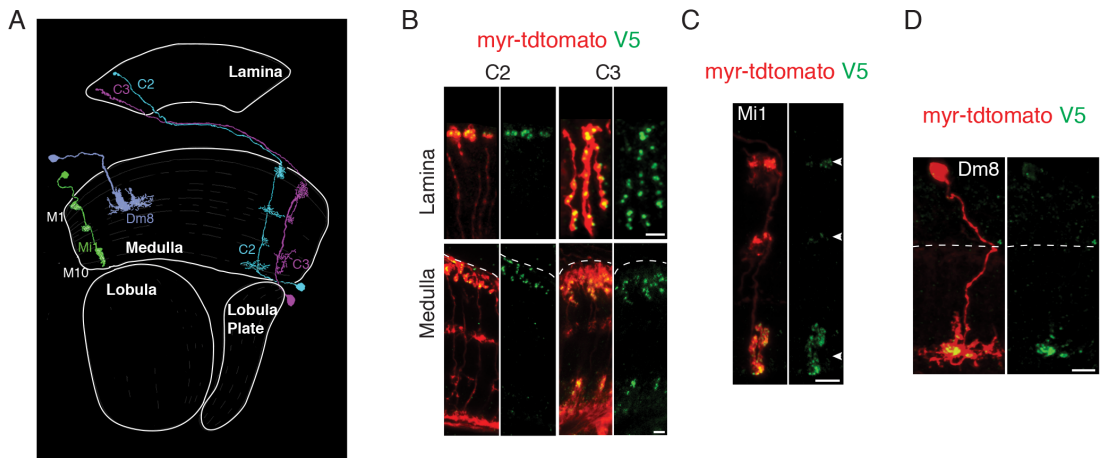

Figure S3-3 BRP presynaptic marker labels presynaptic sites in various neurons in the fly visual system. Related to Figure 2. (A) Schematic drawings of centrifugal neurons C2 and C3, medulla intrinsic neuron Mi1 and Distal Medulla neuron Dm8. Adapted from Fischbach and Dittrich 1989. (B-D) BRP puncta label presynaptic sites in C2, C3, Mi1 and Dm8. Red, myr-tdTomato outlining the neurons expressing the marker; Green, V5 staining labeling presynaptic sites. The dashed lines separate the cortex region comprising the cell bodies (above the line) and the neuropil region comprising the neuronal processes (below the line). The V5 antibody shows non-specific background in the cortex region but is specific in the neuropil region. Scale bars, 5μm.

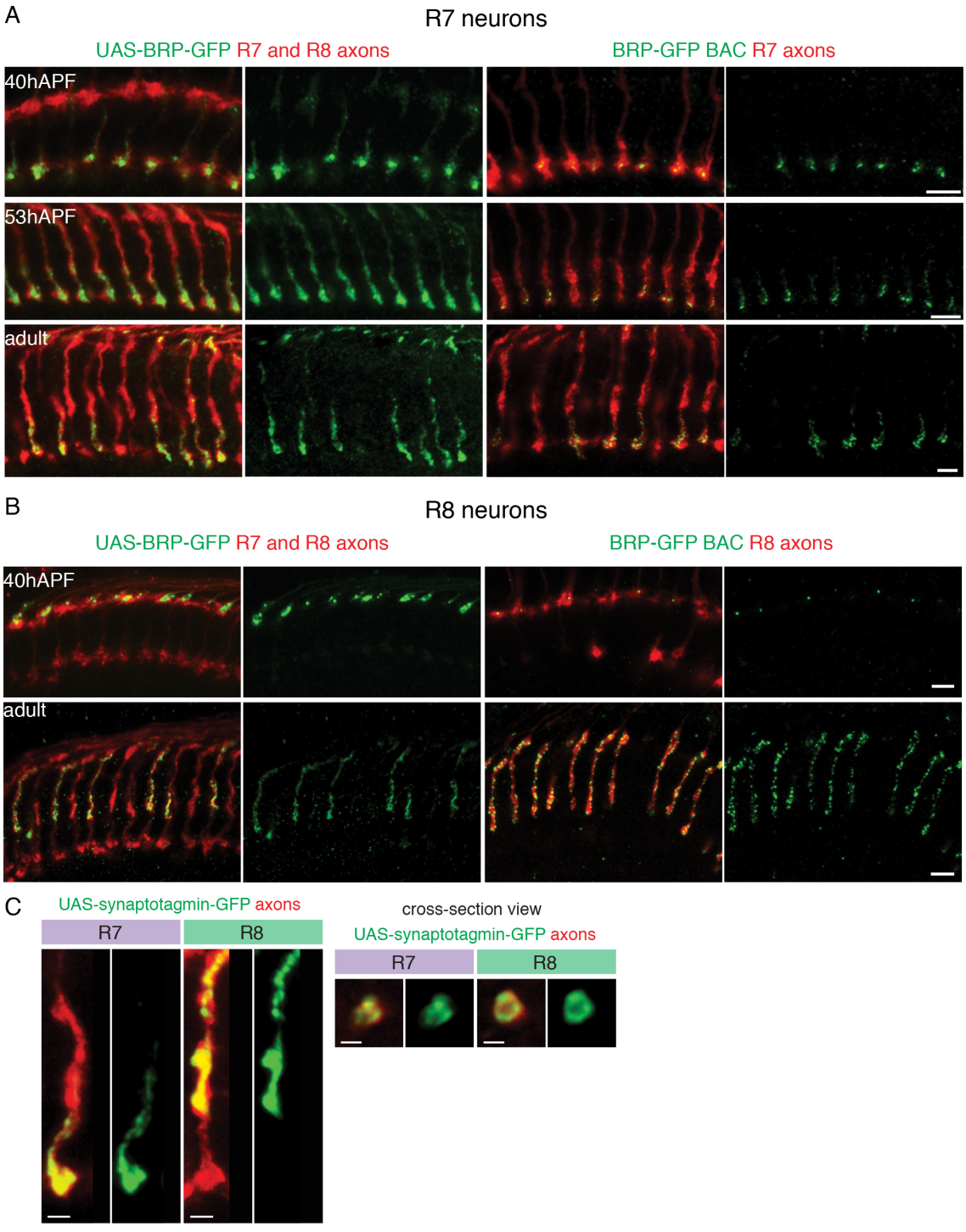

Figure S3-4 Comparison between the GFP-tagged BRP STaR marker and the UAS markers (A and B: UAS-BRP-GFP; C: UAS-synaptotagmin-GFP) in R7 and R8 neurons. Related to Figure 3 and 6. R7 and R8-specific FLP recombinases were used to induce the expression of GFP-tagged BRP STaR marker in R7 and R8 neurons, respectively. R7 and R8-specific Gal4s were used to express the UAS markers in R7 and R8 neurons respectively (R7: R20C11-Gal4 at 40hAPF and 53hAPF, Rh4-Gal4 at adult stage; R8: senseless-Gal4 at 40hAPF and Rh6-Gal4 at adult stage). Red, 24B10 antibody staining

labeling R7 and R8 axons (left panels) or myr-tdTomato labeling R7 or R8 axons (right panels); Green, GFP staining. Scale bars, 5μm (A and B) and 2μm (C).

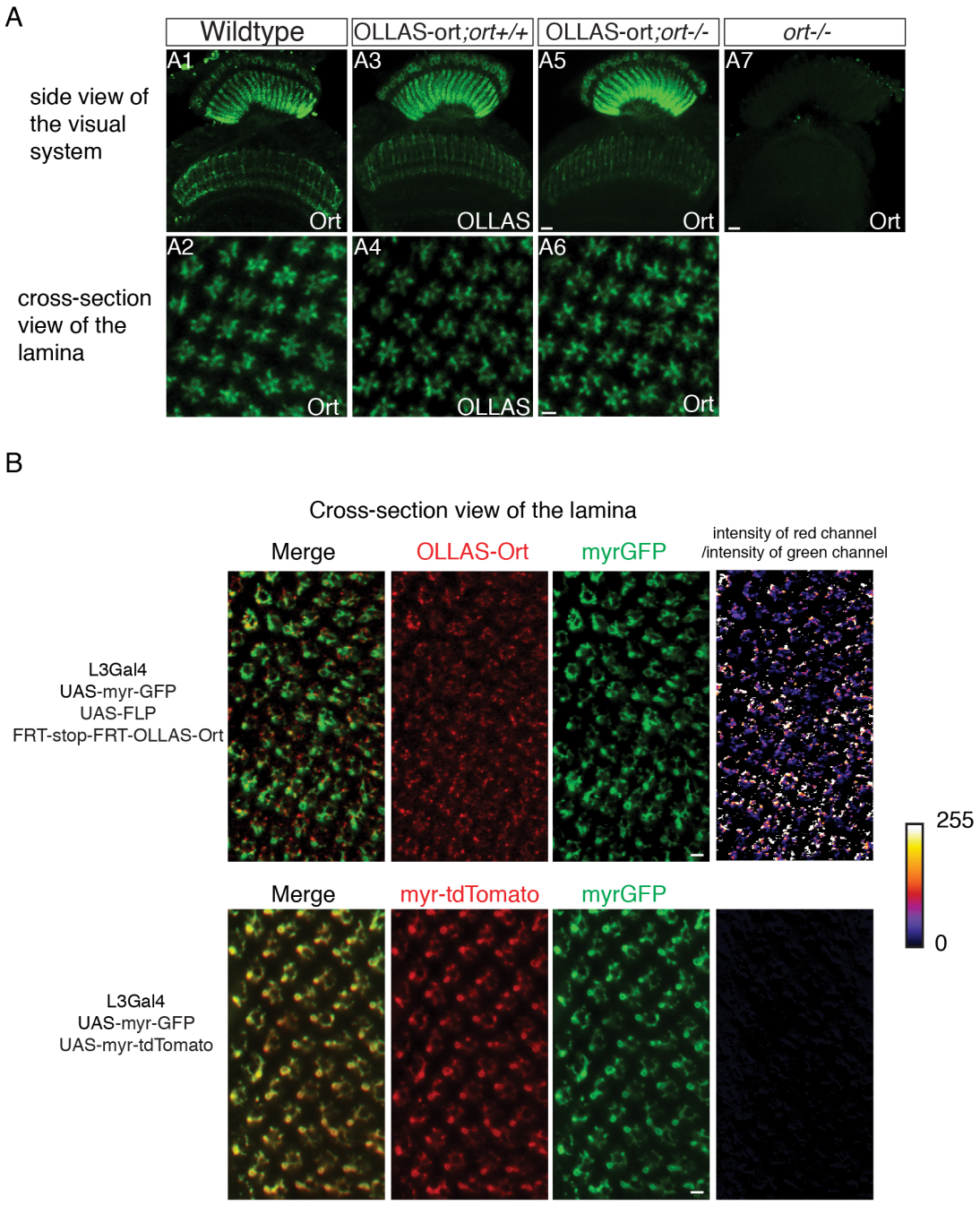

Figure S3-5 The resemblance of OLLAS-tagged Ort to endogenous Ort expression pattern (A) and the enrichment of OLLAS-tagged Ort in L3 secondary dendrites (B). Related to Figure 4. Scale bars, 5μm (A1, A3, A5 and A7), and 2μm (A2, A4, A6 and B). (A1-A2) Ort antibody staining in wild type animals; (A3-A4) OLLAS staining resembles endogenous Ort staining; (A5-A6) The ort construct restores the endogenous expression pattern of Ort; (A7) Loss of Ort staining in ort mutant animals. (B) The difference in intensity distribution between OLLAS-Ort and a general membrane marker myr-GFP in

L3 dendrites was calculated with ImageJ> Process>Image Calculator> Divide. The resulting intensity map (top right) reflected enrichment of OLLAS-Ort in L3 secondary dendrites. The same calculation done on myr-tdTomao showed no enrichment in specific locations relative to myr-GFP (bottom right).

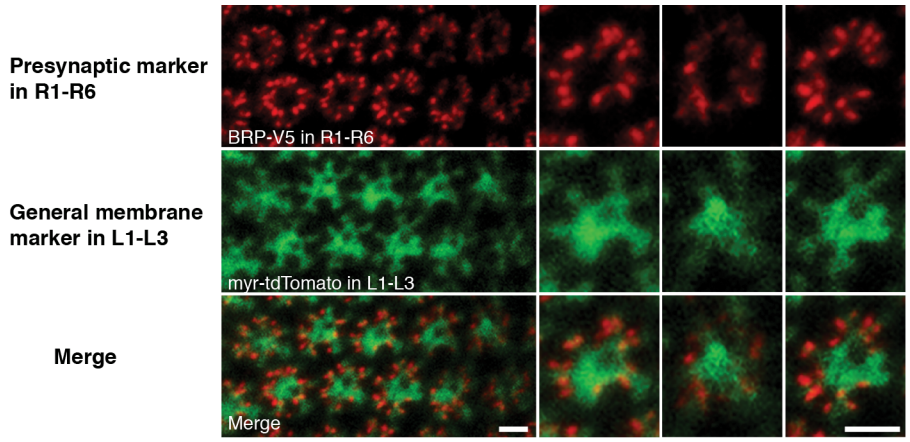

Figure S3-6 General membrane marker myr-tdTomato expressed in L1-L3 dendrites does not appose the presynaptic BRP-V5 puncta in R1-R6 axons. Related to Figure 5. Red, V5 staining; Green, myr-tdTomato, specifically expressed in L1-L3 via Ort (C1-C3)-Gal4. Scale bars, 2μm.

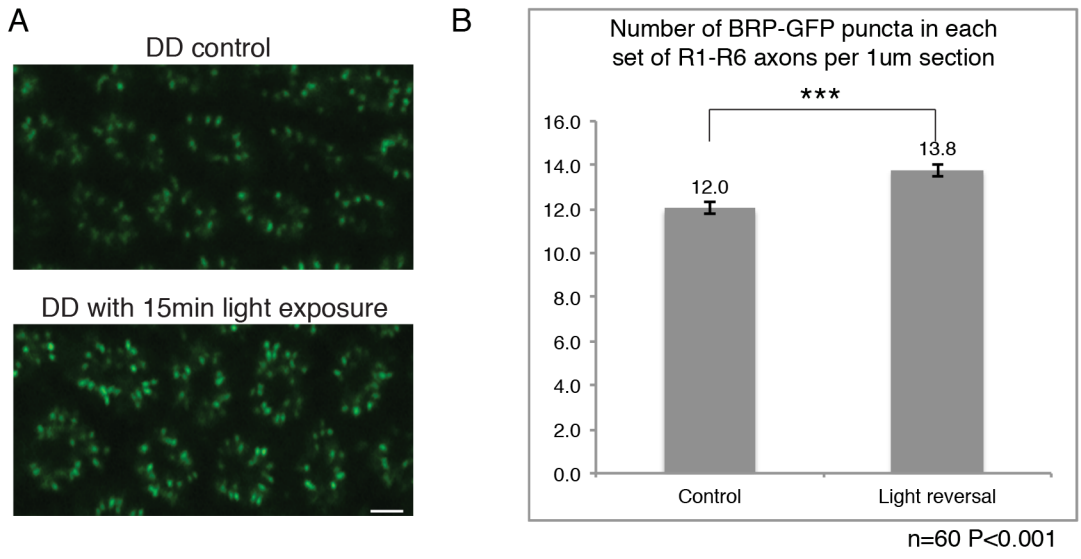

Figure S3-7 Increase in the number of BRP-GFP puncta in R1-R6 neurons after light reversal. Related to Figure 8. DD, constant darkness. Scale bar, 2μm. P value calculated with student t test. Error bars represent standard error.

Supplemental Experimental Procedures

Generation of the BRP presynaptic marker

BAC CH321-79C23 was acquired from CHORI (http://bacpac.chori.org) as the backbone for the BRP marker. BAC recombineering with GalK selection was used to modify the BAC.

The markers were generated in multiple steps. First, the BAC CH321-79C23 was truncated to remove the last 30kb sequence (51373-80506bp of CH321-79C23) that encodes several genes downstream of *brp*, resulting in a ~50kb BAC called CH321-79C23short. Second, cassettes A-F (see below) were PCR amplified and inserted into the CH321-79C23short to replace the stop codon in the *brp* coding sequence (i.e. between 43322 and 43326bp in CH321-79C23short), respectively. This resulted in the final BACs *brp-FSF-V5-2A-LexAVP16, brp-FSF-GFP* and *brp-RSR-V5-2A-LexAVP16,* as well three constitutively tagged control BACs *brp-FRT-V5-2A-LexAVP16, brp-FRT-GFP* and *brp-RSRT-V5-2A-LexAVP16*.

Cassette A: *GS linker-FRT-stop-FRT-V5-2A-LexAVP16;*

Cassette B*: GS linker-FRT-V5-2A-LexAVP16;*

Cassette C: *GS linker-FRT-stop-FRT-GFP;*

Cassette D: *GSlinker-FRT-GFP*;

Cassette E: *GS linker-RSRT-stop-RSRT-V5-2A-LexAVP16;*

Cassette F: *GSlinker-RSRT-V5-2A-LexAVP16*.

To generate cassette A and B, *armL* (50bp homology arm upstream of *brp* stop codon in CH321-

79C23Short)-*GS linker-FRT-stop-FRT-V5-2A-KpnI site* sequence was synthesized by Genewiz, Inc. based on published sequences, using cDNA codons optimized for *D. melanogaster* and cloned into EcoRI-HindIII sites of pUC57-Amp (GenScript). The *FRT-stop-FRT* sequence is the same as in Nern et al., 2011. *LexAVP16* sequence was PCR amplified from pCaSpeR4-*Or83b-LexAVP16* with stop codon and 3' *armR* (50bp homology arm downstream of *brp* stop codon in CH321-79C23Short), and cloned into the above construct via KpnI-HindIII sites, resulting in pUC57-*armL-FSF-V5-2A-LexAVP16-armR* (cassette A). The first FRT site and stop sequence were then removed from pUC57- *armL-FSF-V5-2A-LexAVP16-armR* by RF cloning, resulting in pUC57-*armL-FRT-V5-2A-LexAVP16-armR* (cassette B).

Cassette C and D were generated by replacing the *V5-2A-LexAVP16* sequence in cassette A and B by GFP sequence via RF cloning.

To generate cassette E and F, *armL-GS linker-RSRT-NotI site-V5-2A-KpnI site* sequence was synthesized and cloned into XhoI-HindIII sites of pUC57-Amp. The *RSRT-stop-RSRT* sequence is the same as in Nern et al., 2011 with minor modifications (see below). *LexAVP16* sequence was PCR amplified with 3' *armR* and cloned into the above construct via KpnI-HindIII sites, resulting in pUC57-*armL-RSRT-V5-2A-LexAVP16-armR* (cassette F). The *stop-RSRT* sequence was PCR amplified with flanking NotI sites from pJFRC168-21XUAS-RSRT-dSTOP-RSRT-myrRFP (Addgene) and cloned into pUC57-*armL-RSRT-V5-2A-LexAVP16-armR* via the NotI site, resulting in pUC57- *armL-RSRT-stop-RSRT-V5-2A-LexAVP16-armR* (cassette E).

Generation of the Ort postsynaptic marker

The *ort* genomic region used in this study consists 9227 bp of the genomic sequence of chromosome 3R (3R: 15482050-15491276). The genomic construct was generated by piecing

together three DNA fragments. First, 4337-5662bp of the *ort* genomic region was PCR amplified from BAC CH322-90N09 (CHORI) with 5' XmaI and SpeI sites and cloned into pBluescript (the SpeI site in pBluescript was deleted previously) via XmaI-EagI sites (5656-5662bp of the *ort* genomic region was a natural EagI site). OLLAS-GS linker sequence was generated by primer annealing with a CAA codon (encoding Q24 of Ort protein) added to the 5' end and inserted into the *ort* 4337-5662bp fragment in pBluescript by RF cloning, replacing a small intron (5334-5394bp of the genomic region). Residue 1-24 is the predicted signal peptide for Ort. Second, 1-4336bp of the *ort* genomic region was PCR amplified with a 5' XmaI site and a 3' SpeI site and cloned into the above pBluescript construct via those sites. Third, 5656-9227bp of the *ort* genomic region was PCR amplified with a 5' XmaI site and a 3' KpnI site and cloned into pUC57-Amp. The modified 1-5656bp of the *ort* genomic region was digested out from pBluescript by XmaI and EagI and cloned into the pUC57-*ort* 5656-9227bp construct via those sites, resulting in the pUC57-*ort* genomic construct with a SpeI site between 4336bp and 4337bp of the genomic region (in the non-conserved region of the first intron) and an OLLAS-GS linker inserted after Q24 of Ort.

The FRT-Splicing Acceptor (SA)-stop-FRT was synthesized (Genewiz Inc., see below) with flanking SpeI sites and cloned into the pUC57-*ort* genomic construct via the SpeI site. Then, the entire modified *ort* genomic region was digested out with XmaI and KpnI and cloned into a transformation vector with an attB site and a mini *white* selection marker (pW-attB). The pW-attB vector was generated by replacing the UAS-Multiple Cloning Sites-polyA sequences in pUAST-attB with a new set of Multiple Cloning Sites.

Sequences of key elements used to generate the *brp* and *ort* constructs

GS-linker: GGTGGCGGCGGAAGCGGAGGTGGAGGCTCC

V5: GGCAAGCCCATCCCAAACCCACTGCTCGGCCTGGATAGCACC

2A: CGGGCTAAGAGATCAGGTTCTGGAGCACCAGTGAAACAGACTTTGAATT

TTGACCTTCTCAAGTTGGCAGGAGACGTGGAGTCCAACCCAGGGCCC

RSRT (modified): CTTGATGAAAGAATAACGTATTCTTTCATCAAG

OLLAS: AGCGGCTTCGCCAACGAGCTGGGCCCCCGCCTGATGGGCAAG

SA: AGTCGATCCAACATGGCGACTTGTCCCATCCCCGGCATGTTTAAATATA

CTAATTATTCTTGAACTAATTTTAATCAACCGATTTATCTCTCTTCCGCAGGTC

Generation of transgenic animals

BAC or plasmid DNA constructs were introduced into flies via the PhiC31 integrase-mediated transgenesis system (Bestgene Inc.). All the brp BAC constructs were injected in the VK00033 site on chromosome 3L and all the ort genomic constructs in attP40 site on chromosome 2L.

Antibodies used in this study

The following primary antibodies were used: mouse-anti-V5 (1:200, Serotec MCA2892GA), nc82 (1:10, Developmental Studies Hybridoma Bank) and 24B10 (1:10, Developmental Studies Hybridoma Bank), rabbit-anti-DsRed (1:200, Clontech 632496), rat-anti-OLLAS (1:200, Novus Biologicals NBP1-06713), rabbit-anti-GFP (1:500, Life technologies A11122), chicken-anti-GFP (1:800, Abcam ab13970) and rat-anti-Ort (1:200, see below for the generation of this antibody). The following secondary antibodies were used: Alexa Fluor 647 Goat-anti-mouse,

Alexa Fluor 647 Goat-anti-rat, Alexa Fluor 488 Goat-anti-mouse, Alexa Fluor 488 Goat-anti-rabbit, Alexa Fluor 488 Goat-anti-chicken and Alexa Fluor 568 Goat-anti-rabbit. Each secondary antibody was used at 1:500 dilutions. The secondary antibodies were purchased from Life technologies and are referred as A21235, A21247, A11001, A11008, A11039 and A11011, respectively.

Genotypes of flies used in each experiment

To label presynaptic sites in various visual system neurons (Figure 2 and S3):

w; LexAoP-myr-tdTomato/+; UAS-FLP, *brp*-FRT-stop-FRT-V5-2A-LexAVP16/ X-Gal4 (X-Gal4 =different Gal4s or split Gal4s)

To label presynaptic sites in mature and developing photoreceptor neurons with V5-tagged BRP (Figure 3, 6 and S4):

R1-R6: GMR-FLP/+; LexAoP-myr-tdTomato/+; *brp*-FRT-stop-FRT-V5-2A-LexAVP16/+

R7: w; LexAoP-myr-tdTomato/20C11-FLP; *brp*-FRT-stop-FRT-V5-2A-LexAVP16/+

R8: *senseless*-FLP/+; LexAoP-myr-tdTomato/+; *brp*-FRT-stop-FRT-V5-2A-LexAVP16/+

To label presynaptic sites in mature and developing photoreceptor neurons with GFP-tagged BRP (Figure 3, 6 and S4)

R7: w; GMR-Gal4/20C11-FLP; *brp*-FRT-stop-FRT-GFP, UAS-FRT-stop-FRT-myr-tdTomoto/+

R8: w, senseless-FLP/+; GMR-FRT-stop-FRT-Gal4/+; *brp*-FRT-stop-FRT-GFP, UAS-FRT-stop-FRT-myr-tdTomato/+

For the expression of the presynaptic UAS-BRP-GFP and UAS-synaptotagmin-GFP markers (Figure 3 and S4):

R7: w, UAS-BRP-GFP/+; +; +/Rh4-Gal4 and w;+; UAS-synaptotamin-GFP/Rh4-Gal4 (adult)

w, UAS-BRP-GFP/+; +; +/20C11Gal4 (40hAPF and 53hAPF)

R8: w, UAS-BRP-GFP/+; +; +/Rh6-Gal4 and w;+; UAS-synaptotamin-GFP/Rh6-Gal4 (adult)

To label L3 dendrites in adult and developing animals (Figure 4 and 7):

w; MH56-Gal4/+; 9-9 Gal4/UAS-DenMark (9-9 Gal4 is specific for L3 in the lamina)

To label postsynaptic sites in L3 (developing and adult) and Dm8 neurons (Figure 4 and 7):

L3: w; OLLAS-FRT-stop-FRT-*ort*/+; UAS-FLP/9-9 Gal4

Dm8: w; OLLAS-FRT-stop-FRT-*ort*/R55F02-AD; UAS-FLP/R69A01-DBD

To co-label presynaptic and postsynaptic sites in R1-R6 neurons and L1-L3 neurons (Figure 5B):

w; R27G05-FLP2::PEST/ OLLAS-FRT-stop-FRT-*ort*; GMR-Gal4/UAS-R, *brp*-RSRT-stop-RSRT-V5-2A-LexAVP16

To co-label presynaptic and postsynaptic sites in R7 neurons and Dm8 neurons (Figure 5C):

w; Rh4-R, OLLAS-FRT-stop-FRT-*ort*/R55F02AD; R69A01DBD, UAS-FLP/*brp*-RSRT-stop-RSRT-V5-2A-LexAVP16, LexAop-myr-tdTomato

To co-express BRP-V5 in R1-R6 neurons and a general membrane marker in L1-L3 neurons (Figure S6):

w, GMR-FLP/+; Ort(C1-C3)-Gal4/+; UAS-myr-tdTomato/*brp*-FRT-stop-FRT-V5-2A-LexAVP16

To label the presynaptic sites and axons of R8 neurons for live imaging (Figure 8):

w, senseless-FLP/+; GMR-FRT-stop-FRT-Gal4/+; *brp*-FRT-stop-FRT-GFP, UAS-FRT stop-FRT-myr-tdTomato/+

For the light reversal experiment (Figure S7):

w, GMR-FLP/+; +; *brp*-FRT-stop-FRT-GFP/+

Generation of Ort antibody

The Ort antisera were obtained from rats immunized with polyhistidine (6xHis) fusion proteins corresponding to nucleotide 1000–1368bp of *ort* cDNA as described previously.

Light reversal experiment

Fruit flies were raised in darkness from the embryonic stage. 1 day after eclosion, adult flies were divided into the control group, which were kept in darkness, and the light reversal group, which were exposed to light for 15min. The two groups of flies were then euthanized (control group in darkness and reversal group in light) and dissected for imaging. 5 animals in each group were imaged and 12 R1-R6 axon sets (i.e. lamina cartridges) were quantified in a blind fashion in each animal, resulting in 60 R1-R6 sets for each condition.

References

Bauer, R., Loer, B., Ostrowski, K., Martini, J., Weimbs, A., Lechner, H., and Hoch, M. (2005). Intercellular communication: the Drosophila innexin multiprotein family of gap junction proteins. Chemistry & biology 12, 515-526.

Brand, A.H., and Perrimon, N. (1993). Targeted gene expression as a means of altering cell fates and generating dominant phenotypes. Development 118, 401-415.

Butcher, N.J., Friedrich, A.B., Lu, Z., Tanimoto, H., and Meinertzhagen, I.A. (2012). Different classes of input and output neurons reveal new features in microglomeruli of the adult Drosophila mushroom body calyx. J Comp Neurol 520, 2185-2201.

Capecchi, M.R. (2005). Gene targeting in mice: functional analysis of the mammalian genome for the twenty-first century. Nature reviews Genetics 6, 507-512.

Clandinin, T.R., and Zipursky, S.L. (2002). Making connections in the fly visual system. Neuron 35, 827-841.

Dietzl, G., Chen, D., Schnorrer, F., Su, K.C., Barinova, Y., Fellner, M., Gasser, B., Kinsey, K., Oppel, S., Scheiblauer, S., *et al*. (2007). A genome-wide transgenic RNAi library for conditional gene inactivation in Drosophila. Nature 448, 151-156.

Duffy, J.B., Harrison, D.A., and Perrimon, N. (1998). Identifying loci required for follicular patterning using directed mosaics. Development 125, 2263-2271.

Fan, P., Manoli, D.S., Ahmed, O.M., Chen, Y., Agarwal, N., Kwong, S., Cai, A.G., Neitz, J., Renslo, A., Baker, B.S., and Shah, N.M. (2013). Genetic and neural mechanisms that inhibit Drosophila from mating with other species. Cell 154, 89-102.

Feinberg, E.H., Vanhoven, M.K., Bendesky, A., Wang, G., Fetter, R.D., Shen, K., and Bargmann, C.I. (2008). GFP Reconstitution Across Synaptic Partners (GRASP) defines cell contacts and synapses in living nervous systems. Neuron 57, 353-363.

Fischbach, K.F., and Dittrich, A.P.M. (1989). The optic lobe of Drosophila melanogaster. I. A Golgi analysis of wild-type structure. Cell and Tissue Research 258, 441-475.

Fouquet, W., Owald, D., Wichmann, C., Mertel, S., Depner, H., Dyba, M., Hallermann, S., Kittel, R.J., Eimer, S., and Sigrist, S.J. (2009). Maturation of active zone assembly by Drosophila Bruchpilot. J Cell Biol 186, 129-145.

Gao, S., Takemura, S.Y., Ting, C.Y., Huang, S., Lu, Z., Luan, H., Rister, J., Thum, A.S., Yang, M., Hong, S.T., *et al*. (2008). The neural substrate of spectral preference in Drosophila. Neuron 60, 328-342.

Gengs, C., Leung, H.T., Skingsley, D.R., Iovchev, M.I., Yin, Z., Semenov, E.P., Burg, M.G., Hardie, R.C., and Pak, W.L. (2002). The target of Drosophila photoreceptor synaptic transmission is a histamine-gated chloride channel encoded by ort (hclA). J Biol Chem 277, 42113-42120.

Gohl, D.M., Silies, M.A., Gao, X.J., Bhalerao, S., Luongo, F.J., Lin, C.C., Potter, C.J., and Clandinin, T.R. (2011). A versatile in vivo system for directed dissection of gene expression patterns. Nature methods 8, 231-237.

Golic, K.G., and Lindquist, S. (1989). The FLP recombinase of yeast catalyzes site-specific recombination in the Drosophila genome. Cell 59, 499-509.

Gordon, M.D., and Scott, K. (2009). Motor control in a Drosophila taste circuit. Neuron 61, 373-384.

Groth, A.C., Fish, M., Nusse, R., and Calos, M.P. (2004). Construction of transgenic Drosophila by using the site-specific integrase from phage phiC31. Genetics 166, 1775-1782.

Hamanaka, Y., and Meinertzhagen, I.A. (2010). Immunocytochemical localization of synaptic proteins to photoreceptor synapses of Drosophila melanogaster. J Comp Neurol 518, 1133-1155.

Jenett, A., Rubin, G.M., Ngo, T.T., Shepherd, D., Murphy, C., Dionne, H., Pfeiffer, B.D., Cavallaro, A., Hall, D., Jeter, J., *et al*. (2012). A GAL4-driver line resource for Drosophila neurobiology. Cell reports 2, 991-1001.

Kittel, R.J., Wichmann, C., Rasse, T.M., Fouquet, W., Schmidt, M., Schmid, A., Wagh, D.A., Pawlu, C., Kellner, R.R., Willig, K.I., *et al*. (2006). Bruchpilot promotes active zone assembly, Ca2+ channel clustering, and vesicle release. Science 312, 1051-1054.

Lai, S.L., and Lee, T. (2006). Genetic mosaic with dual binary transcriptional systems in Drosophila. Nat Neurosci 9, 703-709.

Lee, T., and Luo, L. (2001). Mosaic analysis with a repressible cell marker (MARCM) for Drosophila neural development. Trends Neurosci 24, 251-254.

Li, J., Ashley, J., Budnik, V., and Bhat, M.A. (2007). Crucial role of Drosophila neurexin in proper active zone apposition to postsynaptic densities, synaptic growth, and synaptic transmission. Neuron 55, 741-755.

Ma, J., and Ptashne, M. (1987). The carboxy-terminal 30 amino acids of GAL4 are recognized by GAL80. Cell 50, 137-142.

Meinertzhagen, I.A., and O'Neil, S.D. (1991). Synaptic organization of columnar elements in the lamina of the wild type in Drosophila melanogaster. J Comp Neurol 305, 232-263.

Meinertzhagen, I.A., and Sorra, K.E. (2001). Synaptic organization in the fly's optic lamina: few cells, many synapses and divergent microcircuits. Prog Brain Res 131, 53-69.

Nern, A., Nguyen, L.V., Herman, T., Prakash, S., Clandinin, T.R., and Zipursky, S.L. (2005). An isoform-specific allele of Drosophila N-cadherin disrupts a late step of R7 targeting. Proc Natl Acad Sci U S A 102, 12944-12949.

Nern, A., Pfeiffer, B.D., Svoboda, K., and Rubin, G.M. (2011). Multiple new site-specific recombinases for use in manipulating animal genomes. Proc Natl Acad Sci U S A 108, 14198-14203.

Ni, J.Q., Liu, L.P., Binari, R., Hardy, R., Shim, H.S., Cavallaro, A., Booker, M., Pfeiffer, B.D., Markstein, M., Wang, H., *et al*. (2009). A Drosophila resource of transgenic RNAi lines for neurogenetics. Genetics 182, 1089-1100.

Nicolai, L.J., Ramaekers, A., Raemaekers, T., Drozdzecki, A., Mauss, A.S., Yan, J., Landgraf, M., Annaert, W., and Hassan, B.A. (2010). Genetically encoded dendritic marker sheds light on neuronal connectivity in Drosophila. Proc Natl Acad Sci U S A 107, 20553-20558.

Nonet, M.L. (1999). Visualization of synaptic specializations in live C. elegans with synaptic vesicle protein-GFP fusions. J Neurosci Methods 89, 33-40.

Owald, D., and Sigrist, S.J. (2009). Assembling the presynaptic active zone. Curr Opin Neurobiol.

Pantazis, A., Segaran, A., Liu, C.H., Nikolaev, A., Rister, J., Thum, A.S., Roeder, T., Semenov, E., Juusola, M., and Hardie, R.C. (2008). Distinct roles for two histamine receptors (hclA and hclB) at the Drosophila photoreceptor synapse. J Neurosci 28, 7250-7259.

Park, S.H., Cheong, C., Idoyaga, J., Kim, J.Y., Choi, J.H., Do, Y., Lee, H., Jo, J.H., Oh, Y.S., Im, W., *et al*. (2008). Generation and application of new rat monoclonal antibodies against synthetic FLAG and OLLAS tags for improved immunodetection. Journal of immunological methods 331, 27-38.

Pecot, M.Y., Tadros, W., Nern, A., Bader, M., Chen, Y., and Zipursky, S.L. (2013). Multiple interactions control synaptic layer specificity in the Drosophila visual system. Neuron 77, 299-310.

Pfeiffer, B.D., Jenett, A., Hammonds, A.S., Ngo, T.T., Misra, S., Murphy, C., Scully, A., Carlson, J.W., Wan, K.H., Laverty, T.R., *et al*. (2008). Tools for neuroanatomy and neurogenetics in Drosophila. Proc Natl Acad Sci U S A 105, 9715-9720.

Pignoni, F., Hu, B., Zavitz, K.H., Xiao, J., Garrity, P.A., and Zipursky, S.L. (1997). The eye-specification proteins So and Eya form a complex and regulate multiple steps in Drosophila eye development. Cell 91, 881-891.

Prokop, A., and Meinertzhagen, I.A. (2006). Development and structure of synaptic contacts in Drosophila. Semin Cell Dev Biol 17, 20-30.

Rivera-Alba, M., Vitaladevuni, S.N., Mishchenko, Y., Lu, Z., Takemura, S.Y., Scheffer, L., Meinertzhagen, I.A., Chklovskii, D.B., and de Polavieja, G.G. (2011). Wiring economy and volume exclusion determine neuronal placement in the Drosophila brain. Curr Biol 21, 2000-2005.

Rust, M.J., Bates, M., and Zhuang, X. (2006). Sub-diffraction-limit imaging by stochastic optical reconstruction microscopy (STORM). Nature methods 3, 793-795.

Ryan, M.D., and Drew, J. (1994). Foot-and-mouth disease virus 2A oligopeptide mediated cleavage of an artificial polyprotein. EMBO J 13, 928-933.

Rybak, J., and Meinertzhagen, I.A. (1997). The effects of light reversals on photoreceptor synaptogenesis in the fly Musca domestica. Eur J Neurosci 9, 319-333.

Shaw, S.R., Frohlich, A., and Meinertzhagen, I.A. (1989). Direct connections between the R7/8 and R1-6 photoreceptor subsystems in the dipteran visual system. Cell Tissue Res 257, 295-302.

Shimohigashi, M., and Meinertzhagen, I.A. (1998). The shaking B gene in Drosophila regulates the number of gap junctions between photoreceptor terminals in the lamina. J Neurobiol 35, 105-117.

Southern, J.A., Young, D.F., Heaney, F., Baumgartner, W.K., and Randall, R.E. (1991). Identification of an epitope on the P and V proteins of simian virus 5 that distinguishes between two isolates with different biological characteristics. The Journal of general virology 72 (Pt 7), 1551-1557.

Stuart, A.E., Borycz, J., and Meinertzhagen, I.A. (2007). The dynamics of signaling at the histaminergic photoreceptor synapse of arthropods. Prog Neurobiol 82, 202-227.

Stuart, G.W., McMurray, J.V., and Westerfield, M. (1988). Replication, integration and stable germ-line transmission of foreign sequences injected into early zebrafish embryos. Development 103, 403-412.

Tahayato, A., Sonneville, R., Pichaud, F., Wernet, M.F., Papatsenko, D., Beaufils, P., Cook, T., and Desplan, C. (2003). Otd/Crx, a dual regulator for the specification of ommatidia subtypes in the Drosophila retina. Developmental cell 5, 391-402.

Takemura, S.Y., Bharioke, A., Lu, Z., Nern, A., Vitaladevuni, S., Rivlin, P.K., Katz, W.T., Olbris, D.J., Plaza, S.M., Winston, P., *et al*. (2013). A visual motion detection circuit suggested by Drosophila connectomics. Nature 500, 175-181.

Takemura, S.Y., Lu, Z., and Meinertzhagen, I.A. (2008). Synaptic circuits of the Drosophila optic lobe: the input terminals to the medulla. J Comp Neurol 509, 493-513.

Timofeev, K., Joly, W., Hadjieconomou, D., and Salecker, I. (2012). Localized netrins act as positional cues to control layer-specific targeting of photoreceptor axons in Drosophila. Neuron 75, 80-93.

Ting, C.Y., Yonekura, S., Chung, P., Hsu, S.N., Robertson, H.M., Chiba, A., and Lee, C.H. (2005). Drosophila N-cadherin functions in the first stage of the two-stage layer-selection process of R7 photoreceptor afferents. Development 132, 953-963.

Tuthill, J.C., Nern, A., Holtz, S.L., Rubin, G.M., and Reiser, M.B. (2013). Contributions of the 12 neuron classes in the fly lamina to motion vision. Neuron 79, 128-140.

Venken, K.J., Schulze, K.L., Haelterman, N.A., Pan, H., He, Y., Evans-Holm, M., Carlson, J.W., Levis, R.W., Spradling, A.C., Hoskins, R.A., and Bellen, H.J. (2011). MiMIC: a highly versatile transposon insertion resource for engineering Drosophila melanogaster genes. Nature methods 8, 737-743.

Wagh, D.A., Rasse, T.M., Asan, E., Hofbauer, A., Schwenkert, I., Durrbeck, H., Buchner, S., Dabauvalle, M.C., Schmidt, M., Qin, G., *et al*. (2006). Bruchpilot, a protein with homology to ELKS/CAST, is required for structural integrity and function of synaptic active zones in Drosophila. Neuron 49, 833-844.

Warming, S., Costantino, N., Court, D.L., Jenkins, N.A., and Copeland, N.G. (2005). Simple and highly efficient BAC recombineering using galK selection. Nucleic Acids Res 33, e36.

Weng, R., Chen, Y.W., Bushati, N., Cliffe, A., and Cohen, S.M. (2009). Recombinase-mediated cassette exchange provides a versatile platform for gene targeting: knockout of miR-31b. Genetics 183, 399-402.

Wernet, M.F., Labhart, T., Baumann, F., Mazzoni, E.O., Pichaud, F., and Desplan, C. (2003). Homothorax switches function of Drosophila photoreceptors from color to polarized light sensors. Cell 115, 267-279.

White, J.G., Southgate, E., Thomson, J.N., and Brenner, S. (1986). The structure of the nervous system of the nematode Caenorhabditis elegans. Philos Trans R Soc Lond B Biol Sci 314, 1-340.

Yasuyama, K., Meinertzhagen, I.A., and Schurmann, F.W. (2003). Synaptic connections of cholinergic antennal lobe relay neurons innervating the lateral horn neuropile in the brain of Drosophila melanogaster. J Comp Neurol 466, 299-315.

Yeh, E., Kawano, T., Weimer, R.M., Bessereau, J.L., and Zhen, M. (2005). Identification of genes involved in synaptogenesis using a fluorescent active zone marker in Caenorhabditis elegans. J Neurosci 25, 3833-3841.

Zeng, X., Sun, M., Liu, L., Chen, F., Wei, L., and Xie, W. (2007). Neurexin-1 is required for synapse formation and larvae associative learning in Drosophila. FEBS Lett 581, 2509-2516.

Zhang, Y.Q., Rodesch, C.K., and Broadie, K. (2002). Living synaptic vesicle marker: synaptotagmin-GFP. Genesis 34, 142-145.

Chapter 4 Future Prospects

STaR and Super-resolution Microscopy: the feasibility and potential

One important application of the BRP STaR marker is to facilitate synapse quantification in many cell types in the nervous system with light microscopy (see Chapter 3). In the cell types we have successfully acquired the number of presynaptic sites using the BRP marker, the density of the presynaptic sites are not too high and the neighboring BRP fluorescent puncta were easily separable when imaged from optimal orientation using confocal microscope. By contrast, for many neuronal terminals in the medulla (e.g., L2 terminal in Figure 3-2), quantification is hindered by increased density of presynaptic sites leading to unresolvable neighboring puncta with the resolution provided by conventional confocal microscopy. One solution to this issue and to expand the applicability of the STaR markers in synapse quantification is to combine STaR markers with super-resolution microscopy.

Super-resolution microscopy is a form of light microscopy that allows the capture of images with a higher resolution than the diffraction limit (Hell, 2003). As described in the introduction of this thesis, two types of functional super-resolution microscopy are commonly used to image biological samples. The first type exploits the nonlinear response of fluorophores to excitation to enhance resolution. This type is represented by STED microscopy (Klar et al., 2000). The second type of super-resolution microscopy makes several close-by fluorophores (which are normally not resolvable) emit light at separate times so that they become resolvable in time. This type is represented by STORM (Rust et al., 2006).

Preliminary studies indicate that STaR is suitable for both STED and STORM techniques. For instance, with conventional confocal microscopy, a few neighboring BRP puncta in L2 axon terminals are unresolvable and appear as one large fluorescent patch (Figure 4-1 left panel). This patch of staining was resolved into 5 individual puncta with STED microscopy, marking 5 individual presynaptic sites (Figure 4-1 right panel). In the preliminary experiments, we were able to achieve a resolution of 30-80nm with STED and STORM, which is on the same scale with synaptic structures such as synaptic cleft, presynaptic active zone and postsynaptic density. With further optimization of the sample preparation using the existing STaR markers, we should be able to accurately map and quantify of the number of presynaptic sites in neurons with particularly high density of synapses, to better visualize the opposing presynaptic and postsynaptic sites between partner neurons and to study the transport and assembly of presynaptic AZ components and neurotransmitter receptor complexes during synapse formation in great details. Furthermore, generation of additional inducibly tagged synaptic proteins and combining them with super-resolution microscopy would greatly advance our understanding of synapse formation *in vivo* both at the cellular level and at the molecular level.

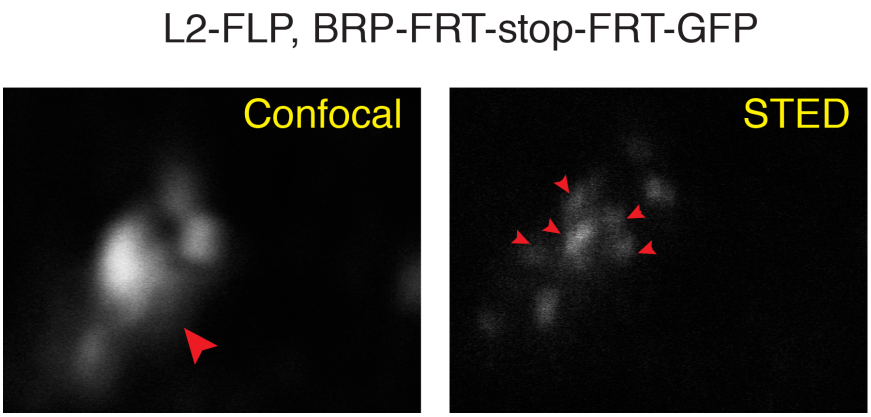

Figure 4-1 STED microscopy resolves neighboring presynaptic sites in L2 axons labeled with the STaR marker

The endogenous BRP presynaptic marker was selectively expressed in L2 neurons and imaged with both conventional confocal microscopy (left) and STED microscopy (right). Single-plane images show the cross-section view of the same L2 axon terminal. The large arrowhead in the left panel points to a large fluorescent patch most likely representing unresolved neighboring presynaptic sites. The small arrowheads in the right panel point to the individual presynaptic sites the large patch in the left panel resolves to.

Using STaR to identify molecular mechanisms underlying synaptic specificity

Through the characterization of synapse formation process in fly photoreceptor neurons (see Chapter 3), we noticed that the presynaptic differentiation in all three types of photoreceptor neurons happened in a synchronous fashion within the same 13-hour time window, between 40h and 53h APF. McEwen and Zhang, also in the Zipursky laboratory, set to generate gene expression profiles in photoreceptor neurons at discrete stages before (40h APF), during (45h APF) and after (53h APF) the initiation of presynaptic differentiation. With a method called Tandem-Tagged Ribosomal Affinity Purification (T-TRAP), they isolated mRNAs specifically from photoreceptor neurons at those three stages and subjected them to RNA-Seq analysis (Doyle et al., 2008). The T-TRAP

method selectively enriches for transcripts that are loaded onto ribosomes, presumably reflecting the transcripts being translated into proteins at each time point.

When ribosomal-enriched gene expression profiles at 40h and 53h APF were compared, a large number of genes were differentially expressed (up- or down-regulated) for at least 5-fold. Using a manually curated list of 16 different functional classifications (Figure 4-2A), we observed statistically significant enrichment in only two categories, genes encoding cell surface proteins and genes involved in phototransduction. Indeed, approximately 39% (127/321) of the genes differentially expressed for more than 5-fold between 40h and 53h APF are genes encoding cell surface proteins (Figure 4-2B). Those include members of gene families implicated in synapse formation in culture and *in vivo* including tetraspanins, SynCAMs, Ig-CAMs and LRRTMs. These 127 cell surface genes are prime candidates for regulating synapse formation in fly photoreceptor neurons and are being tested *in vivo* using the STaR markers (see below). These observations are in support of the prevalent hypothesis that trans-synaptic cell adhesion molecules mediate and stabilize the initial axo-dendritic contacts and initiate bidirectional signaling in the axon and dendrite for the recruitment of synaptic components.

A

Biological category	Up-regulated (5X)	Down-regulated (5X)	Total in fly genome	P-value
cell_surface	100	27	950	1.34E-12
phototransduction	11	1	43	3.82E-11
membrane_transporter	48	6	765	0.063173
actin_binding	9	2	120	0.0724627
ecdysone_inducible	5	4	109	0.0789275
gef	3	0	24	0.0820117
synapse	4	1	44	0.0850172
TF	21	16	751	0.3132098
phosphatase_activity	6	5	178	0.5067386
translation_regulation	2	3	78	0.6423426
gap	0	0	21	0.7960476
microtubule	1	1	63	0.8179043
splicing_regulator	1	2	150	0.9684649
RNA_binding	9	20	741	0.979362
chromatin_assembly	1	1	138	0.9840738
kinase_activity	7	4	373	0.9951578

B

Biological category	Diffrentially expressed (DE) genes (5x)	Percentage of total 5x DE genes (%)
cell_surface	127	39.6
phototransduction	12	3.7
membrane_transporter	54	16.8
actin_binding	11	3.4
ecdysone_inducible	9	2.8
gef	3	0.9
synapse	5	5
TF	37	11.5
phosphatase_activity	11	3.4
translation_regulation	5	1.6
gap	0	0
microtubule	2	0.6
splicing_regulator	3	0.9
RNA_binding	29	9.0
chromatin_assembly	2	0.6
kinase_activity	11	3.4

Figure 4-2 Genes encoding cell surface proteins are significantly enriched in the differentially expressed (DE) gene set between 40h and 53h APF

(A) Numbers of up- and down-regulated genes in 16 functional categories. Only two categories (cell surface and phototransduction) are significantly enriched in the DE dataset compared to the

whole genome. (B) Percentage of DE genes in each category among all DE genes between 40h and 53h APF.

Similarly, gene expression profiles have been generated in R7 neurons and R8 neurons respectively at 40h and 50h APF. Fluorescence-activated Cell Sorting (FACS) was used to specifically isolate R7 or R8 neurons and the mRNAs in each cell type were sequenced (Herzenberg et al., 1976). This method acquires all the transcripts in the specific cell type at each developmental time point and therefore generates the classic transcriptome for that cell type. First, transcripts differentially expressed by more than 5-fold between 40h and 50h APF were identified for R7 neurons and R8 neurons, respectively, as potential regulators of synapse formation in each cell type. Next, comparing differentially expressed genes in R7 neurons to those in R8 neurons led to a collection of R7-specific differentially expressed transcripts and a collection of R8-specific differentially expressed transcripts (Figure 4-3A). Importantly, R7 and R8 photoreceptor neurons are closely related in many aspects of development and function. Between 40h and 50h APF, the most prominent event in these two cell types is the transformation of their axons into synaptic terminals with different synaptic specificity. And the cell-type-specific differentially expressed transcripts in each of the two cell types are likely to account for the synaptic specificity for that cell type.

Both loss-of-function (LOF) and gain-of-function (GOF) analyses can be performed to test the above-identified candidate genes for their involvement in synapse formation and synaptic specificity. We have designed an RNAi-based LOF screen to test those candidate genes in specific photoreceptor neurons with the STaR markers. In this screen, the short-hairpin RNA (shRNA) targeting each gene on the candidate lists is expressed in

all photoreceptor neurons throughout development using the Gal4-UAS system (Figure 4-3B) (Ni et al., 2009). Meanwhile, cell-type-specific FLP activates the endogenous BRP marker selectively in R1-R6 neurons (or in R7 neurons, or in R8 neurons), allowing assessment of presynaptic sites number and distribution in those neurons. Preliminary results have also shown that STaR markers can be incorporated into Mosaic Analysis with a Repressible Cell Marker (MARCM) to test true LOF mutant alleles of candidate genes for their involvement in synapse formation (data not shown) (Lee and Luo, 2001).

To specifically identify the molecules mediating synaptic specificity instead of the general synapse formation process, a GOF approach may be employed in R7 and R8 photoreceptor neurons (Figure 4-3B). For instance, R7 axons span medulla layers M1-M6 but form presynaptic sites predominantly in layers M4-M6. We can ectopically express R8-specific transcripts in R7 neurons and use the endogenous BRP marker to assess whether this results in changes in the distribution of presynaptic sites in R7 axons to layer M1-M3, which are the synaptic layers for R8 neurons.

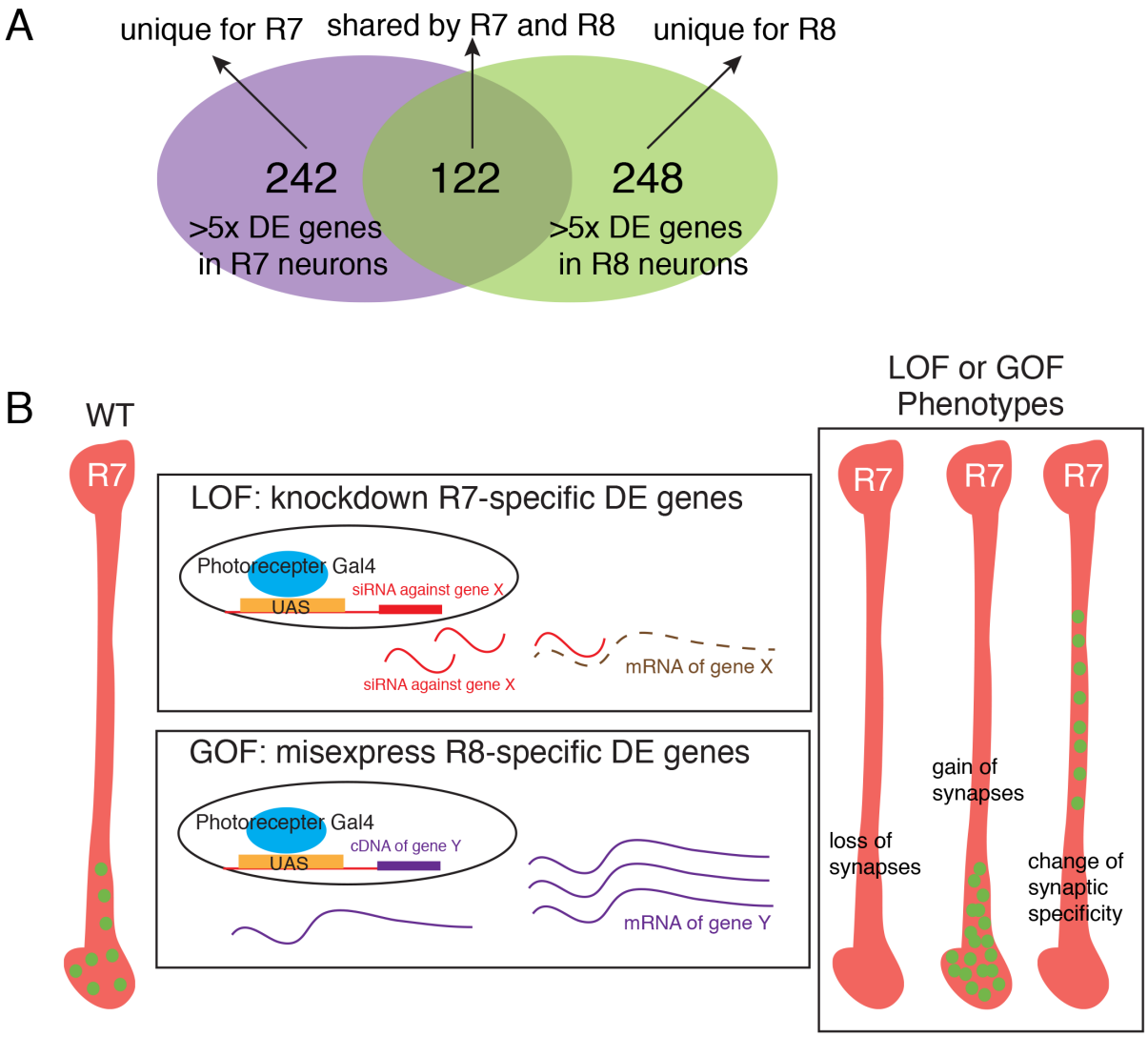

Figure 4-3 Identifying genes regulating synaptic specificity in R7 and R8 neurons

(A) Candidate genes regulating synaptic specificity in R7 and R8 neurons respectively were determined by acquiring the unique gene set differentially expressed for more than 5-fold between 40h and 50h APF in each cell type. The lists of uniquely differentially expressed genes for R7 and R8 neurons contain 242 and 248 genes respectively. (B) Design of LOF and GOF screens to test candidate genes in R7 neurons for synaptic specificity.

Adapting STaR to the mammalian nervous system

The design principle of STaR is not limited to *Drosophila*. The Cre-lox recombination system and the genetic knock-in technique have made it possible to adapt the STaR

design principle to mice (Capecchi, 2005). Currently, most studies in synapse formation and synaptic specificity in the mouse brain use dendritic spines (the specialized dendritic structures hosting postsynaptic sites) as the sole marker for excitatory synapses (Nimchinsky et al., 2002; Rochefort and Konnerth, 2012). The presynaptic side was largely ignored due to a lack of visualization method. Generating an inducible presynaptic marker labeling presynaptic sites in specific neurons will greatly improve the scope and depth of those studies. Also, tools for studying inhibitory synapses *in vivo* are currently lacking. Inducible tagging of proteins specifically localized to the inhibitory synapses (e.g. Gephyrin) will expand our ability to study those synapses in the mammalian CNS (Fritschy et al., 2008). Through the use of multiple recombination systems in mice (e.g., Cre-Lox and the B3 and KD systems), it is possible to simultaneous visualize excitatory and inhibitory synapses in a specific neural circuit (e.g. by inducible tagging of PSD-95 and Gephyrin) and study their homeostasis, which has been implied as the underlying mechanisms for several neurological diseases (Kim and Sheng, 2004; Wondolowski and Dickman, 2013).

In collaboration with William Yang's group at UCLA, we plan to use the well-studied PSD-95 (Dlg4) protein to develop a general strategy to sparsely label genetically defined neurons with tagged endogenous synaptic proteins. PSD-95 was chosen for several reasons. First, PSD-95 is one of the most abundant proteins at the post-synaptic densities of the excitatory synapses, including all cortical and thalamic projection neurons (Kennedy, 2000; Nourry et al., 2003). Second, previous studies have shown that C-terminal tagging of endogenous PSD-95 does not disrupt function or localization (Fernandez et al., 2009). And third, as PSD-95 plays a crucial role at excitatory synapses,

hence sparse labeling of PSD-95 positive synapses in distinct neuronal cell types may help to advance in vivo interrogation of the function and dysfunction of the synapses in various mutants and models of human diseases.

The strategy for tagging PSD-95 is based on the design for modifying the Brp protein in Drosophila. The following cassette will be inserted by gene targeting to the last exon of murine PSD-95 so that the translation STOP codon for PSD-95 will be deleted, and in turn, its PSD-95 open reading frame will continue into the cassette with the following components. First, a floxed sequence containing a translational STOP codon (e.g. TAA, STOP #1 in Figure 4-4) that is in frame with the PSD-95. Thus, in neurons without Cre, the PSD-95 with 12 extra amino acid (from LoxP) will be expressed and translated (termed PSD-95-L, Figure 4-4), and we expect this form of protein should be functional based on the experiments of Fernandez (2009). In neuron with Cre expressed, STOP#1 is removed by recombination, allowing the open reading frame to read through.

As the density of neuronal processes and synapses are extremely high in the mammalian brain and most Cre lines in mice express broadly, we implement a second element to further reduce the number of neurons that the PSD-95 marker labels to achieve sparse labeling of identifiable neurons. This element, termed MORF (MOsaicism with Repeat Frameshift) takes advantage of the fact that microsatellite repeats (e.g. mononucleotide, dinucleotide and trinucleotide) are prone to frameshift mutations. Yang and colleagues have shown that a mononucleotide microsatellite repeat (i.e. G22) mediated frameshifts can be used as a general method to genetically target protein expression to specific neuronal cell types in mammalian brain to enable sparse and stochastic labeling of single genetically-defined neurons for morphological and genetic analyses. Following the floxed

translational STOP#1, we inserted the G22 cassette, and a second translational STOP (in frame with PSD-95-LoxP-G22 frame), which should terminate the translation of the PSD-95 protein product in PSD-95 and Cre-expressing neurons (Figure 4-4). Finally, in a small subset of PSD-95/Cre-expressing neurons a frameshift mutation in the G22 cassette will occur and G22 becomes inframe G3n repeat (e.g. 21, 18), resulting in translation of GFP and, thus, C-terminal tagging of PSD-95. Moreover, this will also lead to translation of the 2A peptide, its self-cleavage followed by translation of the inducible transcription factor tTA (Mansury, 2000). The latter transcription factor can drive expression of reporter gene from TetO promoter (e.g. TdTomato) to highlight the morphology of the cell in which PSD-95 is GFP-tagged or to perform further genetic manipulations in these neurons (Figure 4-4). The above-mentioned cassettes will be inserted into the endogenous PSD-95 genomic locus via the newly developed CRISPR/Cas9-based gene targeting method (Wang et al., 2013).

The synaptic marker based on PSD-95 will be a proof-of-principle example to demonstrate that the STaR method is applicable in the mammalian nervous system. As the CRISPR/Cas9-based method promotes very efficient genome editing such as insertion of exogenous cassettes into the genomic loci of target genes, we are confident that in the future we will be able to generate many STaR synaptic markers that labels different types of synaptic structures in the mammalian nervous system to study important questions in neurobiology.

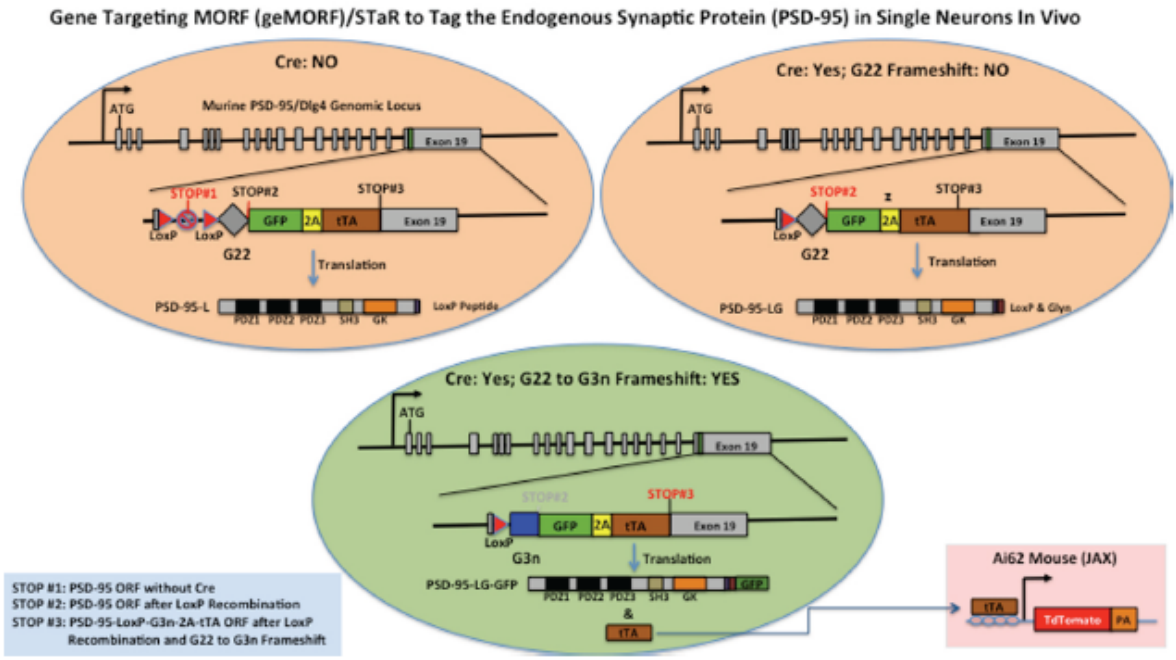

Figure 4-4 Schematic to illustrate gene targeting-mediated MORF strategy to allow Cre-dependent tagging of an endogenous PSD-95 in sparsely distributed single neurons of a specific type in intact mouse brains.

Gene targeting will introduce the floxed translational STOP#1 flanked by two LoxP sites to the last exon (Exon #19) of PSD-95. This LoxP cassette is followed by G22 sequence, a second STOP (#2) that will terminate the PSD-95 translation after Cre-mediated LoxP recombination. Finally, the last part of the cassette, in the G3n open reading frame, is GFP, 2A peptide, and tTA transcription factor. (A). In neurons expressing PSD-95 but not Cre, the targeted PSD-95 allele is expressed but translation will stop at STOP #1 (Red) with a few extra peptide translated from LoxP at C-terminal (PSD-95-L). (B). In neurons expressing Cre (determine labeling cell types), but G22 is not frameshift into G3n, Cre-mediated deletion of the LoxP cassette will remove STOP#1, but the PSD-95 targeted allele will stop translation at STOP#2 (Red), and the produce will be a slightly longer PSD-95 with a C-terminal peptide from LoxP and G22 (PSD-95-LG). (C). In neurons expressing PSD-95 and Cre, and G22 is stochastically frameshifted into G3n, the PSD-95 translation will continue to add a C-terminal tag with GFP (PSD-95-LG-GFP). Moreover, the 2A peptide enable simultaneous translation of a second protein, tTA, to mediate Tet-regulatable transcription (e.g. TdTomato from Ai62 mouse). Thus, only in a small subset of PSD-95/Cre-expressing neurons the endogenous PSD-95 is tagged with GFP and cell body and processes can be visualized with TdTomato.

References

Banovic, D., Khorramshahi, O., Owald, D., Wichmann, C., Riedt, T., Fouquet, W., Tian,

R., Sigrist, S.J., and Aberle, H. (2010). Drosophila neuroligin 1 promotes growth and

postsynaptic differentiation at glutamatergic neuromuscular junctions. Neuron 66, 724-738.

Biederer, T., Sara, Y., Mozhayeva, M., Atasoy, D., Liu, X., Kavalali, E.T., and Sudhof, T.C. (2002). SynCAM, a synaptic adhesion molecule that drives synapse assembly. Science 297, 1525-1531.

Briggman, K.L., and Bock, D.D. (2012). Volume electron microscopy for neuronal circuit reconstruction. Curr Opin Neurobiol 22, 154-161.

Briggman, K.L., Helmstaedter, M., and Denk, W. (2011). Wiring specificity in the direction-selectivity circuit of the retina. Nature 471, 183-188.

Capecchi, M.R. (2005). Gene targeting in mice: functional analysis of the mammalian genome for the twenty-first century. Nature reviews Genetics 6, 507-512.

Chao, D.L., and Shen, K. (2008). Functional dissection of SYG-1 and SYG-2, cell adhesion molecules required for selective synaptogenesis in C. elegans. Mol Cell Neurosci 39, 248-257.

Christopherson, K.S., Ullian, E.M., Stokes, C.C., Mullowney, C.E., Hell, J.W., Agah, A., Lawler, J., Mosher, D.F., Bornstein, P., and Barres, B.A. (2005). Thrombospondins are astrocyte-secreted proteins that promote CNS synaptogenesis. Cell 120, 421-433.

Coyne, J.A., and Orr, H.A. (1998). The evolutionary genetics of speciation. Philos Trans R Soc Lond B Biol Sci 353, 287-305.

Craig, A.M., and Kang, Y. (2007). Neurexin-neuroligin signaling in synapse development. Curr Opin Neurobiol 17, 43-52.

Dalva, M.B., Takasu, M.A., Lin, M.Z., Shamah, S.M., Hu, L., Gale, N.W., and Greenberg, M.E. (2000). EphB receptors interact with NMDA receptors and regulate excitatory synapse formation. Cell 103, 945-956.

Dani, A., Huang, B., Bergan, J., Dulac, C., and Zhuang, X. (2010). Superresolution imaging of chemical synapses in the brain. Neuron 68, 843-856.

de Wit, J., Hong, W., Luo, L., and Ghosh, A. (2011). Role of leucine-rich repeat proteins in the development and function of neural circuits. Annu Rev Cell Dev Biol 27, 697-729.

DeNardo, L.A., de Wit, J., Otto-Hitt, S., and Ghosh, A. (2012). NGL-2 regulates input-specific synapse development in CA1 pyramidal neurons. Neuron 76, 762-775.

Dityatev, A., Dityateva, G., and Schachner, M. (2000). Synaptic strength as a function of post- versus presynaptic expression of the neural cell adhesion molecule NCAM. Neuron 26, 207-217.

Dobzhansky, T. (1937). Further Data on the Variation of the Y Chromosome in Drosophila Pseudoobscura. Genetics 22, 340-346.

Doyle, J.P., Dougherty, J.D., Heiman, M., Schmidt, E.F., Stevens, T.R., Ma, G., Bupp, S., Shrestha, P., Shah, R.D., Doughty, M.L., *et al*. (2008). Application of a translational profiling approach for the comparative analysis of CNS cell types. Cell 135, 749-762.

Dudanova, I., Tabuchi, K., Rohlmann, A., Sudhof, T.C., and Missler, M. (2007). Deletion of alpha-neurexins does not cause a major impairment of axonal pathfinding or synapse formation. J Comp Neurol 502, 261-274.

Dunipace, L., Meister, S., McNealy, C., and Amrein, H. (2001). Spatially restricted expression of candidate taste receptors in the Drosophila gustatory system. Curr Biol 11, 822-835.

Eroglu, C., Allen, N.J., Susman, M.W., O'Rourke, N.A., Park, C.Y., Ozkan, E., Chakraborty, C., Mulinyawe, S.B., Annis, D.S., Huberman, A.D., *et al*. (2009). Gabapentin receptor alpha2delta-1 is a neuronal thrombospondin receptor responsible for excitatory CNS synaptogenesis. Cell 139, 380-392.

Fan, P., Manoli, D.S., Ahmed, O.M., Chen, Y., Agarwal, N., Kwong, S., Cai, A.G., Neitz, J., Renslo, A., Baker, B.S., and Shah, N.M. (2013). Genetic and neural mechanisms that inhibit Drosophila from mating with other species. Cell 154, 89-102.

Feinberg, E.H., Vanhoven, M.K., Bendesky, A., Wang, G., Fetter, R.D., Shen, K., and Bargmann, C.I. (2008). GFP Reconstitution Across Synaptic Partners (GRASP) defines cell contacts and synapses in living nervous systems. Neuron 57, 353-363.

Fernandez, E., Collins, M.O., Uren, R.T., Kopanitsa, M.V., Komiyama, N.H., Croning, M.D., Zografos, L., Armstrong, J.D., Choudhary, J.S., and Grant, S.G. (2009). Targeted tandem affinity purification of PSD-95 recovers core postsynaptic complexes and schizophrenia susceptibility proteins. Molecular systems biology 5, 269.

Fouquet, W., Owald, D., Wichmann, C., Mertel, S., Depner, H., Dyba, M., Hallermann, S., Kittel, R.J., Eimer, S., and Sigrist, S.J. (2009). Maturation of active zone assembly by Drosophila Bruchpilot. J Cell Biol 186, 129-145.

Friedman, H.V., Bresler, T., Garner, C.C., and Ziv, N.E. (2000). Assembly of new individual excitatory synapses: time course and temporal order of synaptic molecule recruitment. Neuron 27, 57-69.

Fritschy, J.M., Harvey, R.J., and Schwarz, G. (2008). Gephyrin: where do we stand, where do we go? Trends Neurosci 31, 257-264.

Gao, S., Takemura, S.Y., Ting, C.Y., Huang, S., Lu, Z., Luan, H., Rister, J., Thum, A.S., Yang, M., Hong, S.T., *et al*. (2008). The neural substrate of spectral preference in Drosophila. Neuron 60, 328-342.

Gerrow, K., Romorini, S., Nabi, S.M., Colicos, M.A., Sala, C., and El-Husseini, A. (2006). A preformed complex of postsynaptic proteins is involved in excitatory synapse development. Neuron 49, 547-562.

Glynn, M.W., Elmer, B.M., Garay, P.A., Liu, X.B., Needleman, L.A., El-Sabeawy, F., and McAllister, A.K. (2011). MHCI negatively regulates synapse density during the establishment of cortical connections. Nat Neurosci 14, 442-451.

Gomes, R.A., Hampton, C., El-Sabeawy, F., Sabo, S.L., and McAllister, A.K. (2006). The dynamic distribution of TrkB receptors before, during, and after synapse formation between cortical neurons. J Neurosci 26, 11487-11500.

Gordon, M.D., and Scott, K. (2009). Motor control in a Drosophila taste circuit. Neuron 61, 373-384.

Graf, E.R., Valakh, V., Wright, C.M., Wu, C., Liu, Z., Zhang, Y.Q., and DiAntonio, A. (2012). RIM promotes calcium channel accumulation at active zones of the Drosophila neuromuscular junction. J Neurosci 32, 16586-16596.

Hell, S.W. (2003). Toward fluorescence nanoscopy. Nat Biotechnol 21, 1347-1355.

Henkemeyer, M., Itkis, O.S., Ngo, M., Hickmott, P.W., and Ethell, I.M. (2003). Multiple EphB receptor tyrosine kinases shape dendritic spines in the hippocampus. J Cell Biol 163, 1313-1326.

Herzenberg, L.A., Sweet, R.G., and Herzenberg, L.A. (1976). Fluorescence-activated cell sorting. Scientific American 234, 108-117.

Hong, W., Mosca, T.J., and Luo, L. (2012). Teneurins instruct synaptic partner matching in an olfactory map. Nature 484, 201-207.

Karuppudurai, T., Lin, T.Y., Ting, C.Y., Pursley, R., Melnattur, K.V., Diao, F., White, B.H., Macpherson, L.J., Gallio, M., Pohida, T., and Lee, C.H. (2014). A hard-wired glutamatergic circuit pools and relays UV signals to mediate spectral preference in Drosophila. Neuron 81, 603-615.

Kaufmann, N., DeProto, J., Ranjan, R., Wan, H., and Van Vactor, D. (2002). Drosophila liprin-alpha and the receptor phosphatase Dlar control synapse morphogenesis. Neuron 34, 27-38.

Kennedy, M.B. (2000). Signal-processing machines at the postsynaptic density. Science 290, 750-754.

Kim, E., and Sheng, M. (2004). PDZ domain proteins of synapses. Nat Rev Neurosci 5, 771-781.

Kim, J., Zhao, T., Petralia, R.S., Yu, Y., Peng, H., Myers, E., and Magee, J.C. (2012). mGRASP enables mapping mammalian synaptic connectivity with light microscopy. Nature methods 9, 96-102.

Kizilyaprak, C., Daraspe, J., and Humbel, B.M. (2014). Focused ion beam scanning electron microscopy in biology. Journal of microscopy.

Klar, T.A., Jakobs, S., Dyba, M., Egner, A., and Hell, S.W. (2000). Fluorescence microscopy with diffraction resolution barrier broken by stimulated emission. Proc Natl Acad Sci U S A 97, 8206-8210.

Klassen, M.P., and Shen, K. (2007). Wnt signaling positions neuromuscular connectivity by inhibiting synapse formation in C. elegans. Cell 130, 704-716.

Ko, J., Kim, S., Chung, H.S., Kim, K., Han, K., Kim, H., Jun, H., Kaang, B.K., and Kim, E. (2006). SALM synaptic cell adhesion-like molecules regulate the differentiation of excitatory synapses. Neuron 50, 233-245.

Lee, T., and Luo, L. (2001). Mosaic analysis with a repressible cell marker (MARCM) for Drosophila neural development. Trends Neurosci 24, 251-254.

Li, J., Ashley, J., Budnik, V., and Bhat, M.A. (2007). Crucial role of Drosophila neurexin in proper active zone apposition to postsynaptic densities, synaptic growth, and synaptic transmission. Neuron 55, 741-755.

Luthy, K., Ahrens, B., Rawal, S., Lu, Z., Tarnogorska, D., Meinertzhagen, I.A., and Fischbach, K.F. (2014). The irre Cell Recognition Module (IRM) Protein Kirre Is Required to Form the Reciprocal Synaptic Network of L4 Neurons in the Drosophila Lamina. J Neurogenet.

Margeta, M.A., Shen, K., and Grill, B. (2008). Building a synapse: lessons on synaptic specificity and presynaptic assembly from the nematode C. elegans. Curr Opin Neurobiol 18, 69-76.

Martinez, A., Alcantara, S., Borrell, V., Del Rio, J.A., Blasi, J., Otal, R., Campos, N., Boronat, A., Barbacid, M., Silos-Santiago, I., and Soriano, E. (1998). TrkB and TrkC signaling are required for maturation and synaptogenesis of hippocampal connections. J Neurosci 18, 7336-7350.

Mauch, D.H., Nagler, K., Schumacher, S., Goritz, C., Muller, E.C., Otto, A., and Pfrieger, F.W. (2001). CNS synaptogenesis promoted by glia-derived cholesterol. Science 294, 1354-1357.

Mayr, B., Kalat, M., and Rab, P. (1988). Heterochromatins and band karyotypes in three species of salmonids. TAG Theoretical and applied genetics Theoretische und angewandte Genetik 76, 45-53.

McAllister, A.K. (2007). Dynamic aspects of CNS synapse formation. Annu Rev Neurosci 30, 425-450.

Meinertzhagen, I.A., and O'Neil, S.D. (1991). Synaptic organization of columnar elements in the lamina of the wild type in Drosophila melanogaster. J Comp Neurol 305, 232-263.

Millard, S.S., Lu, Z., Zipursky, S.L., and Meinertzhagen, I.A. (2010). Drosophila dscam proteins regulate postsynaptic specificity at multiple-contact synapses. Neuron 67, 761-768.

Nam, J., Mah, W., and Kim, E. (2011). The SALM/Lrfn family of leucine-rich repeat-containing cell adhesion molecules. Semin Cell Dev Biol 22, 492-498.

Ni, J.Q., Liu, L.P., Binari, R., Hardy, R., Shim, H.S., Cavallaro, A., Booker, M., Pfeiffer, B.D., Markstein, M., Wang, H., *et al*. (2009). A Drosophila resource of transgenic RNAi lines for neurogenetics. Genetics 182, 1089-1100.

Nimchinsky, E.A., Sabatini, B.L., and Svoboda, K. (2002). Structure and function of dendritic spines. Annu Rev Physiol 64, 313-353.

Nonet, M.L. (1999). Visualization of synaptic specializations in live C. elegans with synaptic vesicle protein-GFP fusions. J Neurosci Methods 89, 33-40.

Nourry, C., Grant, S.G., and Borg, J.P. (2003). PDZ domain proteins: plug and play! Sci STKE 2003, RE7.

Pantazis, A., Segaran, A., Liu, C.H., Nikolaev, A., Rister, J., Thum, A.S., Roeder, T., Semenov, E., Juusola, M., and Hardie, R.C. (2008). Distinct roles for two histamine receptors (hclA and hclB) at the Drosophila photoreceptor synapse. J Neurosci 28, 7250-7259.

Pedelacq, J.D., Cabantous, S., Tran, T., Terwilliger, T.C., and Waldo, G.S. (2006). Engineering and characterization of a superfolder green fluorescent protein. Nat Biotechnol 24, 79-88.

Poon, V.Y., Klassen, M.P., and Shen, K. (2008). UNC-6/netrin and its receptor UNC-5 locally exclude presynaptic components from dendrites. Nature 455, 669-673.

Rivera-Alba, M., Vitaladevuni, S.N., Mishchenko, Y., Lu, Z., Takemura, S.Y., Scheffer, L., Meinertzhagen, I.A., Chklovskii, D.B., and de Polavieja, G.G. (2011). Wiring economy and volume exclusion determine neuronal placement in the Drosophila brain. Curr Biol 21, 2000-2005.

Rochefort, N.L., and Konnerth, A. (2012). Dendritic spines: from structure to in vivo function. EMBO Rep 13, 699-708.

Rust, M.J., Bates, M., and Zhuang, X. (2006). Sub-diffraction-limit imaging by stochastic optical reconstruction microscopy (STORM). Nature methods 3, 793-795.

Sabo, S.L., Gomes, R.A., and McAllister, A.K. (2006). Formation of presynaptic terminals at predefined sites along axons. J Neurosci 26, 10813-10825.

Sanes, J.R., and Yamagata, M. (2009). Many paths to synaptic specificity. Annu Rev Cell Dev Biol 25, 161-195.

Sara, Y., Biederer, T., Atasoy, D., Chubykin, A., Mozhayeva, M.G., Sudhof, T.C., and Kavalali, E.T. (2005). Selective capability of SynCAM and neuroligin for functional synapse assembly. J Neurosci 25, 260-270.

Scott, K., Brady, R., Jr., Cravchik, A., Morozov, P., Rzhetsky, A., Zuker, C., and Axel, R. (2001). A chemosensory gene family encoding candidate gustatory and olfactory receptors in Drosophila. Cell 104, 661-673.

Shen, K., and Bargmann, C.I. (2003). The immunoglobulin superfamily protein SYG-1 determines the location of specific synapses in C. elegans. Cell 112, 619-630.

Shen, K., Fetter, R.D., and Bargmann, C.I. (2004). Synaptic specificity is generated by the synaptic guidepost protein SYG-2 and its receptor, SYG-1. Cell 116, 869-881.

Stocker, R.F. (1994). The organization of the chemosensory system in Drosophila melanogaster: a review. Cell Tissue Res 275, 3-26.

Sun, M., Xing, G., Yuan, L., Gan, G., Knight, D., With, S.I., He, C., Han, J., Zeng, X., Fang, M., *et al*. (2011). Neuroligin 2 is required for synapse development and function at the Drosophila neuromuscular junction. J Neurosci 31, 687-699.

Takemura, S.Y., Bharioke, A., Lu, Z., Nern, A., Vitaladevuni, S., Rivlin, P.K., Katz, W.T., Olbris, D.J., Plaza, S.M., Winston, P., *et al*. (2013). A visual motion detection circuit suggested by Drosophila connectomics. Nature 500, 175-181.

Takemura, S.Y., Lu, Z., and Meinertzhagen, I.A. (2008). Synaptic circuits of the Drosophila optic lobe: the input terminals to the medulla. J Comp Neurol 509, 493-513.

Varoqueaux, F., Aramuni, G., Rawson, R.L., Mohrmann, R., Missler, M., Gottmann, K., Zhang, W., Sudhof, T.C., and Brose, N. (2006). Neuroligins determine synapse maturation and function. Neuron 51, 741-754.

Vicario-Abejon, C., Collin, C., McKay, R.D., and Segal, M. (1998). Neurotrophins induce formation of functional excitatory and inhibitory synapses between cultured hippocampal neurons. J Neurosci 18, 7256-7271.

Wagh, D.A., Rasse, T.M., Asan, E., Hofbauer, A., Schwenkert, I., Durrbeck, H., Buchner, S., Dabauvalle, M.C., Schmidt, M., Qin, G., *et al*. (2006). Bruchpilot, a protein with homology to ELKS/CAST, is required for structural integrity and function of synaptic active zones in Drosophila. Neuron 49, 833-844.

Wang, H., Yang, H., Shivalila, C.S., Dawlaty, M.M., Cheng, A.W., Zhang, F., and Jaenisch, R. (2013). One-step generation of mice carrying mutations in multiple genes by CRISPR/Cas-mediated genome engineering. Cell 153, 910-918.

Wang, Z., Singhvi, A., Kong, P., and Scott, K. (2004). Taste representations in the Drosophila brain. Cell 117, 981-991.

Washbourne, P., Bennett, J.E., and McAllister, A.K. (2002). Rapid recruitment of NMDA receptor transport packets to nascent synapses. Nat Neurosci 5, 751-759.

White, J.G., Southgate, E., Thomson, J.N., and Brenner, S. (1986). The structure of the nervous system of the nematode Caenorhabditis elegans. Philos Trans R Soc Lond B Biol Sci 314, 1-340.

Witte, I., Kreienkamp, H.J., Gewecke, M., and Roeder, T. (2002). Putative histamine-gated chloride channel subunits of the insect visual system and thoracic ganglion. J Neurochem 83, 504-514.

Wondolowski, J., and Dickman, D. (2013). Emerging links between homeostatic synaptic plasticity and neurological disease. Frontiers in cellular neuroscience 7, 223.

Yamagata, M., and Sanes, J.R. (2012). Transgenic strategy for identifying synaptic connections in mice by fluorescence complementation (GRASP). Frontiers in molecular neuroscience 5, 18.

Yamagata, M., Sanes, J.R., and Weiner, J.A. (2003). Synaptic adhesion molecules. Curr Opin Cell Biol 15, 621-632.

Yeh, E., Kawano, T., Weimer, R.M., Bessereau, J.L., and Zhen, M. (2005). Identification of genes involved in synaptogenesis using a fluorescent active zone marker in Caenorhabditis elegans. J Neurosci 25, 3833-3841.

Zeng, X., Sun, M., Liu, L., Chen, F., Wei, L., and Xie, W. (2007). Neurexin-1 is required for synapse formation and larvae associative learning in Drosophila. FEBS Lett 581, 2509-2516.

Zhang, Y.Q., Rodesch, C.K., and Broadie, K. (2002). Living synaptic vesicle marker: synaptotagmin-GFP. Genesis 34, 142-145.